SOME INCLUSION COMPLEXES AND THEIR PROPERTIES

A Thesis submitted for the Degree of
Doctor of Philosophy
in the
University of London

by

John Leonard Whiteman
April 1965

Chemistry Department,
Imperial College,
London,
S. W. 7.

ABSTRACT

A comparative study of the sorption of the elements, sulphur, phosphorus and mercury, has been made in several molecular sieve zeolites such as Linde Sieves X and A, chabazite and gmelinite. The sorption of sulphur by the zeolites with the more open structures is very rapid, and gives isotherms which are remarkably rectangular in view of the high temperature of the sorbents. The zeolites in which the windows between neighbouring sorption cavities are small take up sulphur and also phosphorus much more slowly. A surprising discovery is that the uptake of phosphorus by the zeolite with the most open structure is also slow. Possible mechanisms for these slow processes have been suggested.

The uptake of mercury by the sodium and lead forms of Sieve X is found to be smaller than would be expected from the magnitude of the inter-atomic forces in liquid mercury. The modest uptake in these zeolites has been explained by demonstrating that the sorbed mercury exists as isolated atoms, and that it is the mercury-framework interactions which determine the extent of sorption. When electron interchange between mercury atoms and the cations in the zeolite is possible, much larger uptakes are observed. In mercuric X, the chemisorption of mercury on to the mercuric ion leads to large mercury uptakes, while in silver zeolites the transfer of electrons from mercury atoms to the silver ions allows still larger mercury uptakes to be achieved through the release of

silver atoms which can act as sites for mercury uptake. A comparative study of the mercury sorption of the silver forms of a number of zeolites has been carried out. The silver forms studied showed large uptakes of mercury, and hysteresis was observed in all the isotherms obtained.

D E D I C A T I O N

This work is dedicated to my late mother in appreciation of her unfailing interest and encouragement.

ACKNOWLEDGEMENTS

I wish to acknowledge my indebtedness to Professor R. M. Barrer, FRS, for suggesting this topic of research, for his continued interest and encouragement, and for many helpful discussions.

I am grateful to the U.S. Department of the Army and to Imperial College for financial support.

INDEX

1. INTRODUCTION

1.1. Scope of the Research.

When a gas or vapour comes into contact with the surface of a solid some of the gas molecules may be held, or sorbed, on the surface. Evaporation of these molecules may not take place for some time, and a surface layer may be built up. If the solid is porous and presents a large surface area to the gas, the quantity of sorbed material may be considerable. This ability of porous solids to retain fluids is exploited in a variety of technological processes. It is not surprising, therefore, that sorption has been studied extensively in recent years. Meanwhile theoretical aspects of sorption have not been neglected and much progress has been made towards understanding the principles underlying the process.

A feature of most sorbents which complicates the fundamental study of sorption processes is the lack of precise knowledge of the nature of the sorbing surface. Charcoal and silica gel are widely used in industry and are among the sorbents most frequently studied. Both owe their large surface area to the presence of very fine pores throughout the body of the sorbent. The pores vary in both size and shape, and the sorbing surface is neither uniform nor regular.

Certain features characteristic of crystals allow more precise knowledge of the sorbent. The atoms of crystals are arranged in definite patterns repeated throughout the structure in each direction. A porous crystal has channels and internal surfaces

as regular as the framework itself. It can act therefore as a molecular sieve since molecules which are small enough and have the right shape can pass freely into the channels whereas other molecules which are too large or have the wrong shape are totally excluded. Furthermore, the position of each atom in the repeated pattern, and hence the structure of the sorbent, can be determined accurately from X-ray diffraction studies. Crystals therefore are very suitable sorbents for fundamental studies of sorption processes. Gases or vapours which are sorbed by porous crystals penetrate the structure completely, and may be regarded as included in it. It is then appropriate to give the name "inclusion complex" to the sorbate-sorbent system.

Many minerals of the zeolite family can act as molecular sieves and form inclusion complexes with gases and vapours. The structures and sorption characteristics of zeolites and of their synthetic analogues have been studied extensively both in these laboratories and elsewhere. This work extends that study and compares the sorption by zeolites of several of the less volatile elements. The non-metallic elements, sulphur and phosphorus, exist in the vapour phase as atomic groups whose complexity varies with temperature and pressure. At the temperature of the experiments to be described, sulphur is predominantly octa-atomic, and phosphorus tetra-atomic. At similar temperatures mercury vapour is monatomic. In this work the sorption of these three elements by several zeolites will be studied and compared with the sorption of diatomic iodine which has already been reported (Barrer and Wasilewski, 1961). In addition to the

interest attaching to the study of sorption of each of these elements separately, comparison between them could be expected to throw light on the effect of atomic complexity on the sorption process.

Further study of the sorption of mercury by zeolites has been carried out using the crystals ion exchanged to contain various cations. Natural zeolites contain the cations of alkaline earth and alkali metals. In this study these cations are replaced by the cations of metals whose positions in the electrochemical series fall on either side of that of mercury.

The research is continued with a comparison of the mercury sorption in silver ion-exchanged forms of a number of porous crystals in which the size of the sorbing cavities and the diameter of the windows connecting neighbouring cavities form a graduated series. Study of these was expected to show the effect on sorption of providing an environment in which limited clusters of metal atoms could form. The use of zeolites and of finely divided metals as catalysts in many industrial processes adds considerable interest to such an investigation.

1.2 The Structure of the Sorbents

The porous crystals studied in this work are complex aluminosilicates belonging to the zeolite and felspathoid families of minerals. Each comprises essentially an anionic framework comparably strong in all three dimensions. The basic units from which the anionic framework is constructed are SiO_4^{4-} and AlO_4^{5-} tetrahedra. Each oxygen is shared between two tetra-

hedra and hence the framework is negatively charged only because of the isomorphous replacements of Si^{IV} by Al^{III}. The framework charge is neutralised by its electrochemical equivalent of cations.

In each porous crystal groups of tetrahedra are joined together to form hollow polyhedra. The polyhedra are then joined in simple arrangements to form the frameworks characteristic of the different sorbents. Thus eight tetrahedra form a cubic unit, and twelve a hexagonal prism. The polyhedra can be visualised as having an aluminium or a silicon atom at each apex and oxygens near the middle points of each edge. A more complex polyhedral unit is the cubo-octahedron formed from 24 tetrahedra. Its shape is that of a regular octahedron with each of its six apices cut off by the faces of a cube.

Stacking one or more of these three types of polyhedra in different arrangements produces the frameworks of the five sorbents studied. When large numbers of cubo-octahedra are stacked together in 8-fold co-ordination so that each 6-membered ring is shared between two cages, the structure formed corresponds to the felspathoid sodalite (Halstead and Moore, 1962). Each cage in this sorbent encloses a free space of diameter 6.6 angstroms accessible only through a ring of 6 oxygen atoms. The shape of these cages is shown in figure 1.1, which also shows to the same scale the cages of the other sorbents studied, together with some of the sorbate species. Table 1.1 lists the smallest free diameters of the largest windows in each sorbent, and the size and shape of the cavities which they connect. Also included is the total free volume

THE CAVITIES IN THE SORBENTS

FIG 1.1.

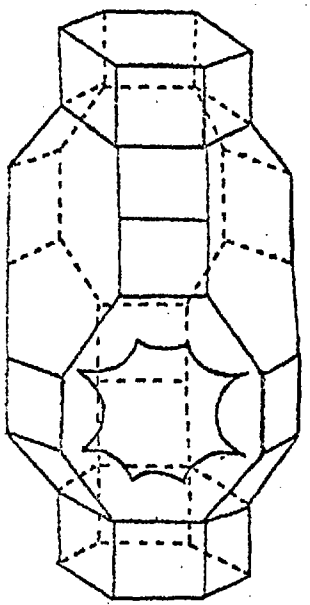

CHABAZITE

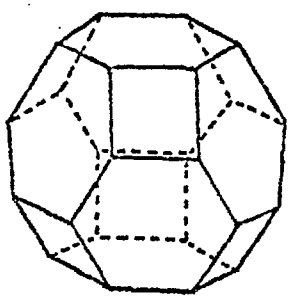

SODALITE

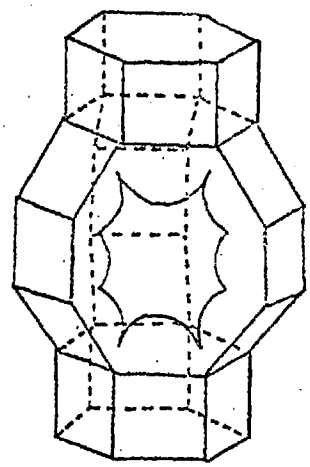

GMELINITE

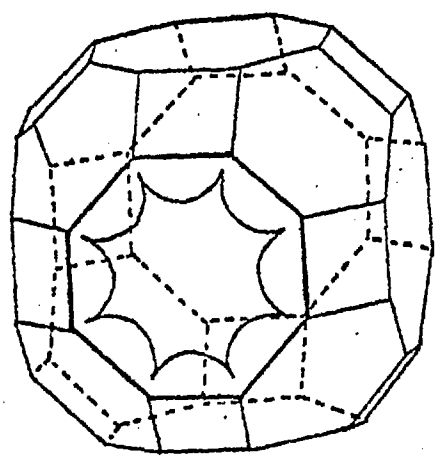

LINDE SIEVE A.

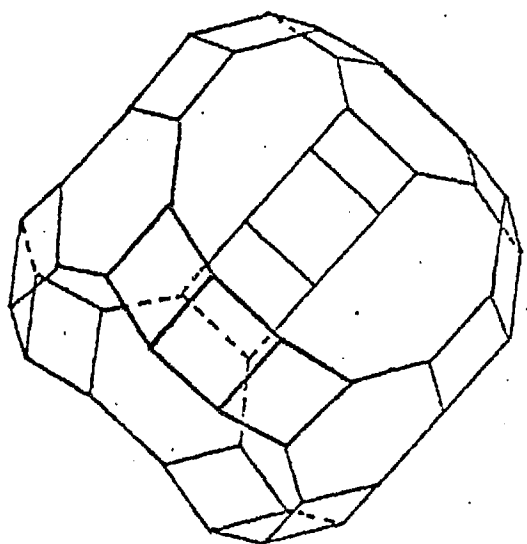

LINDE · SIEVE X

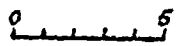

ANGSTROMS

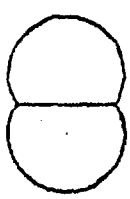

S_2

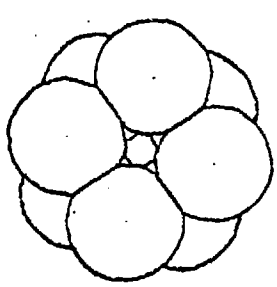

S_8

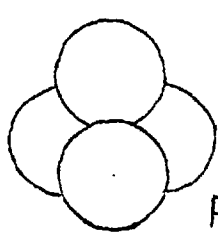

P_4

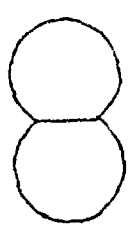

P_2

in the crystal estimated from the volume of liquid water which may be removed from each sorbent.

The cubo-octahedra which compose the sodalite structure, and are therefore known as sodalite cages, may be linked in other ways. When they are arranged in 6-fold co-ordination and linked by cubic units, the structure formed corresponds to Linde Sieve A, a synthetic material with no counterpart in nature (Barrer and Meier, 1958). This arrangement of polyhedra encloses a third cavity which is considerably larger than either of the polyhedra (figure 1.1 and table 1.1). The cuspidate line in the diagram shows

TABLE 1.1

Structure	Shape and free diameter of largest cage (Å)	Smallest free diameter of largest windows (Å)	Free volume (cm^3/cm^3 of crystal)
Natural chabazite	elongated ~11 x 6.6	~3.7	0.46
Synthetic zeolite Ca-form (Sieve 5A)	spherical ~11.8	~4.3	0.46
Synthetic near-faujasite Na-form (Sieve 13X)	spherical ~12	9-10	0.53
Natural gmelinite	elongated ~7.8 x 6.5	~3.4	0.45
Basic sodalite	spherical ~6.6	~2.3	0.30

the peripheries of the eight oxygen atoms which define the free diameter of the largest windows. Arranging cubo-octahedra in 4-fold co-ordination and joining appropriate faces through hexagonal prism units gives the structure of Linde Sieve X, a synthetic sorbent similar to the mineral faujasite.

Another important structure building unit is the hexagonal prism. The anionic frameworks of chabazite and gmelinite may be represented as sequences of layers of hexagonal prisms. These are firmly bonded to one another to produce rigid frameworks which enclose cavities much larger than the prisms themselves (Barrer and Kerr, 1959). The layer sequence is 123,123 in chabazite, and 1212 in gmelinite.

While it is convenient to visualise the formation of super-cages by the stacking of small polygonal units, the concept must not be allowed to obscure the fundamental character of the sorbents. The structural frameworks enclose networks of intersecting channels which run through the zeolites. Even when the channels are interrupted by crystal faults, the presence of interconnecting channels may provide alternative paths for a migrating species. The channels are constricted at regular intervals by windows formed by a ring of oxygen atoms. The minimum free diameters of these windows are listed in table 1.1. It is the windows which control the tempo of diffusion through the sorbent or, by completely excluding larger molecules, determine the molecular sieve effect.

Although the structure of the anionic framework of most zeolites has been determined, the positions of the cations in the structures is less well established. Some have been located in certain windows and cages (e.g.

Broussard and Shoemaker, 1960) while others are believed to move freely through the channel networks. Positions are not necessarily the same in anhydrous and hydrated sorbents and the presence of sorbates may also affect their distribution. These considerations will not be discussed in detail here, but will be introduced later at relevant points in the discussion.

1.3 The Sorbates

The special interest attaching to the study of the sorption of the elements, sulphur, phosphorus and mercury, arises from their forming a series of decreasing molecular complexity in the vapour phase. In the vapour of each element at the temperature of these experiments the predominant molecular species is octa-atomic, tetra-atomic and monatomic respectively. Dissociation of the complex molecules commences at comparatively low temperatures. West (1950) has used vapour pressure measurements to demonstrate that several molecular species are already present in sulphur vapour at 260°C. The calculated mole fractions of S_8, S_6 and S_2 in sulphur vapour at 262°C and 320°C are listed in table 1.2.

Table 1.2

Temperature of vapour	Mole Fractions		
	S_8	S_6	S_2
262°C	0.69	0.30	0.008
320°C	0.59	0.40	0.010

Liquid sulphur also contains complex molecules. At temperatures just above the melting point (119°C) liquid sulphur consists largely of S_8 molecules. As the temperature is raised, polymeric sulphur appears abruptly at 159°C (Gee, 1952). The proportion of polymer in the equilibrium liquid then rises steadily with temperature.

The extent of dissociation of tetra-atomic phosphorus in the vapour is small compared with that of sulphur. Calculation from the equilibrium constant of the dissociation reaction shows the proportion of P_2 molecules in the vapour at 1 cm total pressure to be 1 in 10^6 at 264°C and 1 in 10^5 at 320°C. Mercury vapour is monatomic at all temperatures.

The atomic arrangements in these complex molecules have been established by diffraction methods. Lu and Donohue (1944) showed by electron diffraction that the S_8 molecules in sulphur vapour were in the form of puckered rings similar to those found in rhombic sulphur. Warren and Burwell (1935) calculated the interatomic distances in rhombic sulphur from X-ray diffraction patterns. From their data an overall diameter of 8.5 Å for the molecules can be estimated. The S_6 molecules in rhombohedral sulphur are also in the form of puckered rings (Donohue et al, 1961). Their overall diameter is about 5.8 Å. No determination of the atomic arrangement in polymeric sulphur has been published. Meyer and Go (1934) showed that stretched plastic sulphur contains zig-zag chains of atoms, but their data do not allow the chain dimensions to be calculated. The interatomic distance in S_2 is 1.89 Å (Wells, 1962). Assuming 1.85 Å for the van der Waals' radius of sulphur (Pauling, 1960) enables a value of 5.59 Å to be obtained

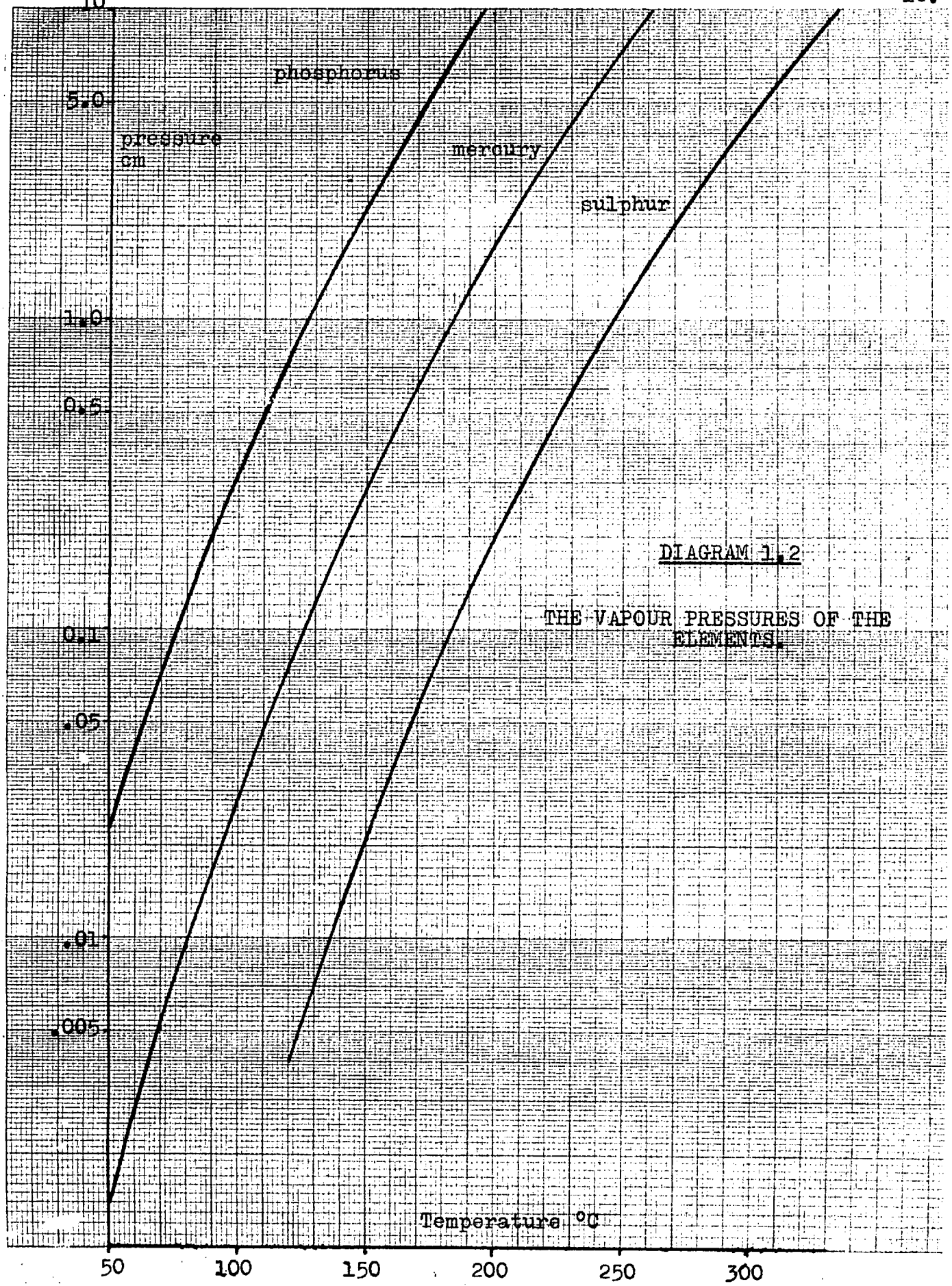

DIAGRAM 1.2

THE VAPOUR PRESSURES OF THE ELEMENTS.

for the length of the S_2 molecule.

The molecules in phosphorus vapour consist of four atoms arranged tetrahedrally (Maxwell et al, 1935). The overall diameter of the approximately spherical molecules is ca. 7.0 Å. P_2 molecules have a length of 6.6 Å and a diameter of 3.5 Å. These two forms of phosphorus, together with the sulphur molecules S_8 and S_2 are shown in fig. 1.1 to the same scale as the sorbents.

Reliable thermodynamic data for sulphur vapour is not available in the literature. No calorimetric determination of the specific heat of the vapour has been reported. Specific heats of each molecular species have been determined by spectroscopic methods, but interpretations of the measurements by different authors has led to a number of conflicting values for thermodynamic functions.

1.4 Some Remarks on Sorption

Sorption at the gas-solid interface is conveniently described in terms of sorption isotherms which relate the amount sorbed to the sorbate pressure at a specified temperature. Most isotherms conform to one of the five types classified by Brunauer et al (1940) which are shown in fig. 1.2. One feature these isotherms have in common is that they all tend to become linear at very low pressures. This behaviour is reminiscent of Henry's Law according to which the solubility of a gas in a liquid is proportional to the gas pressure. The low pressure region of sorption isotherms is accordingly sometimes referred to as the Henry's Law region.

THE FIVE TYPES OF ISOTHERM Fig. 1.3

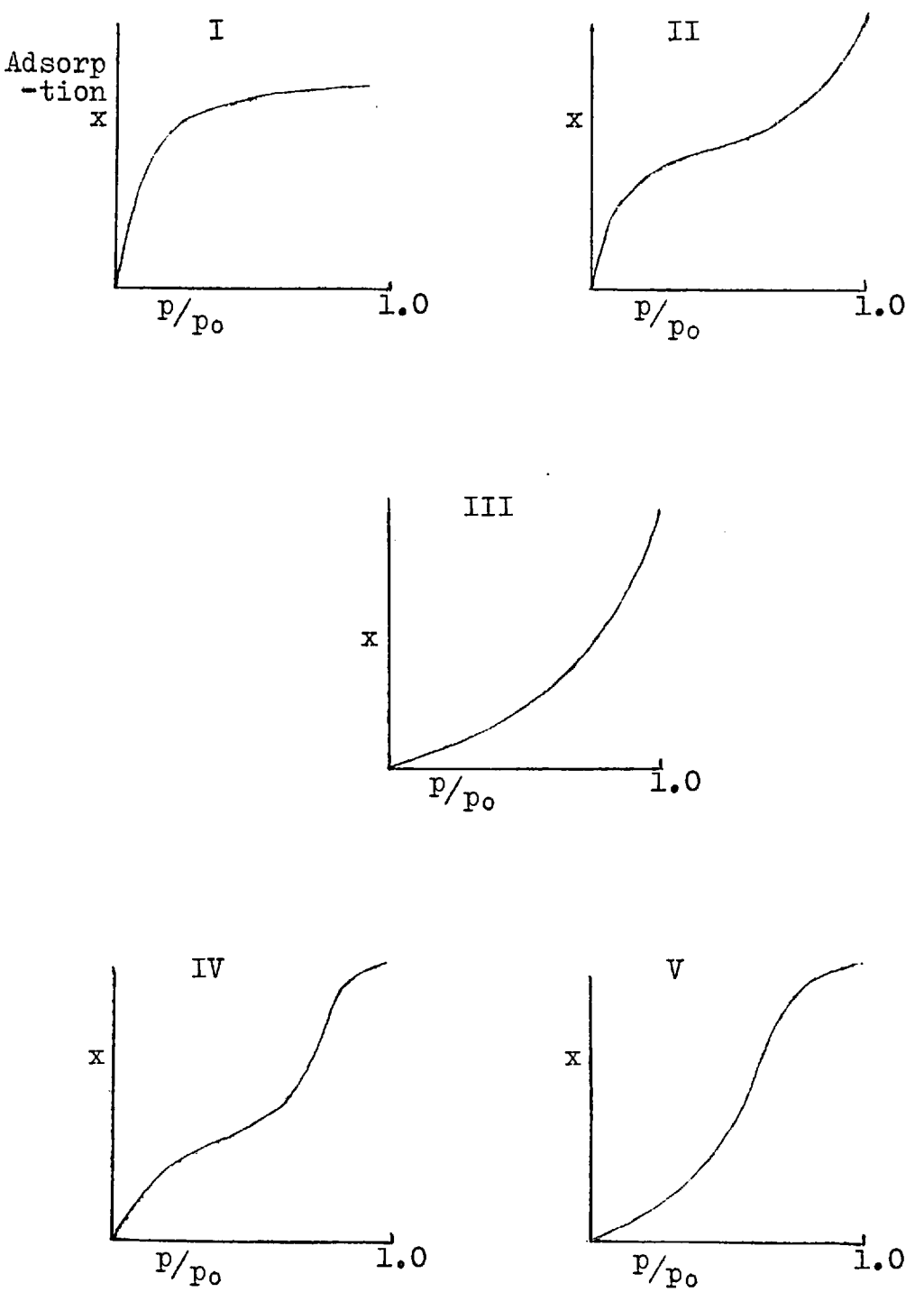

Few generalisations concerning sorption isotherms are possible. The effect on any sorption system of a rise in temperature is always to reduce the extent of sorption at a given pressure. This implies that adsorption is an exothermic process. Large negative heats of sorption produce a sharp knee in type I and II isotherms in the region of low partial pressures. Thus isotherms which are rectangular at low partial pressures are indicative of strong sorbate-sorbent interactions. The steep rise in sorption sometimes found as the partial pressure approaches unity is ascribed to condensation of the sorbate in capillaries and interparticle spaces.

Numerous attempts have been made to fit mathematical expressions to experimentally determined isotherms. The earliest equations were entirely empirical. Later theories based on physical pictures of sorption have been more successful. The kinetic approach to sorption first developed by Langmuir (1918) uses models of sorption and desorption processes. The Langmuir model was limited to a single layer of non-interacting molecules on fixed sites. If θ is the fraction of sites occupied at the pressure p, the equilibrium constant K is given by

$$K = \frac{\theta}{p(1-\theta)} \quad .$$

This relation has also been derived from thermodynamic considerations and is not dependent on the kinetic mechanism originally assumed. Extension of the model to multilayer sorption by Brunauer, Emmett and Teller (1938) led to the well known B.E.T. equation, which will not be discussed in detail. Lacher (1937) developed the model of localized sorption by allowing for interaction between neighbouring molecules. The relation obtained was

$$K = \frac{\theta}{p(1-\theta)} \left\{\frac{2-2\theta}{\beta-1-2\theta}\right\}^{Z} \quad .$$

Here Z denotes the coordination number of a site, and

$$\beta = \left\{1-4\theta(1-\theta)\left[1-\exp\left(-\frac{2w}{ZkT}\right)\right]\right\}^{\frac{1}{2}}$$

where $\frac{2w}{Z}$ is the interaction energy between a pair of sorbed molecules.

Each cavity in the more open zeolites is sufficiently large for multiple occupancy to be possible, and hence sites and cavities cannot be identified with one another. Furthermore, molecules sorbed in a zeolite cavity may be in contact with others in neighbouring cavities to produce a continuous intracrystalline fluid. Under these circumstances it might be expected that an alternative approach in which isotherm behaviour is described in terms of an equation of state for the sorbed fluid would be more appropriate. Thus a two dimensional analogue of van der Waals' equation leads to the isotherm relation

$$K = \frac{\theta}{p(1-\theta)} \exp\left(\frac{\theta}{1-\theta} - \alpha\theta\right)$$

where α is a coefficient depending upon temperature and upon the constants a and b of van der Waals' equation. The simpler equation of state due to Volmer which neglects the forces between sorbed molecules leads to the isotherm

$$K = \frac{\theta}{p(1-\theta)} \exp\frac{\theta}{1-\theta} \quad .$$

The methods of thermodynamics have been applied extensively to sorption data only in the last twenty years. Little progress was made until the necessity rigorously to define the thermodynamic system under study was recognised. Thus sorbent and sorbed gas can be treated as a two-component system in equilibrium with the unadsorbed gas by the methods of solution thermodynamics. Another choice is to

consider the boundary between the two systems to be at the surface of the sorbent. From this approach the methods of adsorption thermodynamics have been developed. The rigorous thermodynamic meaning of the information obtained has been established by the efforts of many workers. Lucid reviews have been presented by Hill (1952) and Everett (1957) .

The value of the thermodynamic approach is that it allows those features of a theoretical equation which follow directly from assumptions in the model to be separated from those of more general validity. Heats of adsorption can be obtained calorimetrically or from the temperature dependence of sorption through the Clausius-Clapeyron relation. Taken in conjunction with the free energy changes represented in sorption isotherms, these heats allow the entropy changes accompanying sorption to be calculated. Everett (1957) has derived the differential heats and entropies of sorption for models in which the sorbed molecules are localised and independent, mobile and independent, and mobile with interactions between sorbed molecules. Comparison of experimental data with these heat and entropy changes allows some conclusions to be drawn concerning the nature of the sorbed phase.

Another useful approach to the nature of sorbed phases uses the methods of statistical thermodynamics. Equilibrium constants and hence entropies of sorption can be calculated for models in which the sorbed molecules are assumed to have various degrees of freedom relative to their environment. These models may present a sufficient spread of entropy levels to allow a model of the sorbed state to be tentatively chosen by comparison with experimental data.

The calculation of sorption energies from considerations of the interaction between individual atoms has received some attention. The forces responsible for physical sorption arise from electrical moments in the atoms involved. Dispersion forces, which are invariably present, arise from the fluctuating electric moments produced by the movement of electrons in their orbits. These moments induce corresponding moments in neighbouring atoms and so lead to attraction. The attractive energy dies away with distance according to an inverse sixth power law, while the repulsive energy originating from the interpenetration of the electron clouds round the atoms dies away more rapidly and is often represented empirically by an inverse twelfth power law. The resultant is a potential well close to the sorbing surface which allows the sorbed atom to vibrate about an equilibrium position but rarely to escape from the region close to the surface. The energy barrier separating equivalent positions on the sorbing surface is usually much lower than that preventing escape.

When the sorbent is an ionic solid additional forces arise. The electrostatic field round an ion will interact with a molecule possessing a permanent dipole giving rise to an attractive force comparable in magnitude with that due to dispersion. If the adsorbed molecule is non-polar the contribution to the attractive force will depend on the polarisability of the molecule and tends usually to be small compared with the dispersion forces.

1.4.1 Sorption Hysteresis

The occurrence of hysteresis in sorption and desorption cycles has been explained in a number of ways. Many of the proposed mechanisms, including those depending on capillary condensation and volume changes in the sorbent, can be eliminated from consideration in the case of zeolites. A more general theory, suggested by Everett et al (1952, 1954, 1955) requires the existence in the system of independent domains each able to exist in at least two physical states. In certain cases, hysteresis has been attributed to the need to nucleate a second phase of sorbent and sorbate on or in the parent phase (Barrer, 1956). The formation of the new phase involves additional positive free energy terms associated with changes in area and with strain. Not until the state of the system has passed the true thermodynamic equilibrium point will the nuclei develop to a critical size beyond which they will then grow spontaneously. On the desorption branch, similar considerations delay the formation of nuclei of the original phase. Variations in the shape and the distribution of nuclei within the sorbent may give a spread in the strain and interfacial free energy terms, thus resulting in the sloping hysteresis loops commonly observed.

1.5 Sorption by Zeolites

The sorption properties of molecular sieves have been investigated extensively both in these laboratories and elsewhere. Considerable progress has been made in correlating the characteristics of individual sorbents with the shape and dimensions of the sorption channels.

Barrer (1959) has classified some porous crystals into five types, each distinguished by the ability to sorb molecules up to a certain limiting size while excluding others which are larger or of unsuitable shape. The size limits cannot be exactly defined, however, since the molecules are not incompressible, nor are the sorbents rigid structures. In general a molecule will pass through an aperture having a slightly smaller minimum free dimension than the critical dimension of the molecule, but as the overlap in dimensions increases, the energy barrier opposing its passage rises rapidly.

The inclusion of many gases and vapours has been reported. Where equilibrium isotherms have been determined, the curves of amount sorbed vs relative pressure often rise steeply at first, considerable sorption being observed at relatively low pressures. The initial steepness of these curves shows the strong affinity between the sorbents and included molecules. This high affinity has its origin in the strong interactions between included molecules and the polar frameworks of the sorbents. Barrer and Stuart (1959) and Barrer and Bratt (1960) have analysed the interaction energy into its constituent components. By sorbing argon, nitrogen (quadrupole molecule) and water (dipole + quadrupole) in different ion-exchanged forms of sieve X, the contributions arising from interactions between the dipoles and quadrupoles of the sorbates and the non-uniform electrostatic field of the sorbents have been evaluated. The energy of inclusion has been calculated for iodine (Barrer and Wasilewski, 1961), ammonia (Barrer and Gibbons, 1963), and carbon dioxide (Barrer and Gibbons 1965) in sieve X by summing the theoretical energy contri-

butions due to dispersion, repulsion and for ammonia and carbon dioxide, electrostatic interactions between individual sorbed molecules and the atoms of the lattice. The values of inclusion energies obtained were in reasonable accord with experimental values, and showed the variation of sorption potential within the cavities.

In the region where partial pressures in the vapour phase are approaching unity, many inclusion isotherms are nearly horizontal. Limiting extents of sorption obtained from these curves are very similar for many vapours when expressed as volumes of sorbate at the appropriate liquid density. This observation suggests that saturation corresponds to complete filling of the accessible cavities in the sorbent and supports the idea that in the more open structures the isotherm might be described in terms of an equation of state. Barrer and Rees (1959) have shown that a modified form of the van der Waals' equation (Hirschfelder et al, 1958) successfully describes the occlusion of argon and nitrogen in several ion-exchanged forms of sieve X.

The analysis of the changes in free energy, ΔG, in enthalpy, ΔH, and in entropy ΔS accompanying sorption computed from experimental data has thrown considerable light on the state of the sorbed molecules. In particular, calculation of the entropy of sorption has enabled comparison with the sorption entropies associated with the limiting isotherm equations applicable to sorption in zeolites (section 1.4) to be made, and hence a tentative selection of a model of the sorbed state has been possible. Interpretations based on this method include the work of Barrer and Sutherland (1956), Garden and Kington (1956), and Barrer and Reucroft (1960).

Although sorption by zeolites has been studied extensively and results of considerable importance have been obtained, little attention has been paid to the uptake of the less volatile elements sulphur, phosphorus and mercury. The interest attaching to the study of the sorption of these elements has already been indicated (Section 1.1). In 1910, Grandjean reported that chabazite can take up considerable quantities of mercury, sulphur, iodine and bromine. The inbibition of sulphur was stated to be slow. The sorption of iodine and bromine by gmelinite was also reported. Wyart (1933) stated that chabazite could sorb as much as 60% by weight of mercury.

Barrer and Woodhead (1948) showed that the extent of sorption of mercury by chabazite was very small when carried out under high vacuum conditions. It was further shown that the large mercury uptakes previously reported were only obtained in the presence of oxygen. An extensive study of the sorption of iodine by chabazite, sieve X and sieve A has been reported by Barrer and Wasilewski (1961). The element is occluded rapidly and copiously in the temperature range 120-300°C. The isotherms were fully reversible and corresponded to type I of Brunauer's classification. Initially high heats of sorption decreased rapidly to a minimum as the amount of iodine sorbed increased, then rose slowly as iodine-iodine interactions became important. The results of this study are very significant in view of the similarities between iodine and the elements studied in the present work.

2. EXPERIMENTAL METHODS

2.1 Introduction

The study of sorption equilibria involving the vapour of sulphur, phosphorus or mercury presents a number of practical problems. These elements are not readily volatile. The lower limit for isotherm measurements, set by the temperature at which 1 cm of vapour pressure is attainable, are 245°C, 185°C and 130°C for S, Hg and P respectively. These temperatures, and for S and P the reactivity of the sorbates prevent the measurement of pressure with a simple mercury manometer and the use of tap grease in the apparatus.

These limitations were overcome by Barrer and Wasilewski (1960) who designed a sealed gravimetric apparatus to study zeolite-iodine isotherms. This apparatus (Sorption System A) was used with a few modifications for NaX-Hg isotherms and zeolite-sulphur and zeolite-phosphorus isotherms.

The maintenance of a uniform temperature in a considerable volume also presented difficulties at these temperatures. No fluid stable for long periods at 320°C and suitable for a constant temperature bath was available, and so electrically heated tubular furnaces were used. Errors arising from temperature gradients in the furnaces were reduced by calibrating all measuring devices under conditions as similar as possible to those encountered during isotherm measurements. To assist thermal stability, the furnaces were of large heat capacity and consequently required at least 12 hours to re-establish thermal equilibrium after a significant change in settings.

Sorption system B was required to study mercury isotherms only. It was designed to be sufficiently flexible to allow successive equilibria at several different pressures to be attained in one day. To this end the gravimetric system was reduced in size and a furnace of low heat capacity was employed. The resulting loss in precision was tolerated since the mercury uptakes were large and consequently percentage errors were small.

Information concerning structural changes in the inclusion complexes was obtained with the aid of X-ray cameras. Photographs were taken of starting materials, of sorbents at various stages during sorption cycles, and finally of the sorbents after a series of experiments had been completed.

2.2 Sorbents

The synthetic Sieves X and A were obtained from Linde Air Products Ltd. as fine powders. Examination under the microscope showed that they were uniformly crystalline, suggesting that little gel was present. Sieve X was used for sorption studies in the sodium form as supplied, after washing with distilled water. Prolonged washing was avoided to minimise hydrolysis of the zeolite.

Two samples of Sieve A were used. One sample of the sodium form, from the same batch as that used by Barrer and Walker (1964), was ion-exchanged to the silver form as described later in this section. The second sample had been ion exchanged to the calcium form (5A) and analysed by Barrer and Meier (1958). This sample was used for sorption studies without further treatment.

Basic sodalite, synthesised in these laboratories (batch S23) was kindly supplied by Dr. R. M. Carr. This sorbent, stated to be at least 95% pure was seen to be uniformly crystalline under the microscope and was not further treated before silver ion exchange.

Chabazite was obtained in rock form from Nova Scotia. Large crystals were selected, washed several times with hot water, crushed between mild steel plates and ground in an agate mortar. Only material passing a 200-mesh sieve was used in sorption studies.

Gmelinite from Antrim was kindly supplied in rock form by Dr. G. P. L. Walker. Crystals free from impurity were hand picked from the rock, and washed with distilled water. The material was crushed between mild steel plates and ground in an agate mortar before being graded through a 200-mesh sieve.

Silver forms of each of the sorbents were prepared by ion exchange using silver nitrate solutions. The powdered sorbent was stirred into a strong solution of $AgNO_3$ at room temperature and allowed to settle. The liquid was then decanted off, fresh solution was added and the mixture again thoroughly stirred. The sorbent was then filtered off. Ion exchange was continued by percolating a strong solution of $AgNO_3$ through the sorbent standing on the filter. The product was washed with distilled water and dried by suction.

A mercuric form of Sieve X cannot be prepared by ion exchange with mercuric nitrate solution owing to the precipitation of red HgO by the buffering action of the sieve on the solution. Ion exchange can be effected in the absence of water. NaX was outgassed at 350°C and

exposed to mercuric chloride vapour at 300°C for 12 hours. After washing with water to remove the soluble chlorides the product was still white. X-ray photographs demonstrated that ion-exchange had taken place.

The lead form of sieve X was prepared by ion exchanging NaX with lead nitrate solution. NaX was stirred into a strong solution of lead nitrate heated on a boiling water bath. After standing on the bath overnight the liquid was decanted off and replaced by fresh hot solution. The mixture was stirred for 12 hours, and then the sorbent was filtered off. Ion exchange was continued by percolating a hot strong solution of lead nitrate through the sorbent on a filter heated by a steam jacket. The product was washed with hot water, sucked dry, and stored in a dessicator.

Attempts were made to prepare a palladium form of sieve X. The low solubility of salts containing palladous ions prevents these salt solutions being used to effect exchange. Complex palladium ammonium salts are more soluble, and ion exchange of NaX with palladous ammonium chloride solution was effected by a method similar to that used to prepare AgX. The replacement of Na^+ ions was demonstrated by X-ray powder photography. However, when the product was heated under evacuation to drive off ammonia, the crystalline structure of the sieve was destroyed.

2.3. Sorbates

The mercury supplied by Johnson Matthey Ltd. was stated to contain less than 1 part per million of other metals. It was freed from volatile contaminants by boiling under vacuum, and then distilled into the reservoir of the sorption system under high vacuum.

The main impurity in sulphur from Hopkin and Williams Ltd. was stated to be iron. The sulphur was freed from volatile impurities by repeated melting under vacuum until a constant low pressure was obtained above the molten sulphur. The sulphur was then distilled into a sorption reservoir cooled in ice.

Phosphorus was obtained from Hopkin and Williams Ltd. in the red amorphous form. Volatile impurities were removed by heating the material with continuous pumping. Colourless phosphorus condensed in the cooler parts of the apparatus and was distilled into a reservoir maintained at 0°C. Care was taken to prevent the pumping line becoming blocked when the phosphorus condensing in it solidified.

2.4. Sorption System A

Sorption system A (figure 2.1) was a totally enclosed glass balance case containing a silica spring balance, a spiral pressure gauge and a thermocouple. The system was surrounded by electric furnaces.

The sorbent, in a pyrex bucket weighing ca. 0.2 g was suspended on a gravimetric spring supported by a hook sealed into the top of the case. A long hollow finger projected into the case and ran parallel to the spring, allowing a thermocouple to be moved so as to be always close to the sample.

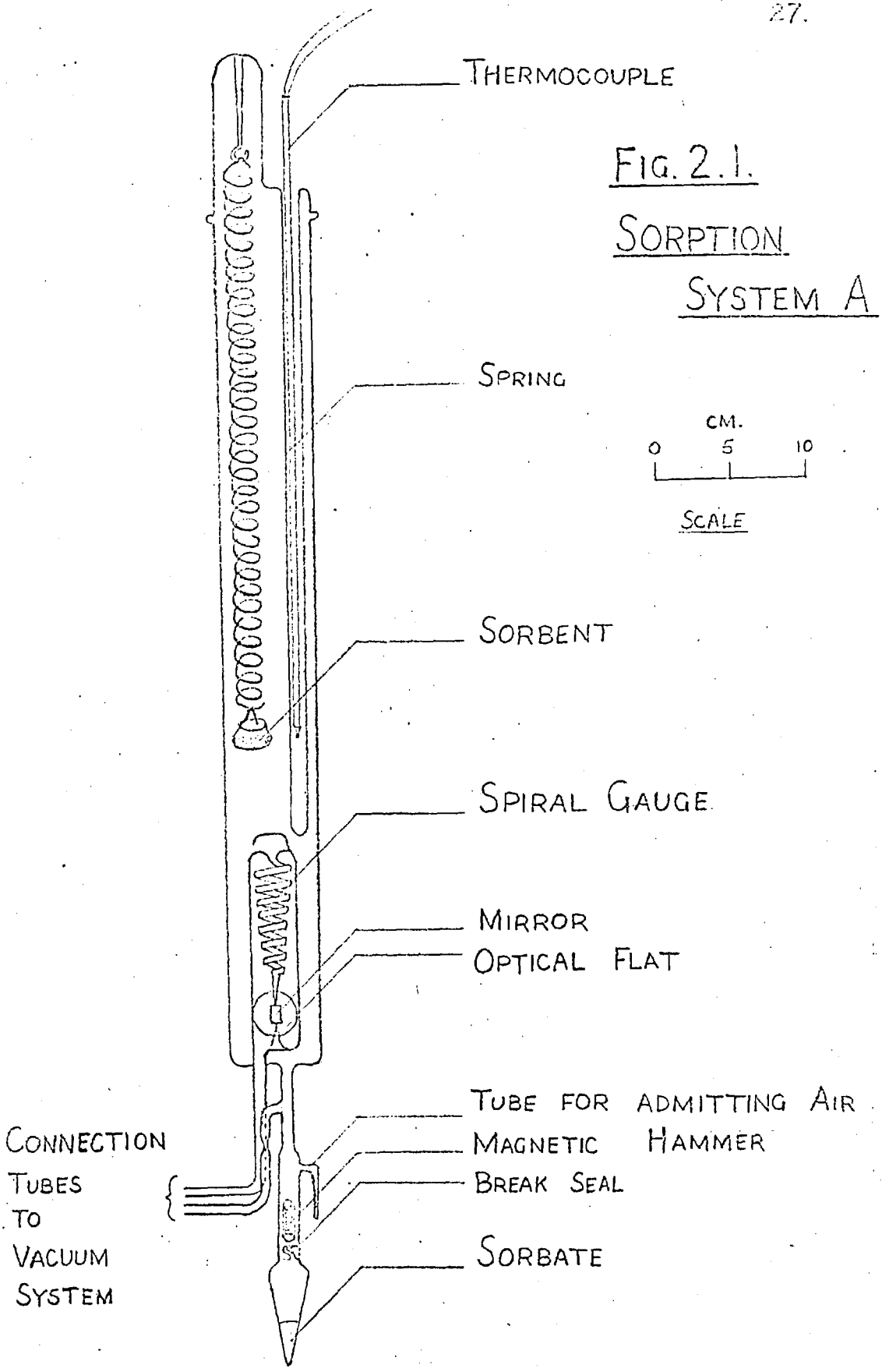

FIG. 2.1.

SORPTION SYSTEM A

A pyrex spiral gauge was sealed into the case below the sorbent so that the inside of the spiral had direct contact with the vapour inside the case. The outside surface of the gauge was in contact with nitrogen whose pressure could be regulated and measured from outside the system through a connecting tube. Movements of the spiral gauge were registered by a beam of light reflected through an optically flat glass window on to a scale by a mirror attached to the apex of the spiral. By recording scale readings for different nitrogen pressures when the pressure inside the balance case was zero, a calibration chart was drawn up. This allowed any pressure inside the case to be computed from the measured nitrogen pressure and the pressure difference across the gauge as recorded on the scale.

This procedure for pressure measurement was preferred to that of adjusting the nitrogen pressure to restore the scale reading corresponding to zero pressure difference across the gauge. Experience showed that at isotherm temperatures, pressure differences across the spiral gauge which will exist when the sorbate pressure is being changed whatever procedure for pressure measurement is adopted, had no effect on pressure readings. At the higher temperatures used for outgassing, however, pressure differences across the gauge caused a deformation which was slow to recover. This gave rise to a slow drift in the indicated pressure when the true pressure was constant. By outgassing with both sides of the pressure gauge evacuated this effect was avoided.

The balance case was evacuated and the sorbent outgassed through a second side arm. This was made with a constriction close to the balance case where it could be

sealed off when the sample was outgassed, thus completing the isolation of the sorption system. An additional side arm was used for the careful admission of air when a series of experiments had been completed. This consisted of a short tube with a narrow end which could be broken after covering with a rubber tube closed by a screw clip.

For temperature measurement a chromel-alumel thermocouple was preferred to a platinum resistance thermometer because of the considerable temperature gradients in the balance case. Temperature differences as great as 5 C deg. between the highest and lowest position of the sample were recorded. In addition the temperature distribution altered as the temperature of the lower furnace changed. A movable thermocouple, always adjacent to the sample was considered to record the sample temperature more reliably than a fixed resistance thermometer several inches long.

A sorbate reservoir, charged with pure sorbate under vacuum, was attached to the bottom of the balance case. Fracture of a break-seal with a magnetic hammer allowed sorbate vapour to enter the balance case and make contact with the sorbent when required.

Three furnaces were used to maintain the temperatures required (Figure 2.2). The main furnace heated the upper chamber of the balance case while the bottom furnace heated the sorbate reservoir. Both of these furnaces were tubular and were mounted on vertical steel rails to preserve their alignment while allowing easy movement when access to the balance case was required. The main furnace was fitted with five windows to allow measurements of spring length and observations of the mirror attached to the spiral gauge.

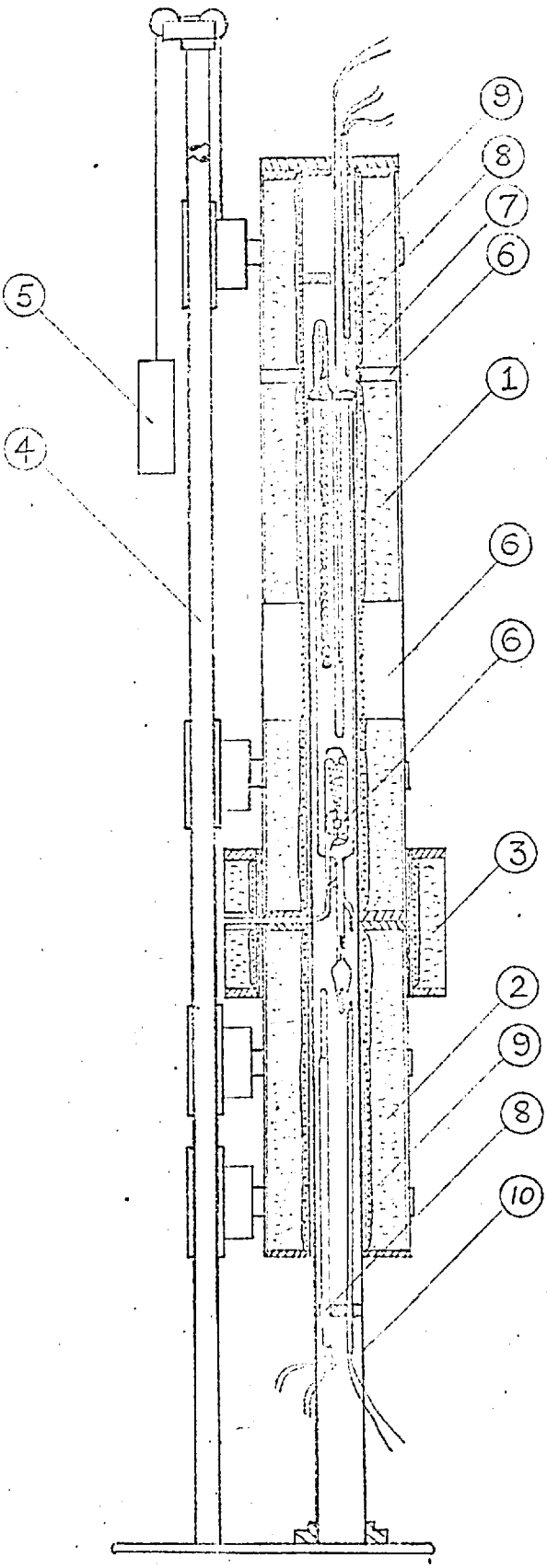

FIG 2.2

THE FURNACE SYSTEM

CM.
0 10 20
SCALE

KEY TO Fig. 2.2

1. Main furnace
2. Lower furnace
3. Junction furnace
4. Steel rails 11ft. high
5. Counterweight
6. Furnace windows
7. Asbestos wool
8. Platinum resistance thermometers for temperature control
9. Thermocouples
10. Steel tube supporting balance case

The third furnace was in the form of two semi-circular segments fitting round the junction of the tubular furnaces. The hole left by slots cut in the two sections of this furnace allowed the tubes connecting the balance case to the vacuum system to pass through.

Each of the tubular furnaces had two insulated heater windings on its steel core. The outer winding in each case supplied most of the heat, while the inner winding of higher resistance allowed the sensitive control of heat input. The furnace cores were mounted in wide asbestos tubes. The free space between tubes and cores was packed with asbestos wool, except for the windows which were unobscured. The two parts of the junction furnace had only a single winding, but were insulated in a similar way.

Power was supplied to the furnace system via a constant voltage regulator and 2KW variacs. The variacs supplied the main windings directly, but the two auxiliary windings were each fed via an electronic controller. The electronic controller was effectively a switch operated by the temperature level in the furnace. A platinum resistance thermometer placed in each tubular furnace was made one arm of a Wheatstone bridge circuit. The other three arms were the compensating leads of the thermometer, a fixed resistance, and a decade box. The out-of-balance current from the bridge was amplified in the controller and used to operate a switch. When the thermometer resistance exceeded the resistance of the decade box, the switch opened. Current which previously flowed directly to the auxiliary winding of the furnace through the closed switch now flowed through a resistance connected across the switch, and the power input to the furnace was reduced.

The furnace then cooled until the control system operated in the opposite sense. In this way the furnace temperature was held constant at a level determined by the resistance of the decade box.

The balance case was concentric with the furnace system, being supported by a stainless steel tube mounted on a cast iron base. Slots in the tube at appropriate positions allowed access to the balance case for observations and adjustments. The space between the balance case and the furnaces was packed with asbestos wool, care being taken to avoid obscuring the windows.

Calibration of the gravimetric spring was carried out inside the furnace system. A balance case was constructed with the same external dimensions as the sorption balance, but without the pressure measuring spiral or the sorbate reservoir (Figure 2.3). Glass weights were made in the form of a chain which was hung on the spring. A small platform on a long vertical rod was raised in the balance case so as to support the lowest link in the chain of weights and reduce the load on the spring. Progressively raising the platform reduced the spring load by a link at a time. In this way the load on the spring could be varied easily.

The spring length was measured for each load with the main furnace at several temperatures. In addition the effect on the spring length of changing the temperature of the small furnace was studied, while maintaining the temperature of the main furnace.

This information was required in order to allow for the effect on the spring length of interaction between the two tubular furnaces. Heat flow between furnaces

FIG. 2.3.

SPRING CALIBRATION SYSTEM

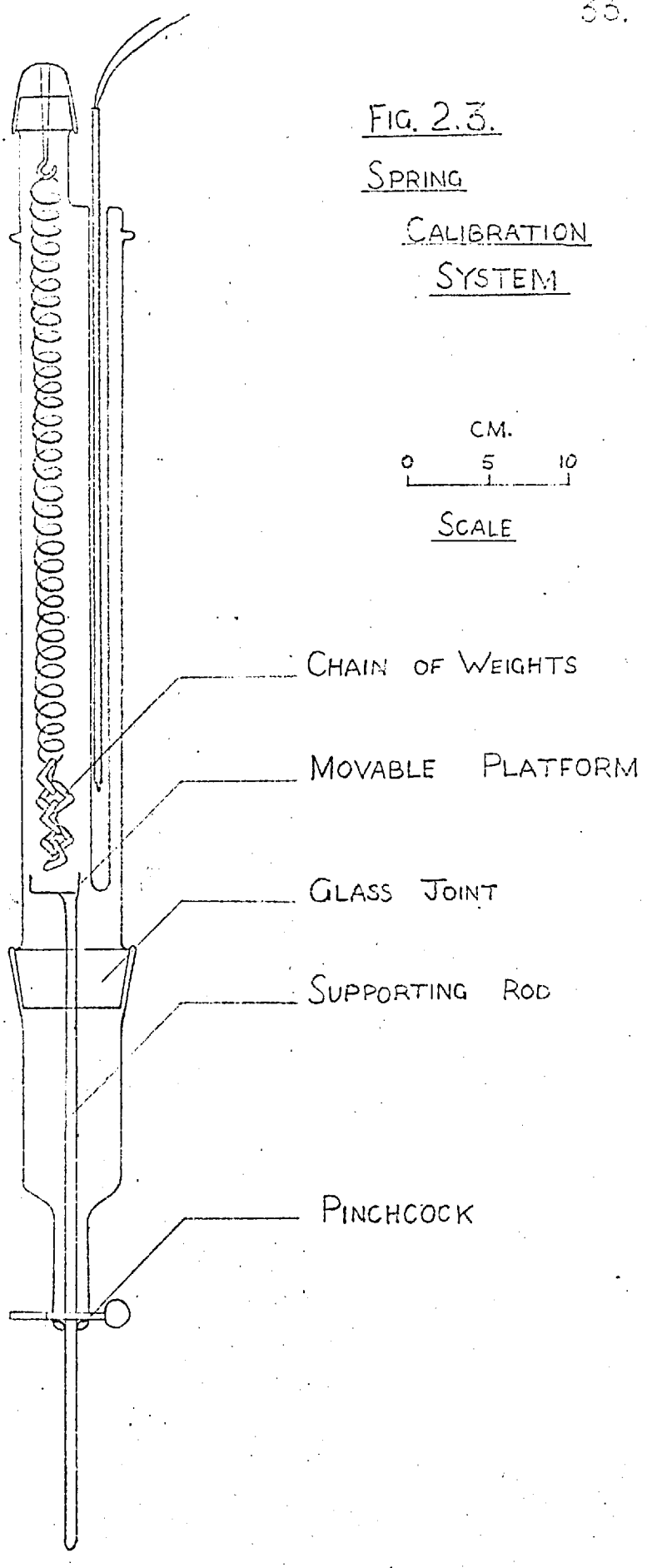

was found to have a significant effect on temperature distributions. When the temperature of the lower furnace was raised more heat flowed to the lower end of the main furnace, tending to raise the sample temperature, but affecting the top end of the spring to a lesser extent. To preserve a constant sample temperature, less power was supplied to the main furnace. The top end of the spring then cooled, resulting in an increase in spring length.

At the low pressure end of isotherms with modest uptakes, this "Furnace Effect" supplied the major part of the spring extension and hence an accurate knowledge of its magnitude was essential. Attempts to reduce the effect by keeping the junction furnace at a steady temperature higher than the maximum temperature reached by the lower furnace encountered difficulties arising from heat flow between the junction furnace and the lower furnace. Even with no power input to the lower furnace, sufficient heat flowed from the junction furnace to prevent the lower sorbate pressures from being attained.

The resistance thermometer which controlled the main furnace temperature was placed inside the furnace level with the top end of the spring, thus supplying temperature data at this point. The alterations to the decade box resistance necessary to maintain a constant sample temperature were determined by trial during a run.

2.5. Sorption System B

The apparatus designed to study mercury isotherms with large weight changes was simpler than sorption system A (Figure 2.4). The balance case containing the gravimetric spring was evacuated through a U-tube at its lower

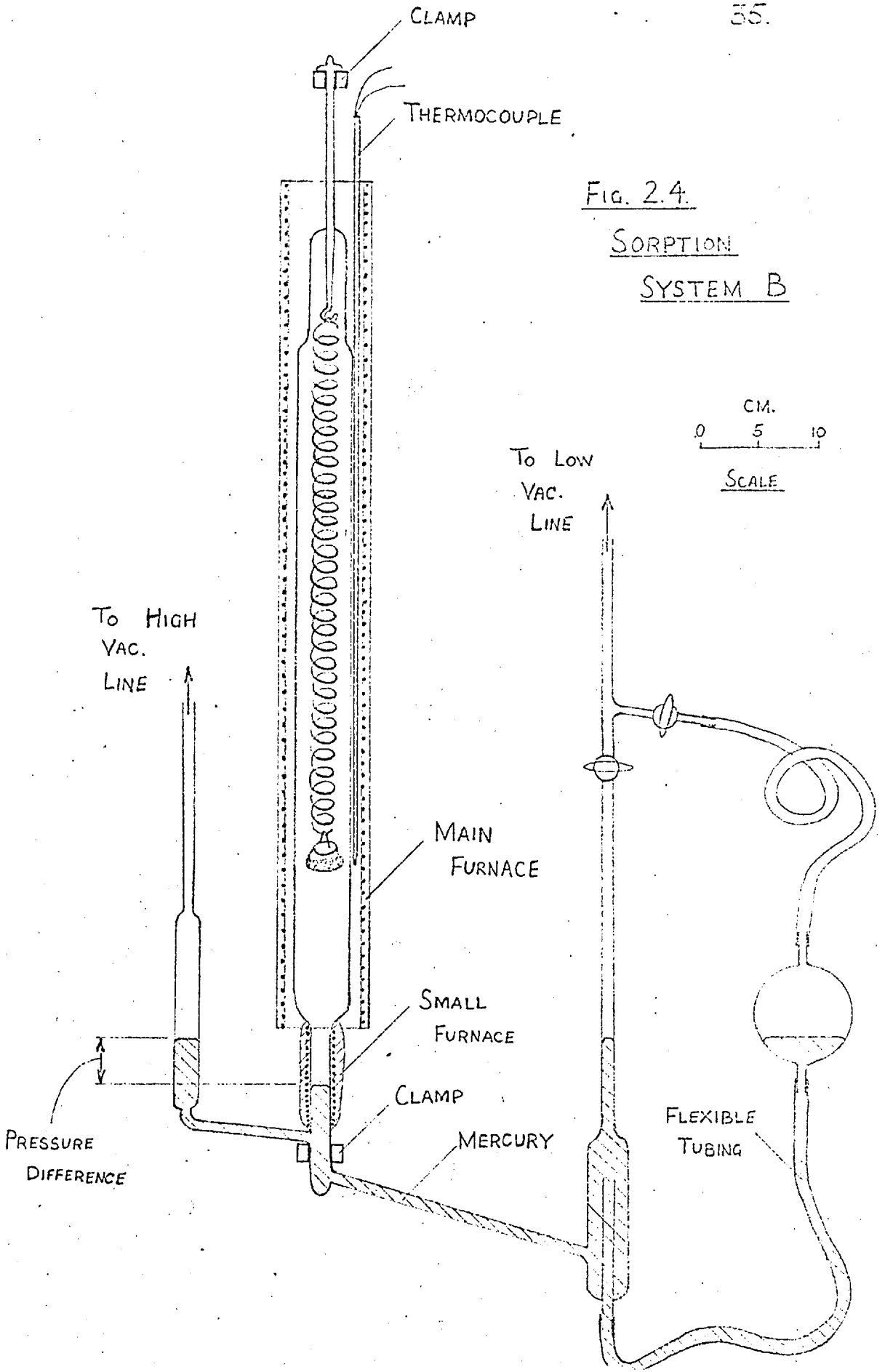

FIG. 2.4.

SORPTION SYSTEM B

end. A vertical tube sealed into the U-tube from below allowed mercury to be run in by raising a mercury reservoir connected to it by flexible tubing. The mercury in the U-tube then sealed the balance case from the pumping line and allowed pressure differences between the balance case and the vacuum line to be measured. This arrangement also allowed the admission of gases and vapours to the balance case when required.

A small furnace, wound directly on to the arm of the U-tube nearest to the balance case heated the mercury to create the vapour pressures required for the experiments. The mercury level in the hot limb of the U-tube was observed through narrow vertical windows cut in the insulation of the furnace.

Expansion of mercury in the hot limb produced an initial indication of negative pressure in the balance case. As the mercury temperature was raised heat conducted through the mercury reduced the difference in density between the two limbs. The true mercury pressure in cms of mercury at 0°C was calculated from the furnace temperature and the observations of mercury levels using the coefficient of expansion of mercury and vapour pressure-temperature curves.

A trap inserted in the mercury line between the U-tube and the reservoir prevented air which penetrated the flexible tubing from entering the balance case.

A small bulb in the mercury line immediately below the balance case retained a small quantity of mercury when the mercury was run out of the U-tube. By placing a liquid air bath round this bulb the mercury pressure in the balance case could be made negligible when required.

The tubular furnace used to maintain the sample temperature was only slightly larger in diameter than the balance case. Sufficient room was left between them to insert a thermocouple which could be moved vertically so as to be always close to the sample. Vertical windows cut in the furnace insulation allowed observation of the spring ends.

The power input to both furnaces was manually controlled. A constant voltage regulator supplied power to two 2KW variacs each connected directly to a furnace. The size and thermal insulation of both furnaces was kept low to reduce their thermal capacity and provide rapid response to changes of power input.

2.6. The Vacuum System

The vacuum system is shown diagrammatically in Figure 2.5.

An Edwards "Speedivac" rotary oil pump (R) backed a single stage mercury diffusion pump (D) to produce vacua of about 10^{-6} cm Hg. An oil trap at (T) prevented oil from entering the diffusion pump in the event of power failure. A buffer volume (V) allowed the diffusion pump to run for long periods without the backing of the oil pump, so that pressure measuring devices could be operated by the oil pump without disturbing the high vacuum. A cold trap (C) which prevented mercury vapour from the diffusion pump entering the high vacuum line also facilitated the removal of condensible vapours from the system.

Low pressures were measured by the McLeod gauge (G). The continuous-reading Pirani gauge (P) was used to

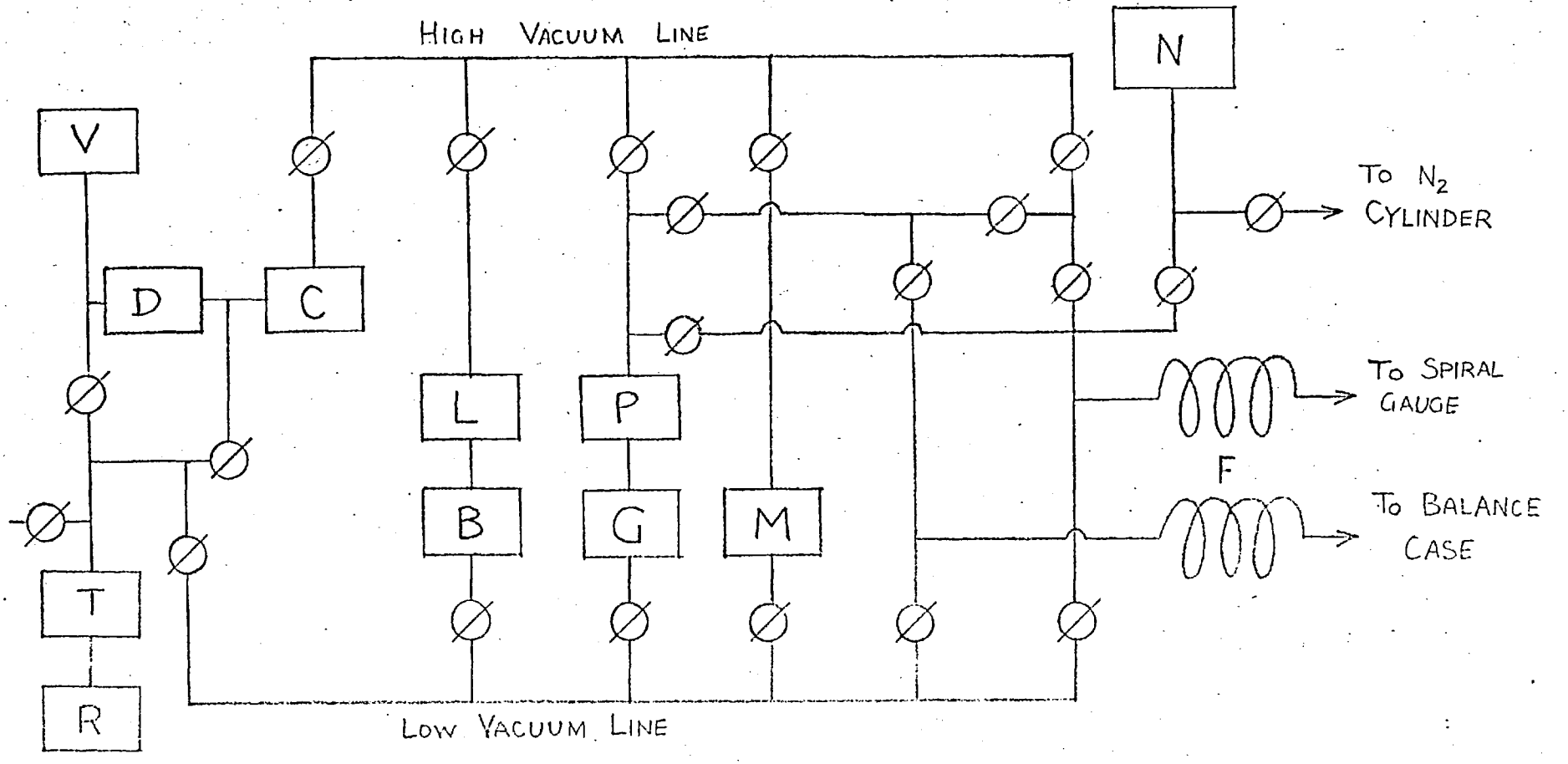

FIG 2.5. THE VACUUM SYSTEM

determine the completion of outgassing and to aid leak detection.

The pressure of the pure dry nitrogen supplied from the storage bulb (N) was measured by the manometer (M). Flexible glass spirals (F) connected the nitrogen line and the pumping line to sorption system A. Flexible connections were necessary to allow movement of the balance case due to the expansion of its steel supporting tube when the furnace temperature was raised.

Sorption system B was placed at (B) and connected to the high vacuum line via the liquid air trap (L).

2.7. The Accuracy of Sorption Measurements

Gravimetric sorption studies require the measurement of three variables: weight, temperature, and pressure. In this study the dependent variable, weight, was determined with the greatest accuracy.

The measurement of spring length by cathetometer is capable of high precision. The height of both ends of the spring was read to .001 cm and hence the error in spring length was ±.002 cm, which corresponds to ±.03 mg.

The total weight of the bucket and the outgassed sorbent was calculated from the length of the spring at room temperature. The weight of the bucket and of the glass links used for spring calibration was determined on a balance weighing to 0.1 mg and hence the sample weight is accurate to ±0.2 mg, which corresponds to ±.05% of a 0.4 g sample.

Uncertainty in the sample weight was important only when weight changes were large. When the weight

changes were small, as in the case of NaX-Hg isotherms for which the greatest spring extension was 0.27 cm, the measurement of spring length to ±.002 cm introduced an uncertainty of ±0.7% in the weight change. The uncertainty was proportionally higher for smaller spring extensions.

Where spring extensions were small, an additional uncertainty arose from the "Furnace Effect" (see Section 2.4). The magnitude of this effect was determined by changes in the spring length, thus adding a further uncertainty of ±.002 cm to the extension measurements. The total uncertainty for the largest weight change in the NaX-Hg isotherms is therefore 1.4%. At lower pressures the uncertainty increases and at the lowest pressure (0.13 cm of Hg) for which the spring extension was .040 cm, the weight changes are subject to an uncertainty as high as 10%.

All temperatures were measured with chromel-alumel thermocouples, calibrated by comparison with a platinum resistance thermometer in a well-stirred oil bath. The resistance thermometer had been standardised at the National Physical Laboratory. Thermocouple calibration by this method is stated to be accurate to 0.2 C deg. (Roeser and Wensel, 1941). No changes were detected in the calibration of thermocouples used for three years at the modest temperatures of these experiments.

The reliability of sorbent temperatures measured by a device not actually embedded in the sample is difficult to estimate. In all cases thermocouples were moved so as to be at the same height as the sample when measurements were taken. In Sorption System A the thermocouple

and the sample were close together in the centre of the furnace as far from the furnace windows as possible. The thermocouple reading probably corresponds to the sample temperature to within 0.5 C deg. Temperature differences between isotherms are probably accurate to 0.2 C deg. The thermocouple in Sorption System B was outside the sorption balance, being inserted between the furnace and the balance case. The estimated temperature difference between sample and thermocouple was 1 C deg.

Different methods were adopted for the measurement of vapour pressures in the two sorption systems. In Sorption System A the nitrogen pressure was measured in a manometer to ±.002 cm with the aid of a cathetometer. The sensitivity of the spiral pressure gauge was 1.5 cm on the scale for 1.0 mm pressure change. The scale was read to ±.02 cm which corresponded to ±.013 mm pressure. Calibration of the pressure measuring device was based on a set of pressure readings subject to the same uncertainty, giving a total uncertainty of ±.026 mm.

The thermostatting system was found to hold each temperature constant to within 0.2 C deg. This introduced a significant fluctuation in the pressure of the more volatile sorbates at their highest pressures. A change of 0.2 C deg in the reservoir temperature produced a pressure change of .04 cm in 6.0 cm of phosphorus vapour.

At the low pressure end of isotherms, pressures were estimated from reservoir temperatures with the aid of vapour pressure-temperature curves. When significant drifts in the pressure readings of the spiral gauge were encountered (see Section 2.4) all vapour pressures were estimated by this method.

Mercury pressures were measured directly in Sorption System B with the aid of cathetometers. The main errors probably arose in the corrections required to compensate for density changes in the heated mercury. It is estimated that the errors were less than 0.5% of the vapour pressure except at pressures below .05 cm where they may have risen to 1% of the recorded pressure. Pressure measurement below .03 cm was avoided.

2.8 X-ray Powder Photography

Two methods were used to obtain X-ray powder photographs. Starting materials and products which remain unchanged on exposure to the atmosphere were mounted under sellotape in the sample holder of a four-unit Guinier camera. Samples of inclusion complexes whose compositions depend on the atmosphere to which they are exposed were enclosed in capillary tubes and mounted in a 9 cm Debye-Scherrer camera. The inclusion complexes were prepared by sealing a capillary tube containing the sorbent on to a wider tube connected to a vacuum pump and heated by a tube furnace. Provision was made to expose the sorbent to any vapour by heating a reservoir containing the appropriate sorbate. Inclusion complexes of any available composition could be prepared with the aid of temperature-pressure data for the sorbate and the inclusion isotherm of the complex. It was not possible to maintain the complex at the temperature of its formation while exposing it to X-rays. Both X-ray cameras were used with filtered Cu K_α radiation. Diffraction patterns were recorded on Ilford film, and the positions of lines on the film were measured to 0.005 cm with a film measuring rule fitted with a vernier scale.

3. RESULTS AND DISCUSSION

3.1 Zeolite-Sulphur Inclusion Complexes

Sulphur vapour is sorbed rapidly and copiously by molecular sieves 5A and NaX, giving them a sandy colour. Two isotherms have been obtained for each sorbent. Sorbent temperatures were chosen to include the largest possible temperature interval. The upper temperature limit was set by the silica springs which show hysteresis effects after temperature cycles above 325°C. A lower temperature limit of 250°C was chosen. Below this temperature the saturated vapour pressure of sulphur is too small to allow a sufficient number of distinct points on the isotherm to be obtained. Diagrams 3.1.1 and 3.1.2 show the isotherms obtained for 5A and NaX respectively. The isotherms are remarkable for their rectangular character, despite the high temperature of the sorbents. The affinity between the crystals and sulphur is strong; nevertheless by further heating and evacuation the sulphur can be removed.

Comparison of X-ray powder photographs of the sorbents taken before sorption of sulphur and after its removal showed that no change had occurred in the structure of the sieves. An X-ray photograph of a sample of NaX containing sorbed sulphur showed only minor changes from the pattern observed with the sulphur-free sorbent, suggesting that the structure undergoes only slight perturbation when sulphur is sorbed. The apparent absence of a regular pattern which might be ascribed to the sulphur itself was of interest, but was in accord with the observations of Barrer and Wasilewski (1961) of the NaX-iodine

DIAGRAM 3.1.1

5A-SULPHUR ISOTHERMS

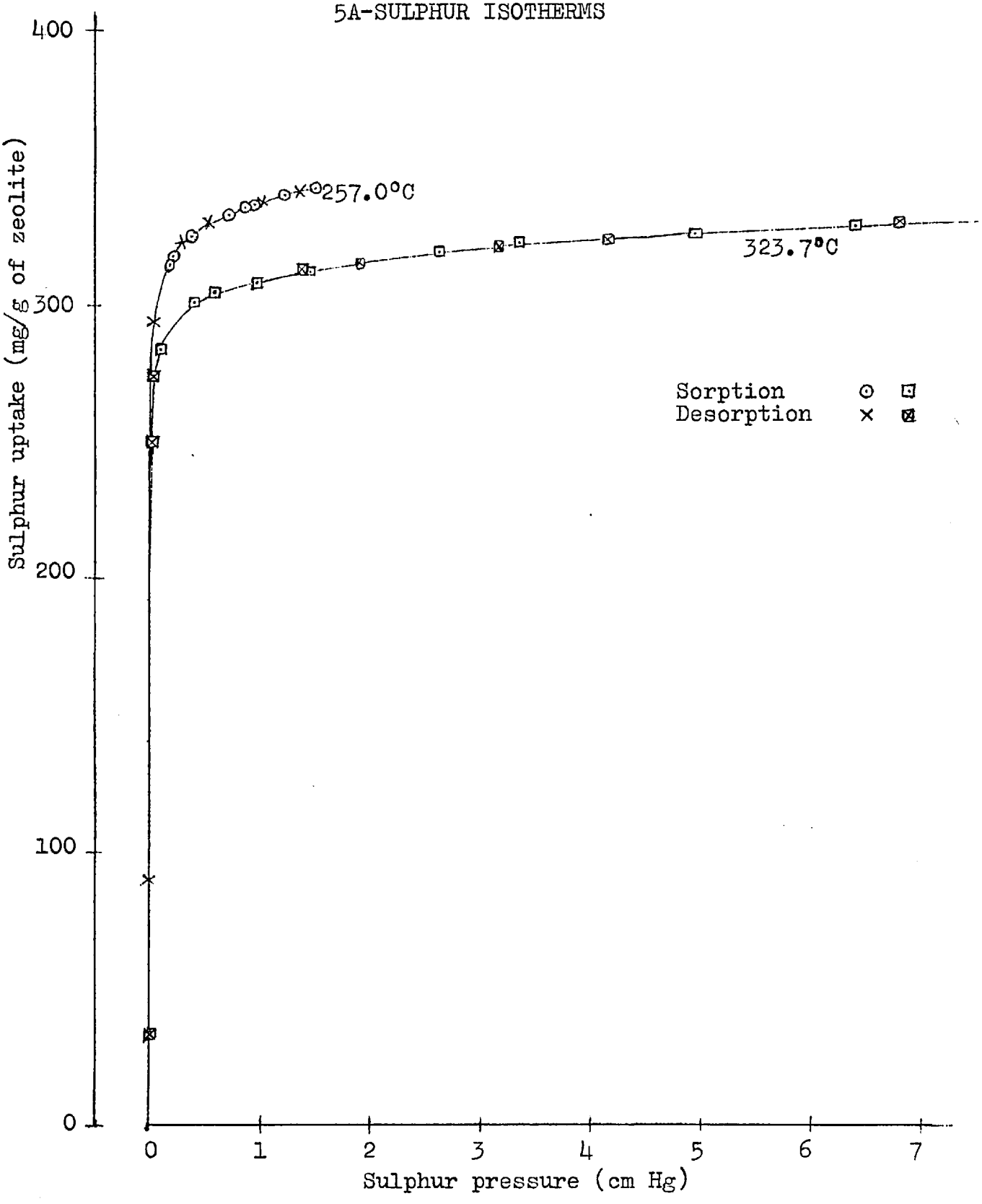

DIAGRAM 3.1.2

NaX-SULPHUR ISOTHERMS

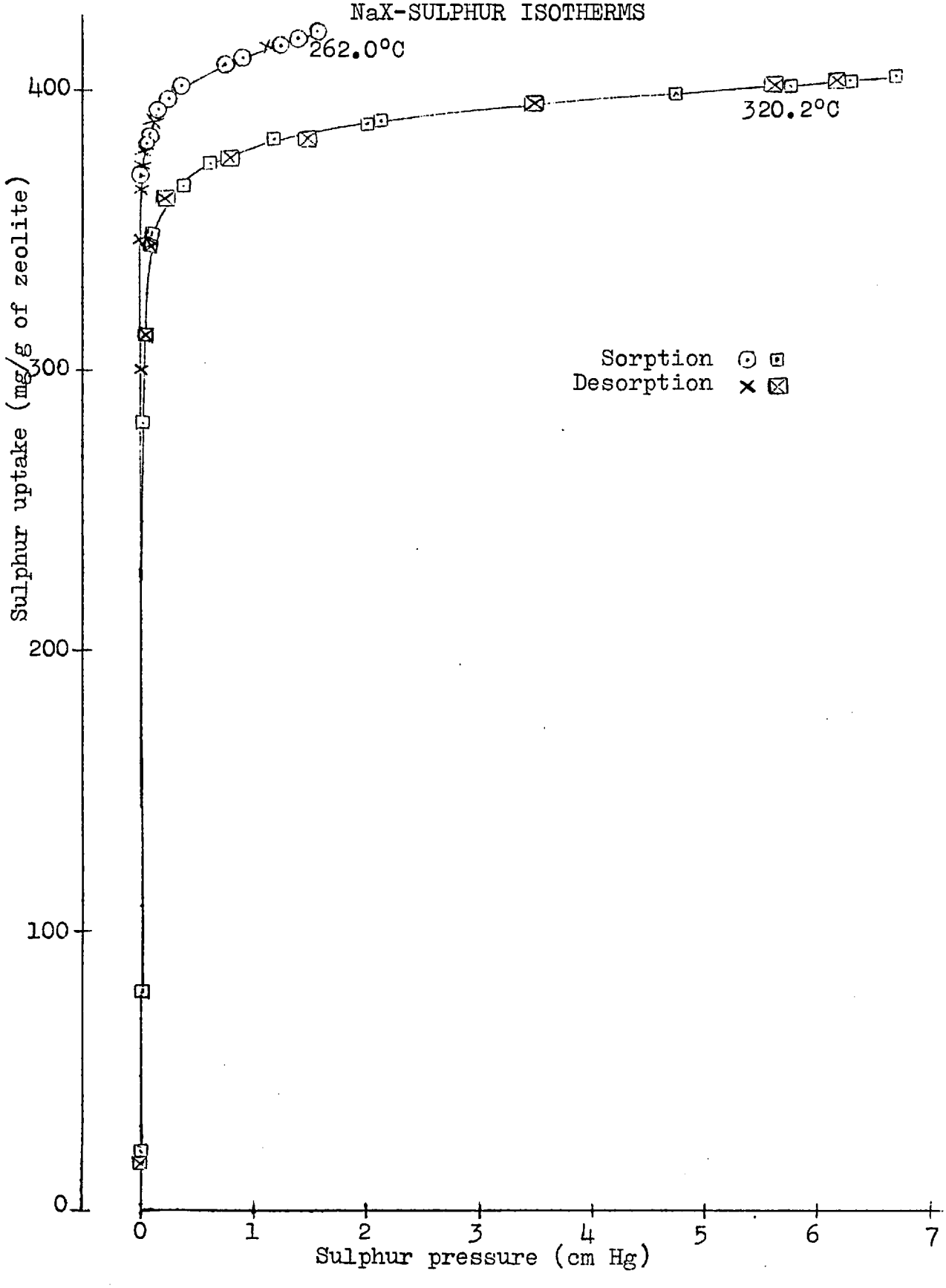

and NaX-bromine complexes.

The isosteric heat of inclusion, $\overline{\Delta H}$, is -30.2 kcal/mole for NaX and -24.5 kcal/mole for 5A, in each case determined near saturation of the crystals. The uncertainties in the published values of standard thermodynamic functions for sulphur vapour (see Section 1.3) prevent the calculation of the standard entropy of the sorbed sulphur. Precise treatment of the sorption data is therefore impossible. An indication of the molecular complexity of sorbed sulphur is provided by comparison of the weight of sulphur sorbed by each zeolite with the free volume of the zeolite. Table 3.1 records the weight of sulphur taken up by 1 g of each anhydrous zeolite when saturated with the sorbate.

Table 3.1

Zeolite	Temp. °C	Sat. uptake mg/g Xtal.	Density of liquid sulphur g/cc	Volume uptake cc/g Xtal.	Supercage volume cc/g Xtal.	Fractional filling
5A	323.7	331.7	1.681	0.197	0.25	0.79
	257.0	342.5	1.721	0.199	0.25	0.80
NaX	320.2	405.0	1.684	0.240	0.32	0.75
	262.0	421.7	1.718	0.246	0.32	0.77

Also shown is the volume of liquid sulphur equivalent to each uptake at the isotherm temperature and the free volume available in the supercages of each sorbent. The final column in table 3.1 shows the ratio between the two previous columns, indicating the fraction of the total available volume actually occupied by sulphur atoms,

assuming the molecular volume to be that of liquid sulphur. The amount by which the fractional filling falls below unity may be an indication of the complexity of the sulphur molecules in the sorbed state and hence the difficulty of accommodating them in a manner economical of space within the zeolite.

Natural chabazite was found to sorb sulphur vapour very slowly compared with the rates in 5A and NaX. A plot of the uptake against the square root of time at two temperatures (diagram 3.1.3) shows a linear relationship, suggesting that an activated diffusion is taking place. By regarding the particles of powdered zeolite as spherical, one may estimate an energy of activation for the process. The equation for diffusion into spheres can be expressed in the form (Crank 1956, and Adams and Hippisley 1922),

$$\frac{d(M_t-M_0)}{dt} = \frac{6(M_\infty-M_0)D}{a^2}\left\{-\tfrac{1}{2} + \sum_1^\infty \frac{\sqrt{\pi}}{x}\left[\tfrac{1}{2} + \exp - \frac{n^2\pi^2}{x^2}\right]\right\}$$

where $\frac{1}{x} = \frac{a}{\pi\sqrt{Dt}}$, D is the diffusion constant, a the radius of the crystals, and M_0, M_t and M_∞ are the weights taken up at times t=0, t=t and t=∞ respectively.

For small t, only the first term is important, and hence,

$$\frac{d(M_t-M_0)}{dt} = \frac{-3(M_\infty-M_0)D}{a^2} + \frac{3(M_\infty-M_0)D}{a^2}\frac{\sqrt{\pi}}{x} + \frac{6(M_\infty-M_0)}{a^2}\frac{D}{x}\exp - \frac{\pi^2}{x^2}$$

$$= \frac{-3(M_\infty-M_0)D}{a^2} + \frac{3(M_\infty-M_0)}{a}\sqrt{\frac{D}{\pi t}} + \frac{6(M_\infty-M_0)}{a\pi}\sqrt{\frac{D}{t}}\exp - \frac{a^2}{Dt} \quad .$$

DIAGRAM 3.1.3

THE SLOW UPTAKE OF SULPHUR BY NATURAL CHABAZITE

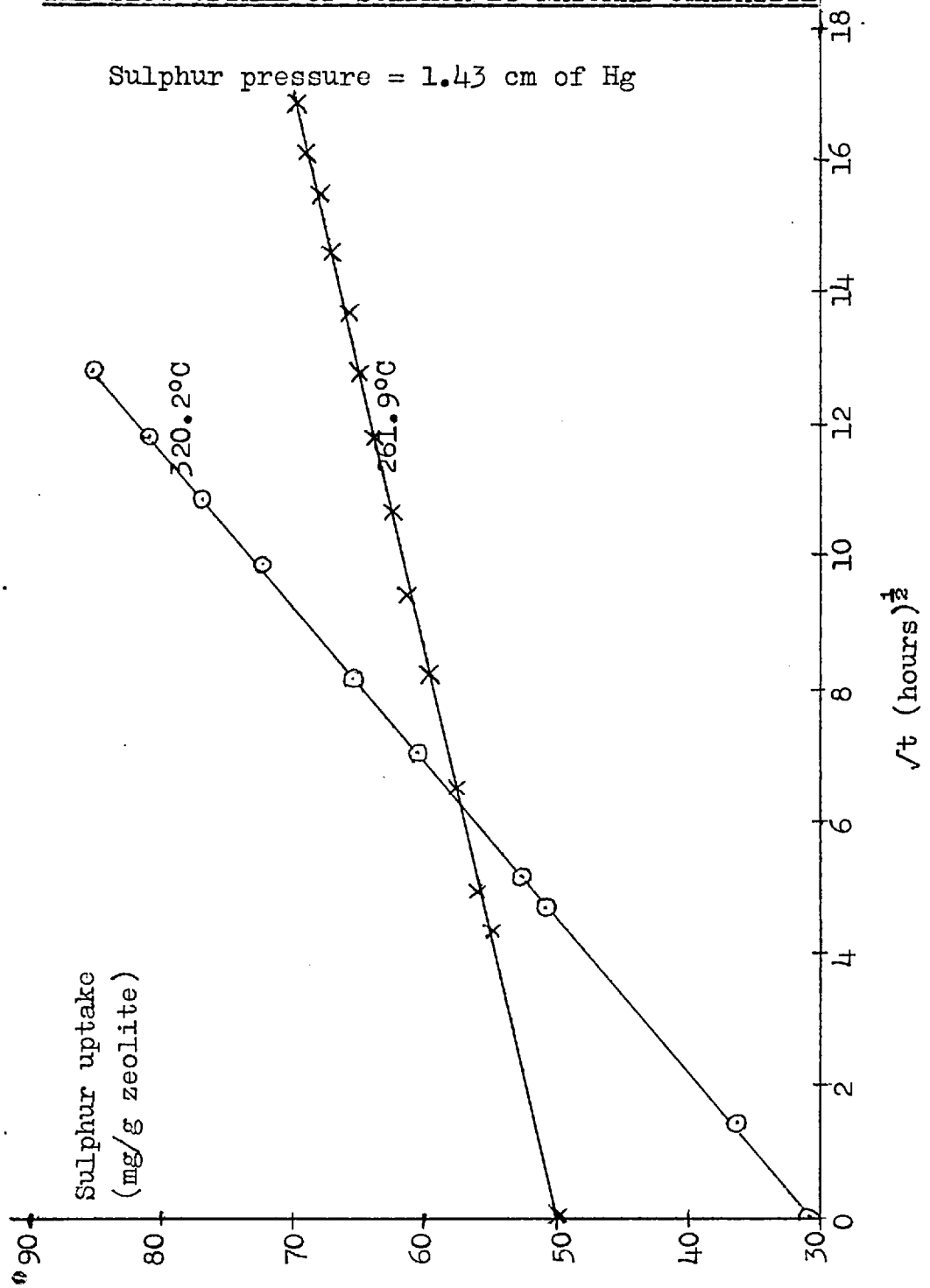

For very small t, the exponential term is negligible, and a plot of $\frac{d(M_t-M_0)}{dt}$ versus $\frac{1}{\sqrt{t}}$ should be linear with slope $\frac{3(M_\infty-M_0)}{a}\sqrt{\frac{D}{\pi}}$, and intercept $\frac{-3(M_\infty-M_0)D}{a^2}$. Hence, $\frac{\text{intercept}}{\text{slope}} = \frac{-\sqrt{D\pi}}{a}$. Diagrams 3.1.4 and 3.1.5 show the plots of these functions at 261.9°C and 320.2°C respectively. The slopes and intercepts of the two graphs are listed in table 3.2 together with the derived functions.

TABLE 3.2

Temp. °C	Slope of graph (mg. $hr^{-\frac{1}{2}}$)	Intercept mg.hr^{-1}	D/a^2 hr^{-1}	M_0 mg/g	$(M_\infty-M_0)$ mg/g
261.9	0.688	-.016	1.8×10^{-4}	50.0	29.8
320.2	2.50	-.075	2.8×10^{-4}	30.6	88.5

The negative intercepts in diagrams 3.1.4 and 3.1.5 are small due to the low values of D, and hence large errors are introduced into the derived functions. In particular, the values of $(M_\infty-M_0)$ obtained correspond to unrealistic values of M_∞. M_∞ can, however, be estimated independently from a knowledge of the free volume of the sorbent. Using the density of liquid sulphur appropriate to each experimental temperature, and assuming that only 75% filling of the cages is possible due to packing difficulties similar to those experienced when sulphur is sorbed by 5A and NaX, values of 370 mg/g and 360 mg/g are obtained for M_∞ at 261.9°C and 320.2°C

DIAGRAM 3.1.4

THE SLOW UPTAKE OF SULPHUR BY NATURAL CHABAZITE

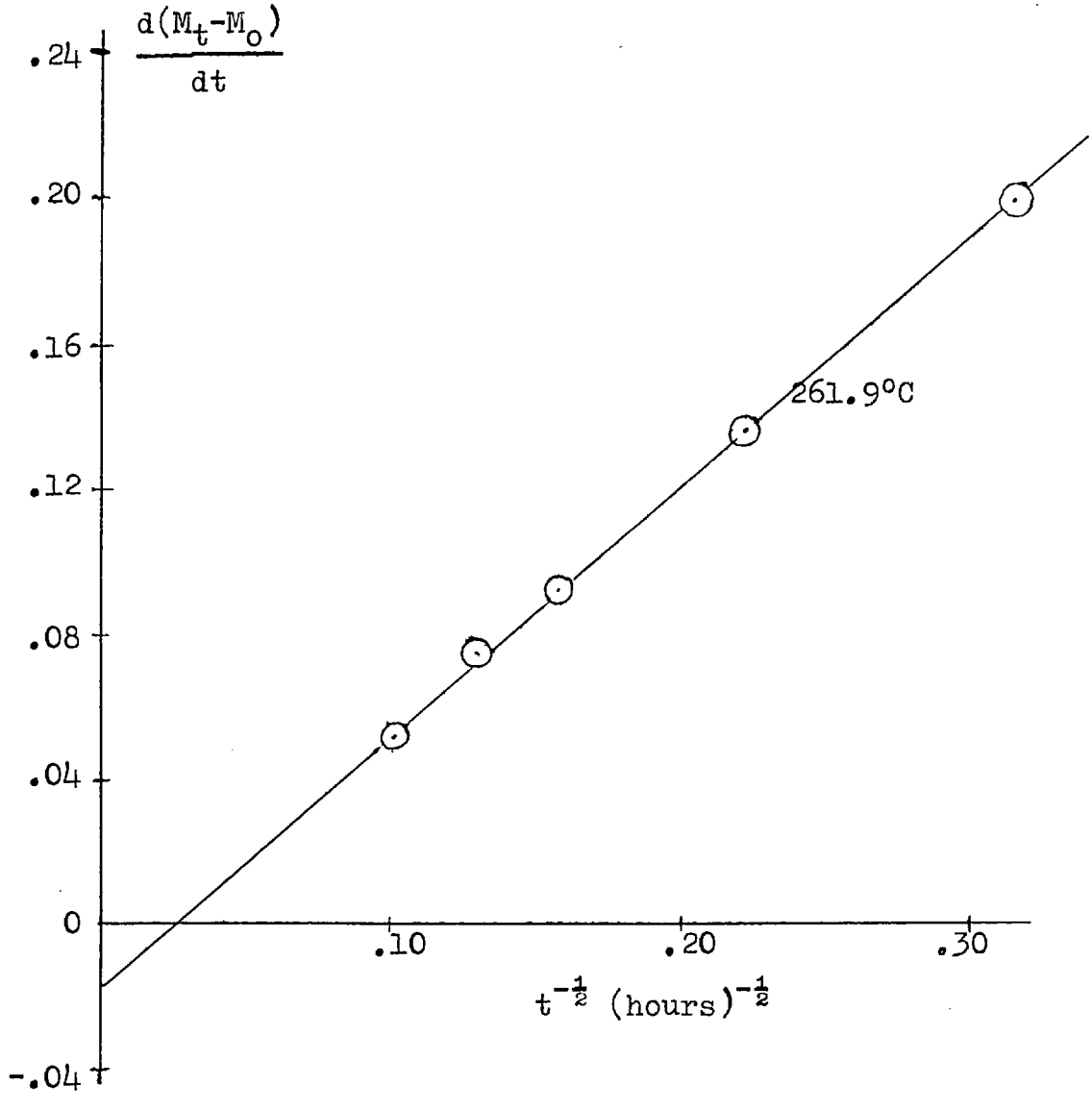

DIAGRAM 3.1.5

THE SLOW UPTAKE OF SULPHUR BY NATURAL CHABAZITE

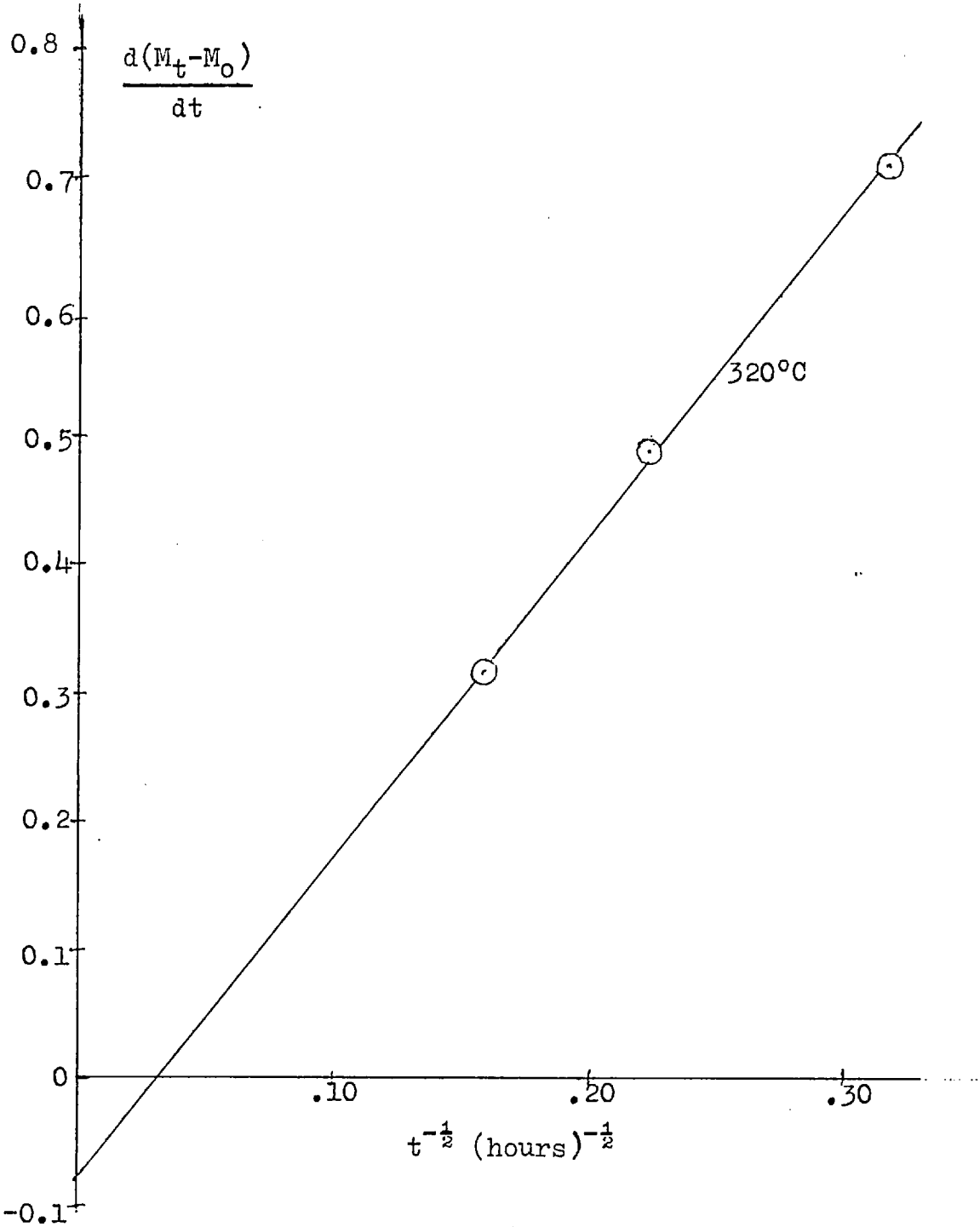

respectively. Using these values of M_∞ together with the slopes listed in table 3.2, an activation energy of 27.3 kcal $mole^{-1}$ for the slow process is obtained.

This activation energy gives a further indication of the molecular complexity of sorbed sulphur. The windows joining neighbouring cages in chabazite have a minimum free diameter of 3.7Å and would be expected to prevent the diffusion of the ring forms of sulphur. The S_2 molecule has a diameter of 3.7Å in directions perpendicular to the axis of the molecule and hence the entry of this species should not require an energy of activation as high as 27.3 kcals $mole^{-1}$. Liquid sulphur is known (Gee, 1952) to contain a large proportion of its molecules in the form of long chains. In these chains the sulphur atoms are not arranged in line, but are staggered about the centre line of the molecule, thus increasing its width. It is possible that the slow diffusion process observed in chabazite is determined by the rate of passage of chain molecules through the tortuous channels and narrow windows of this zeolite. An energy of activation of 27.3 kcal $mole^{-1}$ is not unreasonable for this process.

3.2 Zeolite-Phosphorus Inclusion Complexes

3.2.1 Sieve 5A-Phosphorus

Linde Sieve 5A occludes phosphorus very slowly at temperatures between 260°C and 325°C. Diagrams 3.2.1 and 3.2.2 show the slow uptakes observed when the crystals are exposed at 264.3°C to pressures of phosphorus vapour of 1.45 cm and 7.64 cm respectively. Diagrams 3.2.3 and 3.2.4 show the corresponding uptakes at 323.6°C with the same phosphorus vapour pressures. The rates of increase

SIEVE 5A – PHOSPHORUS AT 264·3°C

DIAGRAM 3.2.1.

PHOSPHORUS PRESSURE = 1·45cm

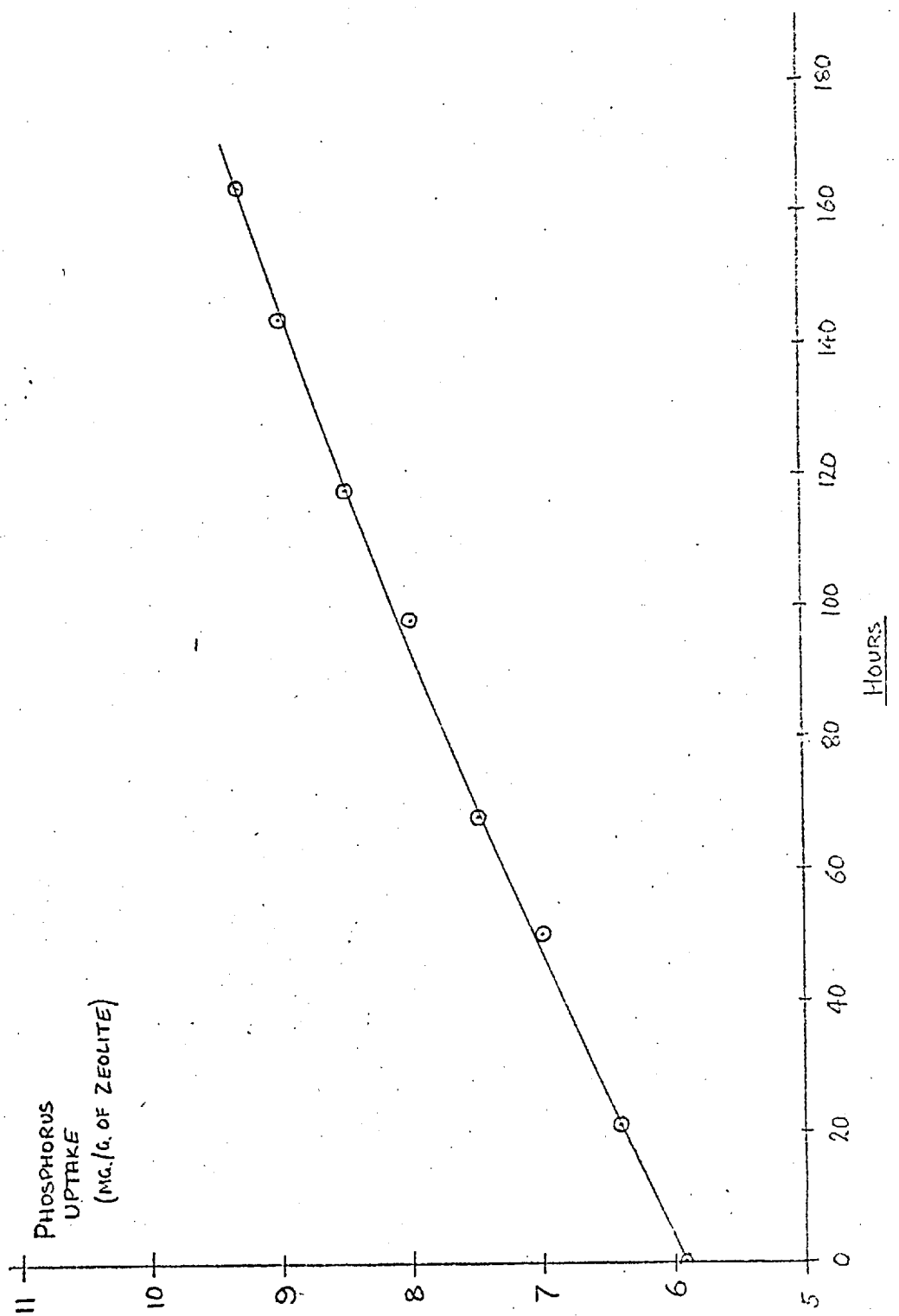

SIEVE 5A – PHOSPHORUS AT 264·3°C

DIAGRAM 3.2.2.

PHOSPHORUS PRESSURE = 7·64cm.

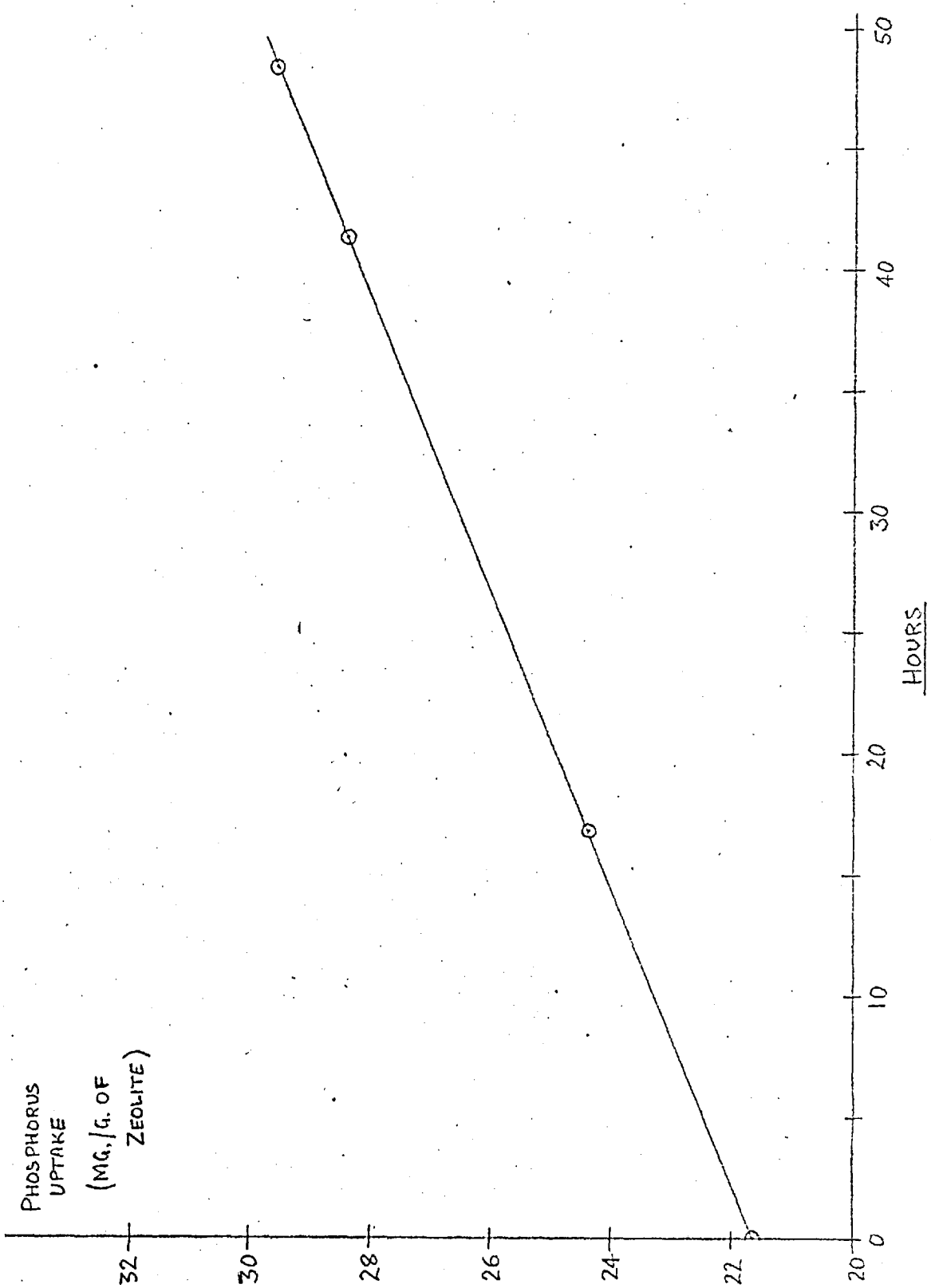

SIEVE 5A – PHOSPHORUS AT 323·6°C

DIAGRAM 3.2.3.

PHOSPHORUS PRESSURE = 1·45 CM.

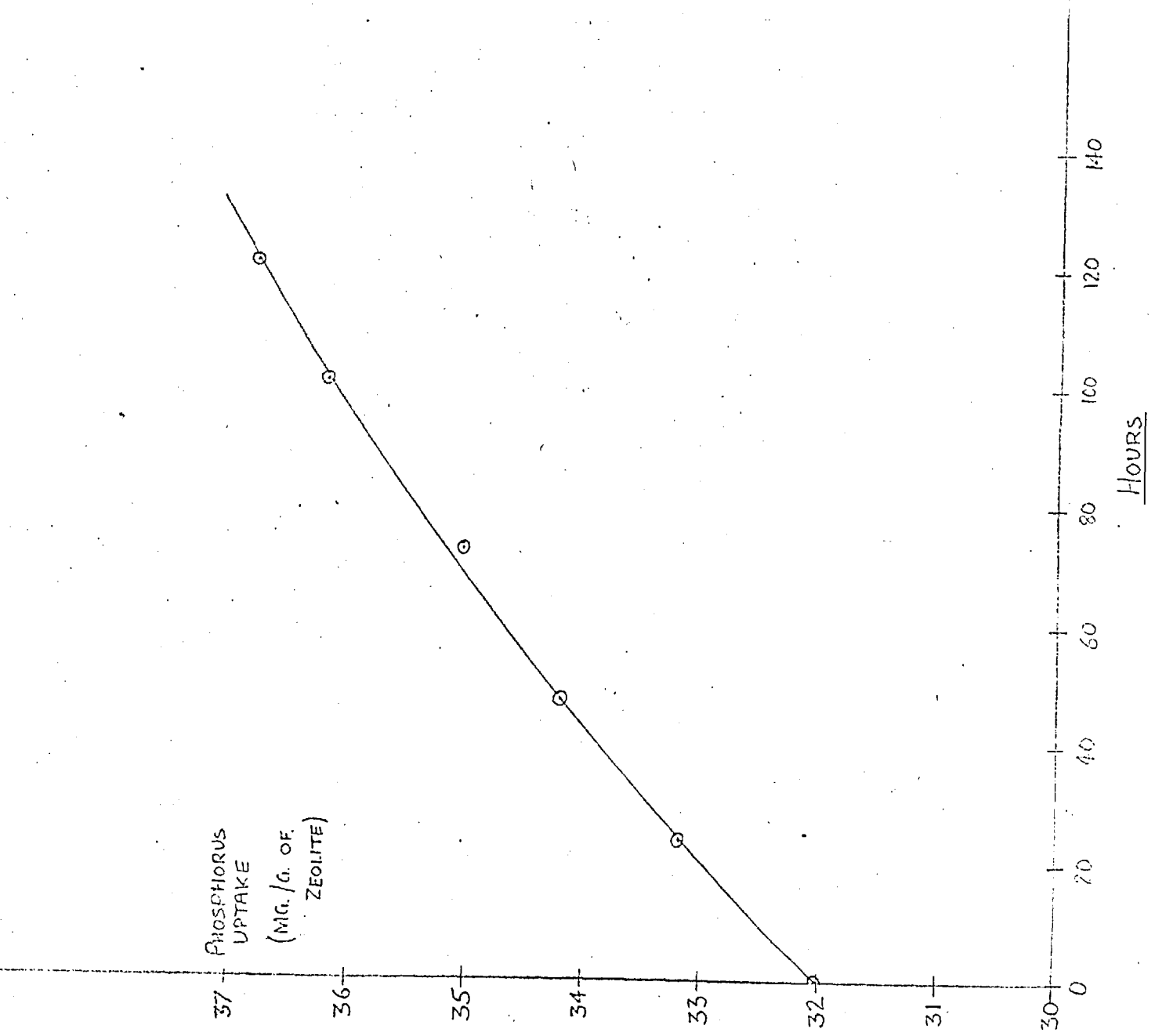

SIEVE 5A – PHOSPHORUS AT 323·6°C

DIAGRAM 3.24

PHOSPHORUS PRESSURE = 7·64 cm.

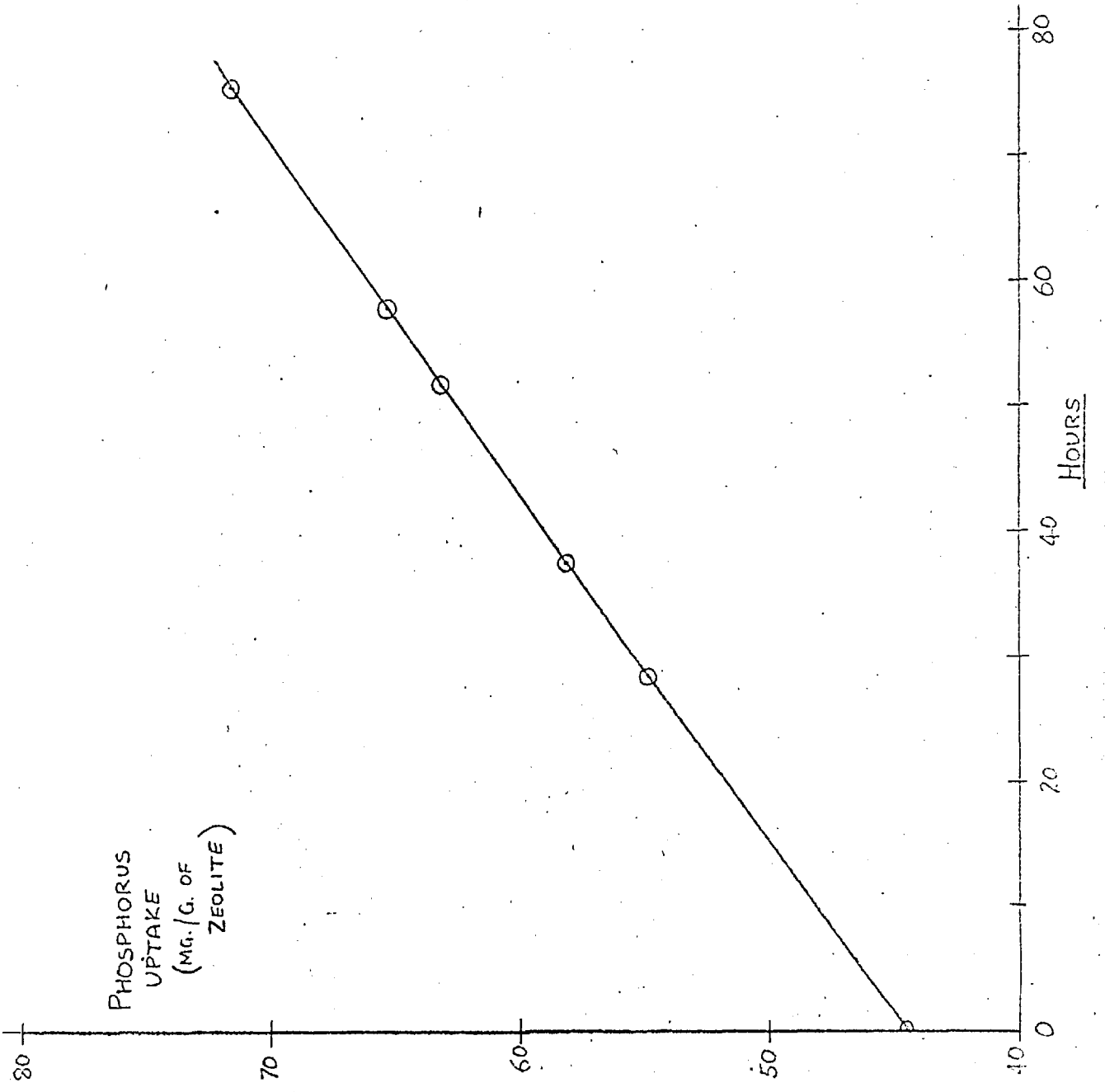

in weight of the complexes are nearly constant at each sorbent temperature and phosphorus pressure.

A slow rate of uptake of phosphorus by sieve 5A might be expected from considerations of the relative sizes of the cage windows in the sorbent and the diameter of the phosphorus molecules. The windows joining neighbouring sorption cavities in sieve 5A have a minimum diameter of about 4.3Å and should prevent the entry of tetrahedral P_4 molecules, whose diameter is about 7.0 Å. P_2 molecules, with a length of 6.6Å and a diameter of 3.5Å should be able to move freely through the structure. The concentration of P_2 is very low at the temperature of these experiments, however, being about 1 in 10^6 of the molecules present at 264.3°C and about 1 in 10^5 at 323.6°C. Furthermore the equilibrium between P_2 and P_4 is affected by the total pressure in such a way that the concentration of P_2 varies with the square root of the total pressure.

Examination of the experimental data enables several possible mechanisms for the slow process to be eliminated. The linearity of the uptake versus time graphs rules out diffusion as the rate controlling process. Since only P_2 can enter the structure the slow rate of uptake might be explained by the low concentration of this species in the gas phase. If this were rate determining, the rate of uptake would vary in the same way as the concentration of P_2 varies with changes in the temperature and total pressure of the phosphorus vapour. While the concentration of P_2 varies with the square root of the total pressure, the rate of uptake increases more rapidly than this when the pressure is raised and so this explanation may be ruled out.

The most probable explanation is that the rate determining process is the slow dissociation of P_4 molecules sorbed on the external surface of the crystals. The P_2 formed would diffuse rapidly into the crystals and more P_4 would then dissociate in the approach toward the equilibrium between P_4 and P_2 on the surface. The phosphorus concentration on the external surface must remain constant at constant temperature and total vapour pressure, giving rise to a steady rate of uptake of phosphorus as the dissociation on the surface proceeds. The concentration of phosphorus on the surface might be expected to rise rapidly as the total vapour pressure is raised and on the external surfaces of the crystallites might follow a type III isotherm similar to that found with Br_2 or I_2 on silica gel. This behaviour would account for the rapid increase in the rate of uptake of phosphorus as the pressure is raised. Although the amount of phosphorus on the surface in equilibrium with a fixed pressure of phosphorus would fall as the temperature is raised, the rate of dissociation of P_4 could rise rapidly with temperature and hence the increase in rate of uptake with temperature which is observed is not unreasonable.

The desorption of phosphorus from 5A was studied by observing the weight changes which occurred when the pressure of phosphorus vapour was made negligibly small by cooling the reservoir to room temperature. At room temperature the pressure of phosphorus vapour over solid yellow phosphorus is below 0.01 cm of mercury. Desorption of phosphorus from 5A was found to be a first order process, giving linear plots of the logarithm of phosphorus content against time. Diagram 3.2.5 shows the plots of $\log(n/n_o)$ against time at three sample temperatures. n_o and n are the weights of phosphorus occluded in 1 g of anhydrous 5A

The Slow Desorption of Phosphorus from Sieve 5A.

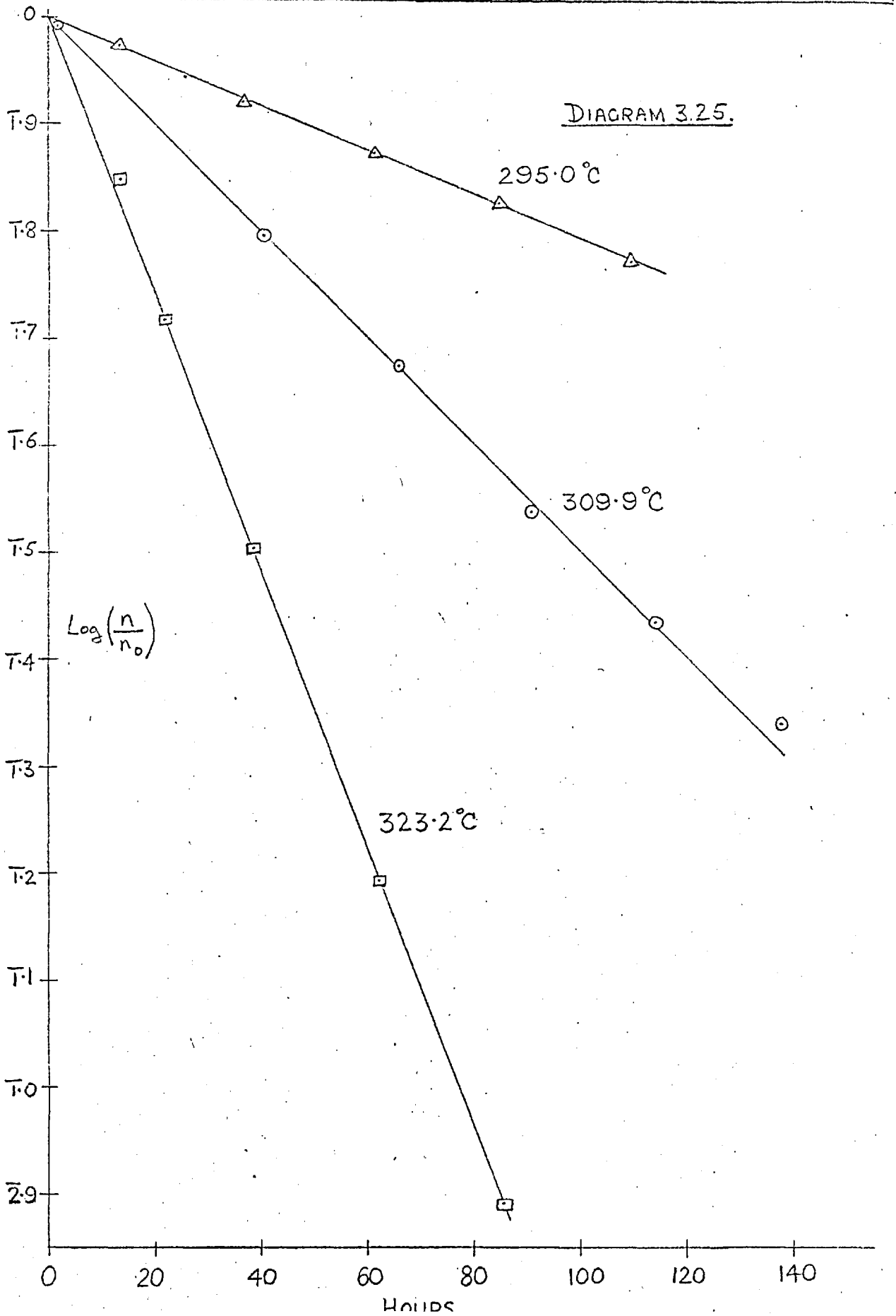

Diagram 3.25.

at times t=0 and t=t respectively. The rate of removal, -dn/dt, at temperature T, is then given by

$$-\frac{dn}{dt} = kn \ .$$

Rearranging gives

$$\frac{dn}{n} = -kdt,$$

and integrating gives

$$\ell n\ n = -kT + A$$

where A is a constant. When t=0, $n=n_o$ and hence

$$A = \ell n\ n_o \ .$$

Hence, $$\log \frac{n}{n_o} = -\frac{k}{2.303}t \ .$$

The slope of the linear plots in diagram 3.2.5 is therefore -k/2.303. Application of the Arrhenius equation to these first order rate constants gives an average energy of activation of 43.8 kcal $mole^{-1}$ for the rate determining step in desorption.

During desorption the pressure of phosphorus vapour surrounding the crystals was very small, and if as before a type III isotherm equation is assumed for this system, the amount of phosphorus sorbed on the external surface of the crystals should also be small. Only P_2 molecules can pass through the windows of the sorption cages and hence in order for phosphorus to reach the surface and so leave the complex, dissociation of P_4 to P_2 must first take place. If the P_2 produced diffuses rapidly inside the crystals and does not recombine too quickly, an almost uniform distribution of phosphorus within the crystals will be maintained. If the dissociation of P_4 inside the crystals is the rate controlling step and its rate is proportional to the concentration of

P_4 in the sieve, then the rate of desorption of phosphorus from the sieve could be first order. The experimental data is fully consistent with this mechanism.

3.2.2 NaX-Phosphorus

The occlusion of phosphorus by NaX was found to be fully reversible giving isotherms which correspond to type V of Brunauer's classification. Diagrams 3.2.6 and 3.2.7 show the isotherms at 265.1°C and 323.8°C respectively. Both sorption and desorption processes were very slow and took place at rates which diminished as the process proceeded (diagram 3.2.8). In the case of NaX these slow processes cannot be ascribed to the restricted entry of phosphorus molecules since in this zeolite the cage windows have a free diameter of 9-10Å while the maximum diameter of tetrahedral P_4 molecules is only about 7Å.

Sorption heats ($-\Delta\bar{H}$) for phosphorus in NaX have been calculated from the isotherms by the use of the Clausius-Clapeyron relation. Diagram 3.2.9 shows the variation of sorption heat with phosphorus uptake. For comparison, the latent heat of condensation of phosphorus vapour, $\Delta\bar{H}_c$ = -12.6 kcal/mole. The initial rise of $-\Delta\bar{H}$ to the steady value of 27.5 kcal/mole, which is reached before uptakes corresponding to only 30% filling of the cages have been obtained, demonstrates that a large contribution to the heat of sorption comes from phosphorus-phosphorus interactions.

Calculation using the volume of the supercages in NaX and the density of liquid phosphorus at 323.8°C (1.49 g/cm^3) shows that complete filling of the supercages

NaX-PHOSPHORUS ISOTHERM AT 265.1°C

DIAGRAM 3.2.6

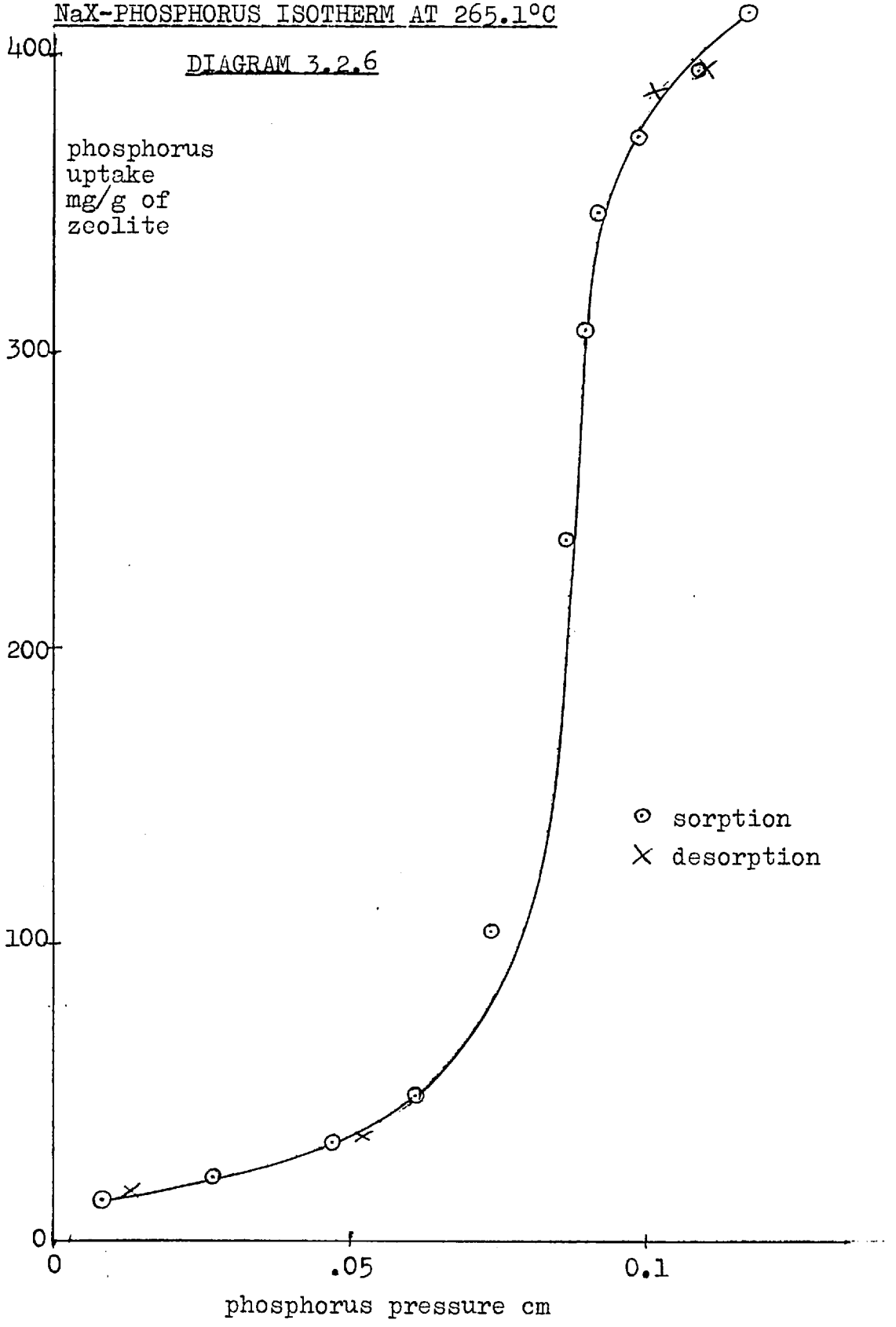

NaX-PHOSPHORUS AT 323.8°C

DIAGRAM 3.2.7

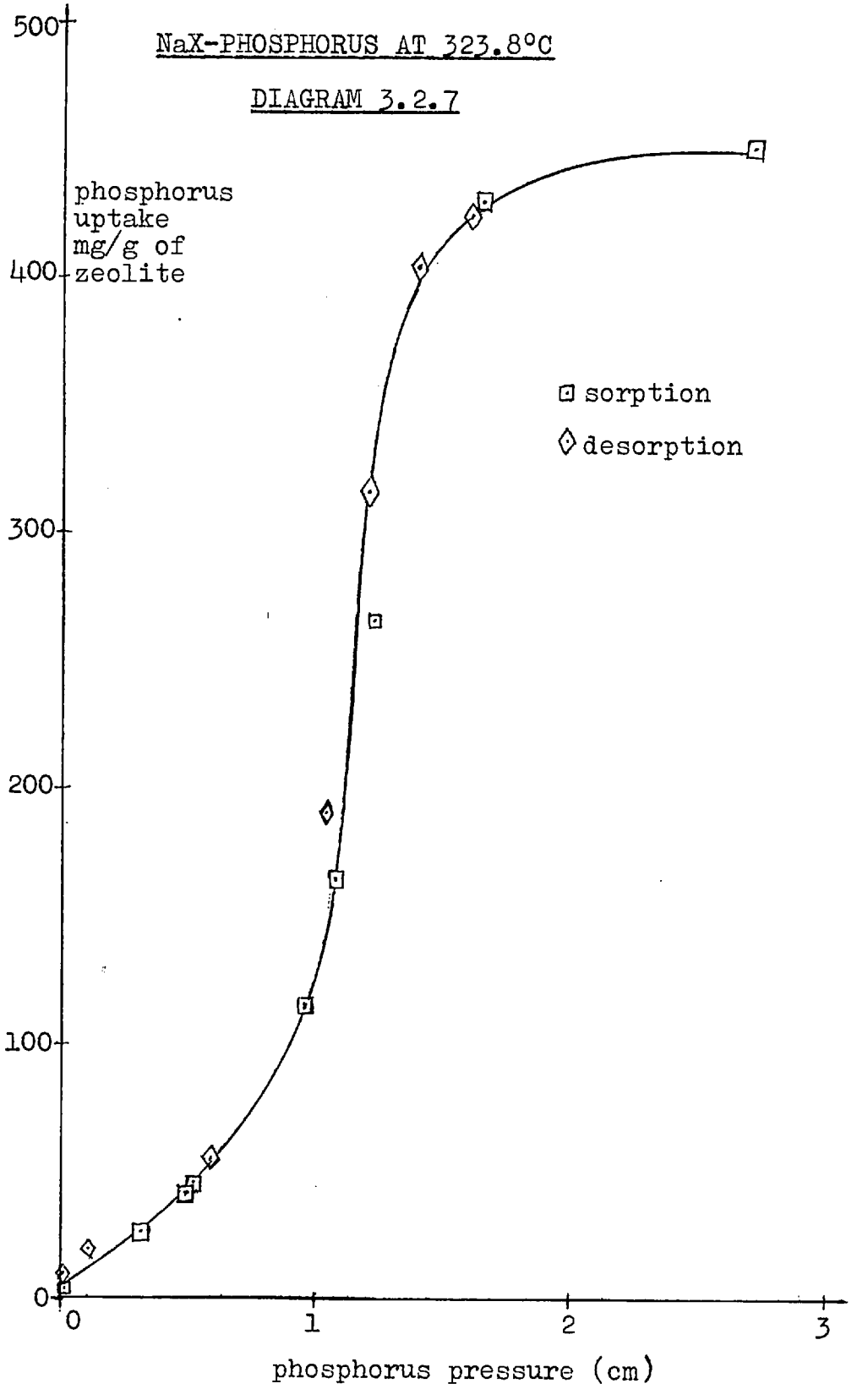

DIAGRAM 3.2.8

NaX-P at 265.1°C

Phosphorus pressure = 0.087 cm

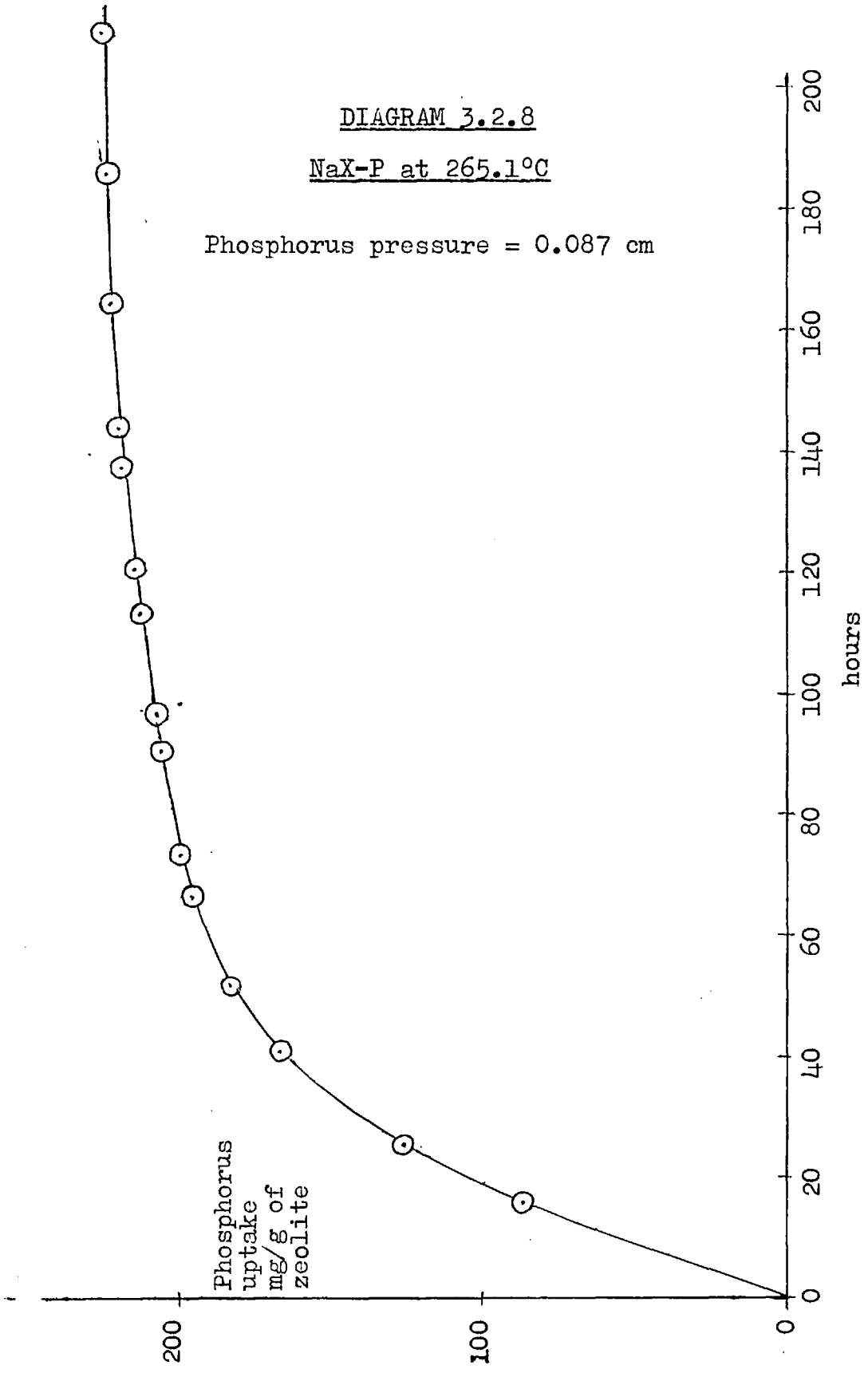

DIAGRAM 3.2.9

HEAT OF SORPTION OF PHOSPHORUS IN NaX

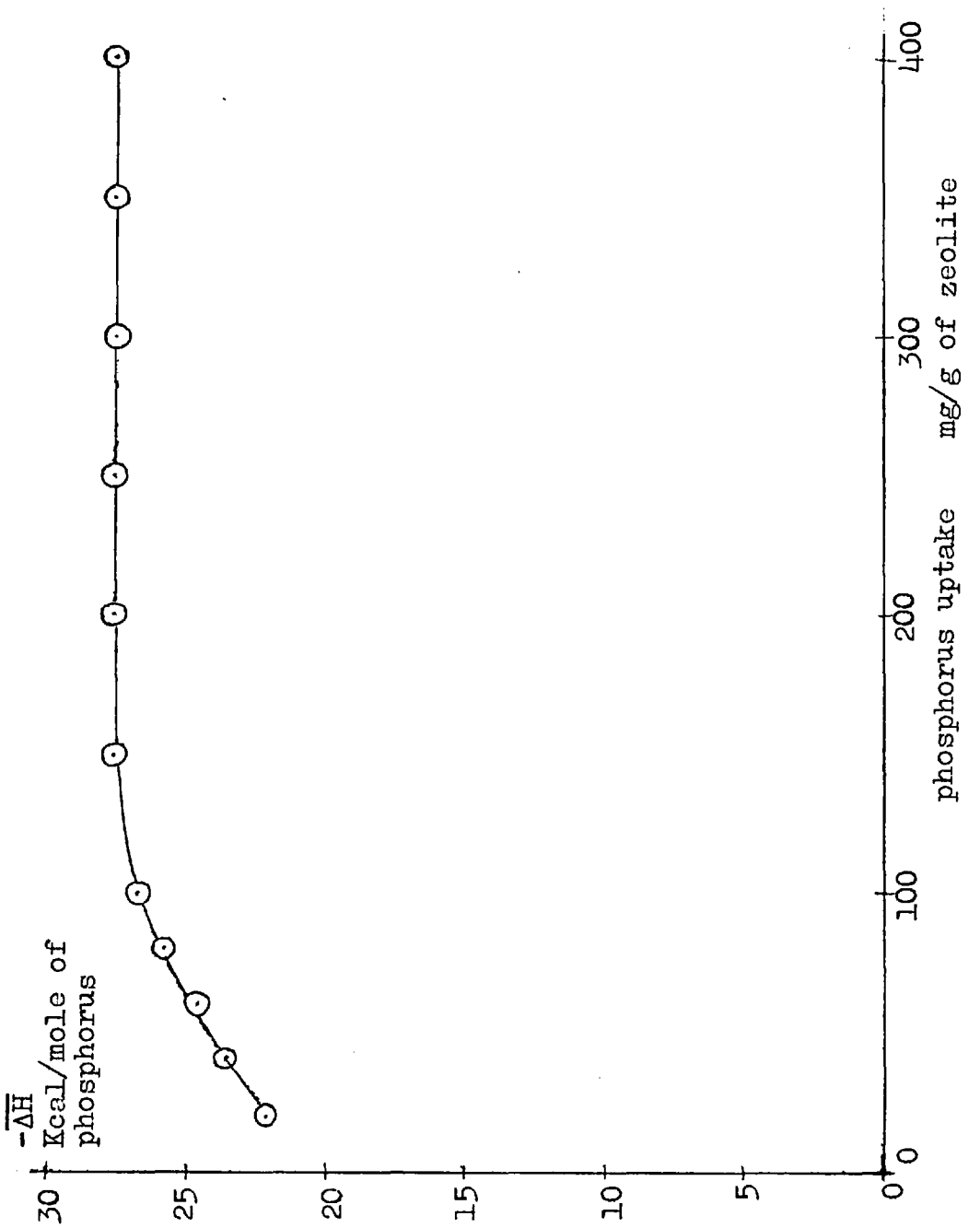

at this temperature corresponds to an uptake of 480 mg of phosphorus per g of anhydrous NaX. If the flat part of the isotherm at 323.8°C may be taken as the maximum uptake attainable at this temperature, the uptake of 450 mg/g which is observed represents only 94% filling of the intracrystalline volume available. This comparison suggests that the phosphorus is present in the structure in forms of greater molecular complexity than P_4.

3.3 Zeolite-Mercury Inclusion Complexes

3.3.1 NaX-mercury

The sorption of mercury vapour by NaX was found to be fully reversible, the uptake of mercury being proportional to its vapour pressure. The magnitude of the uptake was very small, being only about one half that observed for the mercury-chabazite system at the same temperature and pressure (Barrer and Woodhead, 1948). The isotherms obtained are recorded in diagram 3.3.1. The curve on the graph sets the upper limit of mercury pressure obtainable at each isotherm temperature. Passing beyond this line results in the condensation of liquid mercury.

The heat of sorption has been calculated from the integrated form of the Clausius-Clapeyron relation,

$$\Delta H = R\left(\frac{T_1 T_2}{T_1 - T_2}\right)\left(\ell n \frac{p_1}{p_2}\right)_x$$

p_1 and p_2 being the equilibrium pressures for a fixed sorption x of mercury at sorbent temperatures T_1 and T_2 respectively. The average value obtained was $\Delta H = -8.2_8$ kcal/g.atom of mercury which is larger than the heat of -5.8 kcal/g atom found for chabazite (Barrer and Woodhead, 1948). This heat of sorption is considerably smaller than the latent heat of condensation of mercury, ΔH_c = -13.6 kcal/g.atom, suggesting that, as separated atoms, mercury does not show the great polarisability that is found in the liquid state, but behaves more like the permanent gases.

Since the heat of sorption is 5.3 kcal/g.atom less negative than the heat of condensation, transfer of mercury from liquid mercury to NaX will be an endothermal

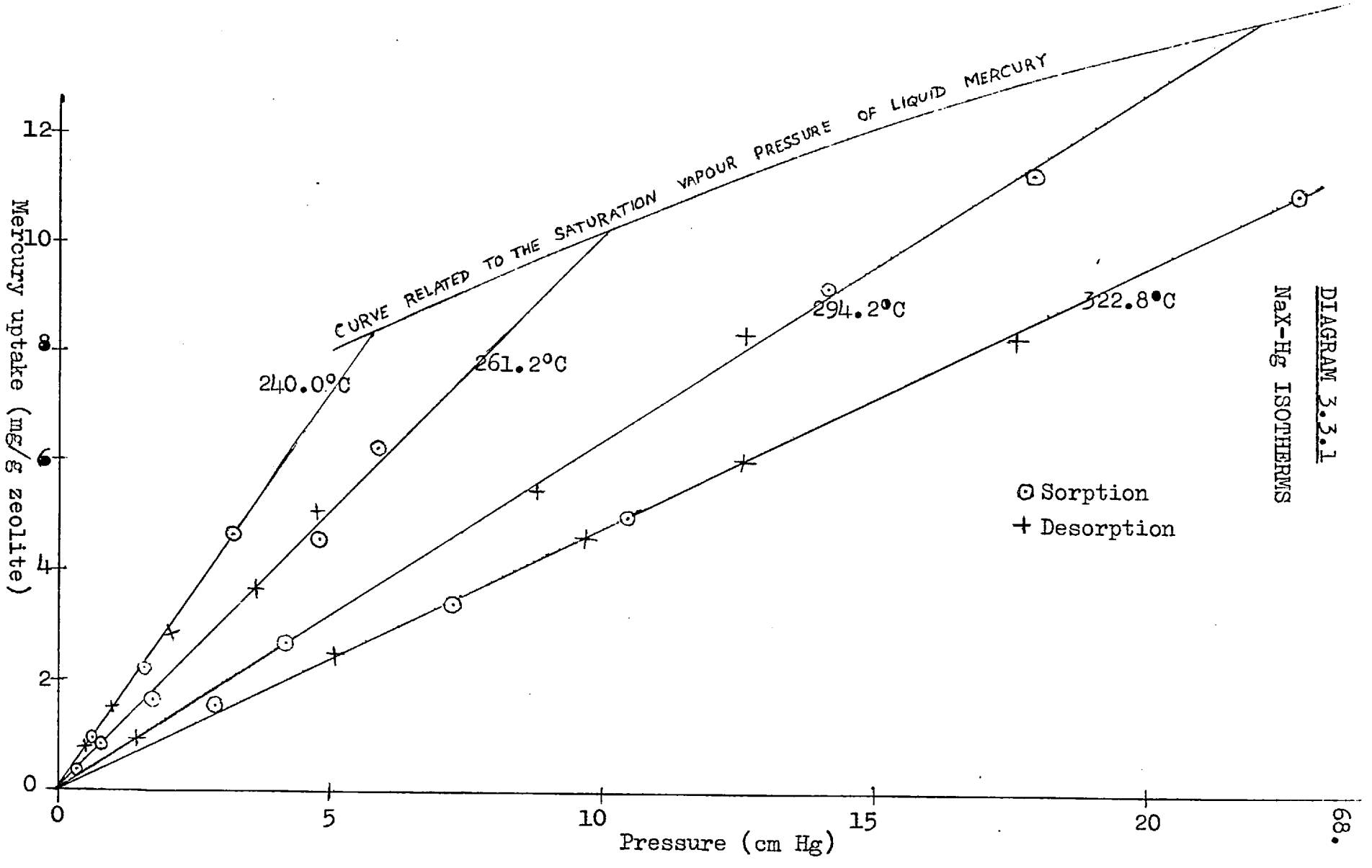

DIAGRAM 3.3.1
NaX-Hg ISOTHERMS

process, favoured by high temperatures. The uptake of mercury has been shown to be very small at temperatures in the region of 300°C and hence the sorption of mercury by NaX will be negligible at room temperature and below. This conclusion is important in view of the widespread use of mercury as the manometric fluid in sorption studies involving NaX.

Adsorption equilibrium

Distribution coefficients for mercury between the vapour and condensed phases can be evaluated in the Henry's law region where the mercury uptake is proportional to pressure. If the sorbent is regarded as inert, a treatment by adsorption thermodynamics is appropriate, using the intracrystalline volume of the sorbent for the sorption volume of the system. At the same time, however, calculation of the buoyancy arising from the displacement of mercury vapour by the sorbent is based on the total volume of the crystal framework and the intracrystalline volume. Thus the sorption measured is analogous to a Gibbs surface excess.

The free energy of transfer of a mole of sorbate from pure gas phase, where its activity is a_g, to an infinite amount of sorbed phase where its activity is a_s is

$$\Delta A = -RT\ell n\left(\frac{a_s}{a_g}\right)_{eq} + RT\ell n\left(\frac{a_s}{a_g}\right) .$$

$(a_s/a_g)_{eq}$ is the thermodynamic equilibrium distribution coefficient, k_a. We may write c_i as the concentration of adsorbed atoms, expressed as the number of atoms per cm^3 of intracrystalline volume, and c_g as the number of

atoms per cm^3 in the gas phase. The activity coefficients are f_i and f_g for the two phases respectively. Then

$$k_a = \frac{c_i}{c_g}\frac{f_i}{f_g} = k_i \frac{f_i}{f_g} .$$

If the standard state in the gas phase is chosen to be p=1 atm , then $c_g = 1/kT$ (where k is the gas constant expressed in cm^3 atm $deg^{-1}mole^{-1}$). It is convenient to choose the standard state in the adsorbed phase as one in which $c_i = 1/kT$. This standard state is one of high dilution in which Henry's law is valid, and so

$$\Delta E = \Delta E_o$$

where ΔE is the experimental energy of sorption in the Henry's law range and ΔE_o refers to this energy in the standard state. Then

$$\Delta A_o = \Delta E_o - T\Delta S_o = \Delta E - T\Delta S_o$$

where ΔA_o and ΔS_o are the standard free energy and entropy of adsorption respectively. Since the Henry's law range is one of high dilution one would expect $f_i/f_g \approx 1$ and so $k_i \approx k_a$.

Standard entropies of adsorption

In the Henry's law range, sorption equilibria may be written

$$K = \theta/p$$

where θ is the fraction of filling of the intracrystalline volume at sorbate pressure p, and K the distribution coefficient.

Writing C_s for the number of atoms required to fill 1 cm^3 of intracrystalline volume, θ can be replaced by C_i/C_s and p by $C_g kT$, giving

$$K = \frac{C_i}{C_g} \frac{1}{kTC_s} = k_i \frac{1}{kTC_s} \qquad (1)$$

$$\therefore k_i = KC_s kT \qquad (2)$$

Values of K have been tabulated for models in which the adsorbed atoms are assumed to have various translational and vibrational degrees of freedom in the adsorbed phase (Barrer, 1956). Thus in model I the adsorbed atoms have two translational and one vibrational mode relative to their sorption sites, in model II one translational and two vibrational modes, while in model III they have three vibrational modes. The models serve as limiting reference states, giving different standard entropies of sorption with which experimental entropies may be compared. Thus, for state I,

$$K_I = \frac{1}{kT} \frac{1}{N_S^{11}} \left(\frac{kT}{2\pi m}\right)^{\frac{1}{2}} \frac{1}{\nu} \exp \chi/RT \qquad (3)$$

where N_S^{11} denotes the number of atoms required to cover 1 cm^2 of intracrystalline area. The atom of mass m has a mean frequency of vibration ν which can be estimated only approximately using the expression (Hill, 1952):

$$\nu = \nu_A \sqrt{\frac{\Delta E M_A}{M \Delta E_A}} \qquad (4)$$

where M is the molecular weight of a given sorbate of sorption energy ΔE, while M_A and E_A are these quantities for a reference molecule of assigned frequency. The reference molecule was argon for which ν_A was taken as 1.0×10^{12} sec^{-1} when ΔE_A was 1.5 kcal/mole (Orr, 1939). The term χ in equation (3) is given for state I by

$$\chi = -\Delta E + \tfrac{1}{2}RT \quad . \qquad (5)$$

Substituting from equation (2) into equation (3),

$$k_i = \frac{c_S kT}{kTN_s''} \left(\frac{kT}{2\pi m}\right)^{\frac{1}{2}} \frac{1}{\nu} \exp\left(\frac{-\Delta E + \frac{1}{2}RT}{RT}\right) \qquad (6)$$

Since $c_S = N_s''/d$ where d is the atomic diameter, equation (6) becomes

$$k_i = \left(\frac{kT}{2\pi m}\right)^{\frac{1}{2}} \frac{1}{\nu d} \exp\left(\frac{-\Delta E}{RT} + \frac{1}{2}\right) \qquad (7)$$

$$\therefore \ell n k_i = \ell n\left[\left(\frac{kT}{2\pi m}\right)^{\frac{1}{2}} \frac{1}{\nu d}\right] - \frac{\Delta E}{RT} + \frac{1}{2} \qquad (8)$$

$$\therefore \frac{\delta \ell n k_i}{\delta T} = \frac{1}{2T} + \frac{\Delta E}{RT^2} \quad .$$

The standard entropy of sorption ΔS^o is given by

$$\Delta S_o = \frac{\delta}{\delta T}(RT\ell nK) = RT\ell nK + RT\,\frac{\delta \ell nK}{\delta T}$$

and therefore for model I,

$$(\Delta S_o)^I = R\ell n\left[\left(\frac{kT}{2\pi m}\right)^{\frac{1}{2}} \frac{1}{\nu d}\right] + R \quad .$$

In Table 3.3.1 are given the distribution coefficients k_i, the experimental standard entropies of adsorption, and the calculated standard entropies for States I, II and III of the adsorbed molecules.

TABLE 3.3.1

Temp. ^oK	k_i	$-\Delta E$ (kcal/mole)	$\nu \times 10^{-11}$ sec^{-1}	cal $mole^{-1}deg^{-1}$			
				$-\Delta S_o$ (expt)	$-\Delta S_o^{I}$	$-\Delta S_o^{II}$	$-\Delta S_o^{III}$
513.2	60.9	7.2_6	9.8_2	5.97	1.3_8	2.7_6	4.1_4
534.2	44.2	7.2_2	9.7_8	6.00	1.3_4	2.6_8	4.0_2
567.4	29.5	7.1_5	9.7_3	5.86	1.2_7	2.5_4	3.8_1
596.0	23.3	7.0_9	9.6_9	5.61	1.2_1	2.4_2	3.6_3

Comparison of experimental and calculated values of ΔS^{o} shows that the experimental values exceed even those calculated for adsorbed states having freedom equivalent to three vibrational modes relative to the surface. The larger standard entropy changes which may arise when the sorption of molecules possessing internal degrees of freedom takes place are not possible with monatomic mercury. Calculated values of ΔS_o are very sensitive to uncertainties in ν (Barrer and Rees, 1961). The values of ν used in the calculations are only approximate, and this is one probable source of the discrepancies between the experimental ΔS_o and the calculated ΔS_o^{III}. Perturbation of the solid by the sorbate is another. It is reasonable to suggest that the results come nearest to the model for the NaX-mercury system in which the adsorbed mercury atoms are localised and execute vibrations about their mean positions close to the cavity walls.

3.3.2 PbX-Mercury

Diagram 3.3.2 shows the lead X-mercury isotherms obtained at two experimental temperatures. The isotherms were fully reversible and obeyed Henry's law. The isosteric heat of sorption, $\Delta H = -9.10$ kcal/g atom of mercury, exceeded the heat of sorption of mercury in NaX by 820 cal/g atom. The greater heat of sorption is attributed to the greater polarizing power and polarisability of the divalent Pb ion, giving a larger contribution from the ion-induced dipole interaction and perhaps from the dispersion energy.

Comparison of the amounts of mercury occluded by an equal number of unit cells of NaX and PbX may be made through the distribution coefficients k_i. These

DIAGRAM 3.3.2

PbX-MERCURY ISOTHERMS.

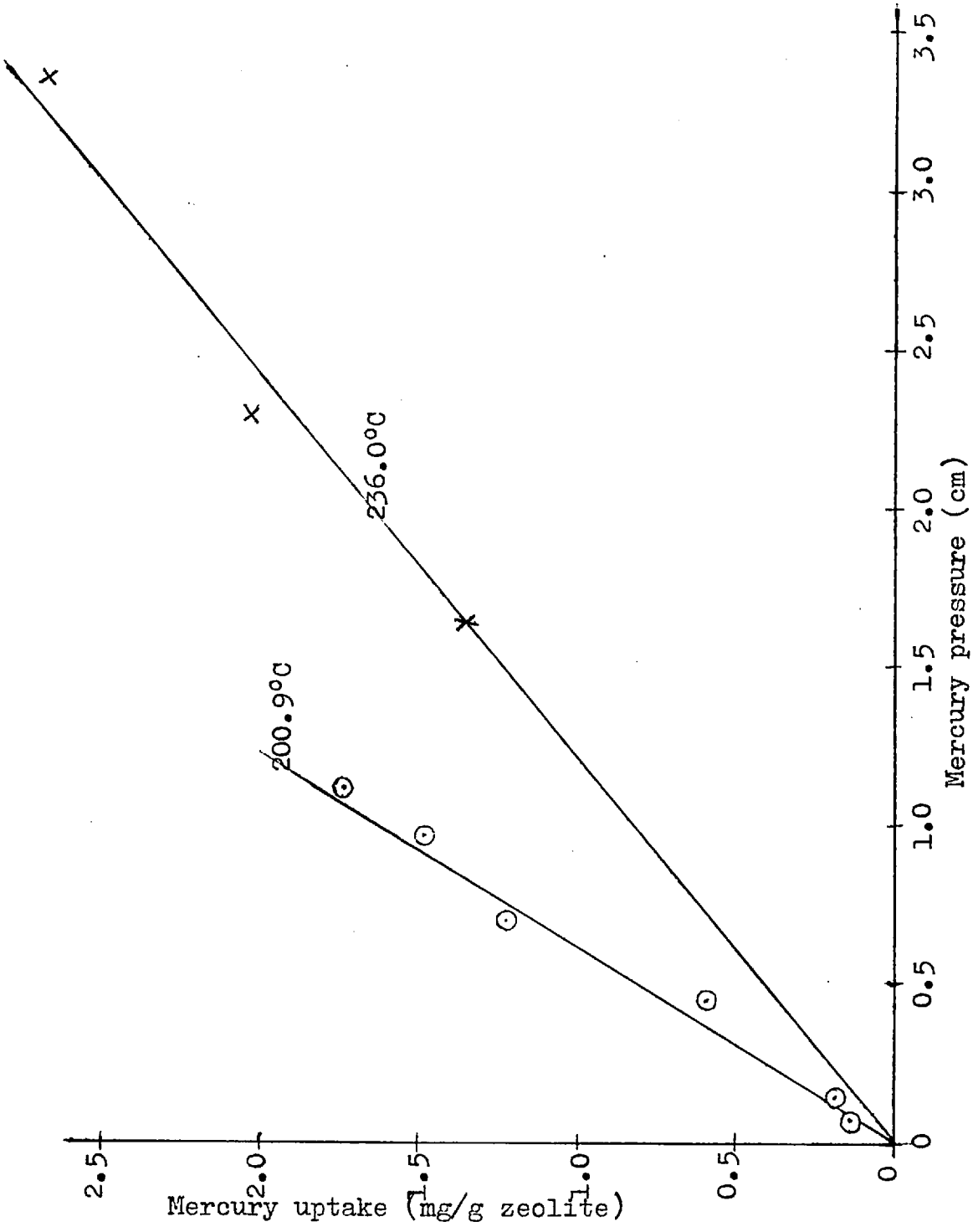

are listed for PbX at the two experimental temperatures in table 3.3.2. While values of k_i for PbX and NaX both fall as the temperature is raised, the distribution coefficient for PbX at 509.2°K is already lower than that for NaX at 513.2°K. Hence NaX takes up more mercury than the equivalent volume of PbX under similar conditions of temperature and mercury vapour pressure.

TABLE 3.3.2

Temp. °K	k_i	$-\Delta E$ (kcal/g.atom)	$vx10^{-11}$ (sec^{-1})	cal $mole^{-1}deg^{-1}$			
				$-\Delta S_o$ (expt)	$-\Delta S_o^{I}$	$-\Delta S_o^{II}$	$-\Delta S_o^{III}$
474.1	98.4	8.1_6	10.4	8.5_8	1.5_3	3.0_6	4.5_9
509.2	54.1	8.0_9	10.3_5	8.4_1	1.4_6	2.9_2	4.3_8

Table 3.3.2 also lists experimental values of ΔS_o together with values of ΔS_o calculated from models of the adsorbed atoms similar to those used in section 3.3.1. Again the experimental values of $-\Delta S_o$ exceed even that calculated for model III suggesting that in PbX, as in NaX, sorbed mercury atoms are localised, and execute vibrations close to the walls of the zeolite cages. Additional perturbation of the sorbent in PbX may arise from the higher energy of sorption in this material.

3.3.3 Mercuric X - Mercury

Mercuric X takes up mercury rapidly and copiously at temperatures in the region of 250°C. The isotherm obtained at 235.7°C is shown in diagram 3.3.3. Experimental evidence suggests that the first step in the process

MERCURIC X – Hg ISOTHERM AT 235·7°C

DIAGRAM 3.3.3.

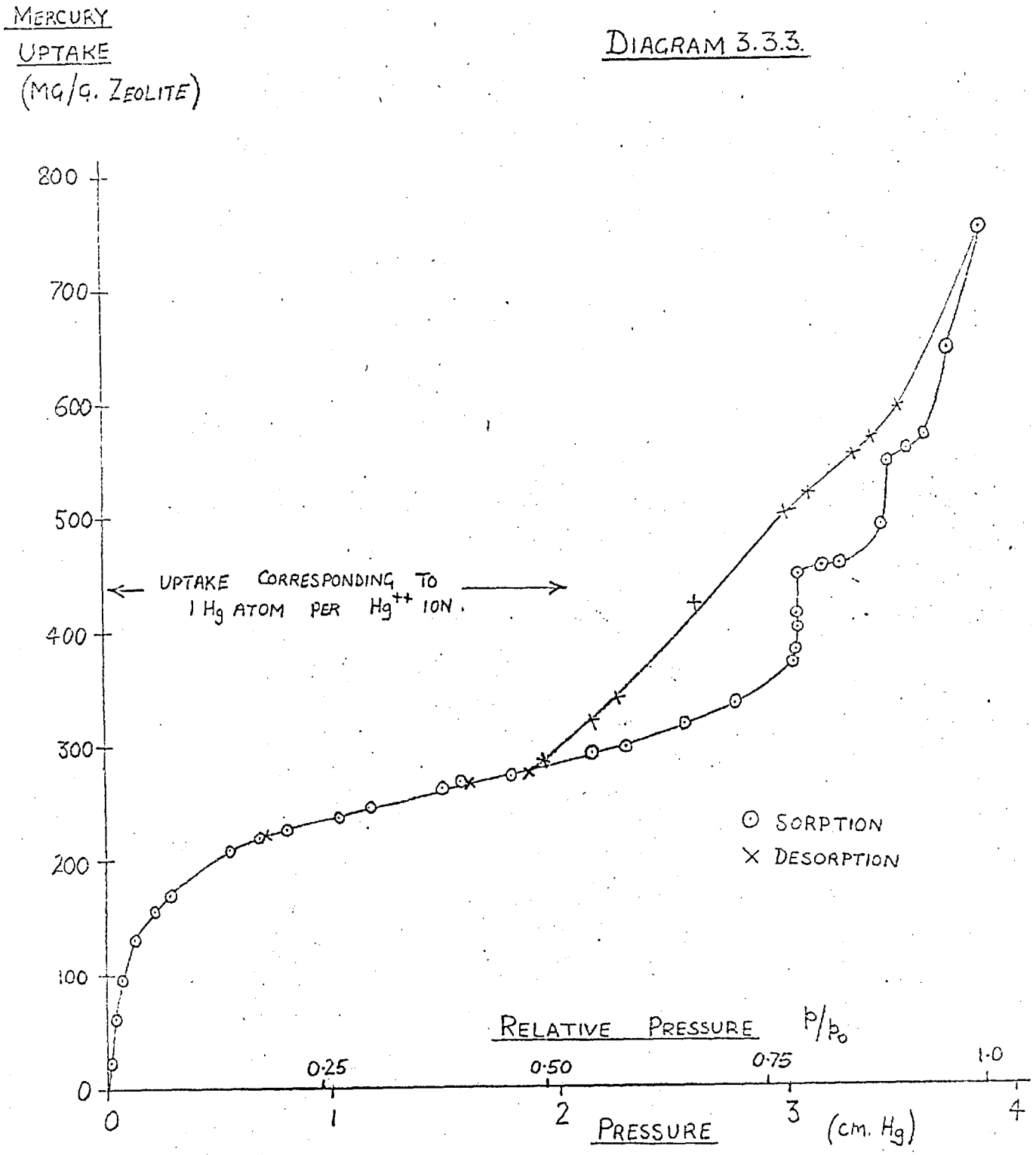

is the reduction of mercuric ions (Hg^{2+}) to mercurous ions (Hg_2^{2+}) by the chemisorption of neutral mercury atoms. At a relative pressure (p/p_o) of 0.79 the uptake increases rapidly with pressure, giving a step in the isotherm. The top of this step corresponds to the inclusion of 1 mercury atom for each mercuric ion in the structure, suggesting that this point marks the completion of the reduction of mercuric ions to mercurous. Further increase in pressure produces a second step in the isotherm at a relative pressure of 0.89, followed by a rapid increase in uptake as the relative pressure approaches unity. The desorption curve does not follow the steps of the sorption branch, but takes a smoother path above the latter, joining the sorption branch at a relative pressure of 0.5.

Interesting colour changes were also observed in the complex. The zeolite was initially white. During the uptake of mercury it became successively yellow, green, grey, and finally black. During desorption these colours were displayed in the reverse order.

The inflection in the isotherm in the region of relative pressure 0.5 may be explained in relation to the positions of the cations in the zeolite. The sample of NaX from which the HgX was prepared contains 86 cations per unit cell (Barrer and Walker, 1964). The Na^+ ions are situated as follows: each supercage shares four 6-membered ring windows with sodalite cages and these windows each contain a monovalent ion. There are 8 supercages per unit cell, so 32 cations occupy the sodalite window positions. The unit cell contains 16 hexagonal prism units each of which contains a monovalent ion. The remaining 38 Na^+ ions per unit cell have not been located, but they are probably in the large cavities, and so are readily accessible for exchange (Broussard and Shoemaker, 1960).

When attempts were made to replace small monovalent ions, e.g. Na^+ (radius 0.95 Å) by larger monovalent ions, e.g. Rb^+ (radius 1.48 Å) it was found that only 54 of the 86 ions can be replaced (Barrer and Shamsuzzoha, 1964). The Rb^+ ion is too large to pass through the 6-membered windows of sodalite cages as the smallest free diameter of these windows is about 2.3 Å. The 16 Na^+ ions in the hexagonal prism units cannot therefore be replaced by Rb^+ ions. In the supercages the Rb ion can only rest adjacent to the sodalite cage windows, whereas the equilibrium position of the Na^+ ions is in the plane of the windows. The position of the positive charge is therefore displaced slightly into the supercages. In order to balance this charge displacement, the cations in the other 3 windows may be slightly displaced towards the centre of their respective sodalite cages, making the exchange of the next Na^+ more difficult. When a second Na^+ ion in a sodalite cage window is replaced the Na^+ ions in the other two windows are displaced even farther into the cages. The charge distribution then prevents any further replacement of the Na^+ ions in sodalite cage windows. The maximum number of Na ions which can be replaced by Rb ions is therefore 54 per unit cell (see Table 3.3.3). When divalent ions replace the Na in the structure, considerations of size again limit the extent of ion exchange. Ions too large to pass through the sodalite cage windows will not replace the ions in hexagonal prism cages. However, one divalent ion replaces two monovalent ions, so it is usually possible to exchange all the ions situated in sodalite cage windows.

The radius of the divalent mercuric ion is 1.10Å, which allows it to pass through the sodalite cage windows.

Complete exchange of Na^+ and Hg_2^{2+} should t herefore be possible (table 3.3.3). When the mercuric ion chemisorbs a mercury atom to give a mercurous ion (Hg_2^{2+}) its charge is unaltered, but its size is increased. It is possible that this increase in size prevents the reduction of the mercuric ions in the hexagonal prisms, and also distorts the charge distribution around the sodalite cage windows so that only one divalent ion in this position can be exchanged in each supercage. The situation envisaged is the distribution shown in table 3.3.3 as $(Hg_2^{2+}, Hg^{2+})X$. This intermediate stage represents reduction of 63% of the mercuric ions present.

The shape of the initial part of the isotherm suggests that the conversion of mercuric to mercurous ions takes place in two stages, only about 65% of the total exchange being effected in the first stage. The desorption branch of the hysteresis loop joins the sorption branch at the point where about 65% of the mercuric ions have been exchanged. Below this point the sorption and desorption of mercury was completely reversible.

Diagram 3.3.4 shows the lower section of the isotherm obtained at 271.0°C. Failure of the apparatus prevented mercury uptakes at higher pressures being recorded. The mechanism proposed for the reversible uptake of mercury may be written

$$Hg^{2+} + Hg \rightleftharpoons Hg_2^{2+} \quad . \qquad (1)$$

The equilibrium constant K_1 is given by

$$K_1 = \frac{a_{Hg^{2+}}}{a_{Hg_2^{2+}} p} \qquad (2)$$

where $a_{Hg^{2+}}$ and $a_{Hg_2^{2+}}$ are the activities of mercuric and mercurous ions respectively, and p is the vapour pressure

TABLE 3.3.3

Material	Ion	Ionic radius Å	Number of ions per unit cell				% Exchange
			In sodalite cage windows	In hexagonal prisms	In super cages	Total	
NaX	Na^+	0.95	32	16	38	86	
(Rb,Na)X	Rb^+	1.48	16	0	38	54	63%
	Na^+	0.95	16	16	0	32	
$Hg^{2+}X$	Hg^{2+}	1.10	16	8	19	43	100%
$(Hg_2^{2+}Hg^{2+})X$	Hg_2^{2+}	-	8	0	19	27	63%
	Hg^{2+}	1.10	8	8	0	16	
$Hg_2^{2+}X$	Hg_2^{2+}	-	16	8	19	43	100%

DIAGRAM 3.3.4

MERCURIC X-Hg ISOTHERM AT 271.0°C

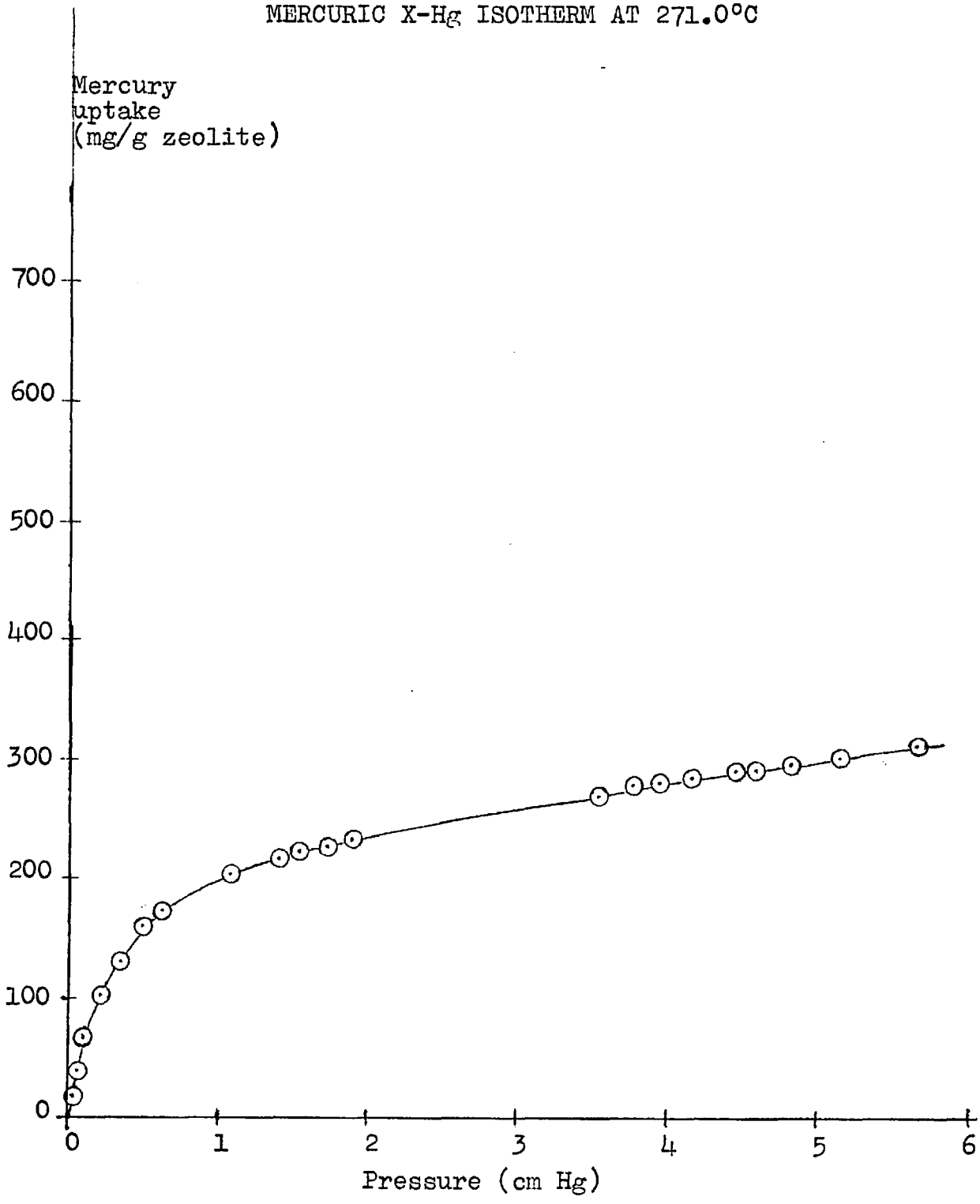

of mercury. K_1 may be expressed in terms of concentrations and if the unit of concentration is taken as g. atoms or ions per litre of zeolite or of gas phase, then 1 cm pressure of mercury vapour at absolute temperature T represents a concentration of $\frac{273}{T} \times \frac{1}{22.4} \times \frac{1}{76} = \frac{0.16}{T}$ g atoms/litre. If m is the active mass of Hg^{2+} ions in 1 litre of sorbent, then after x g ions have been reduced to mercurous ions,

$$K_1 = \frac{x}{(m-x)} \quad \frac{T}{0.16p} \quad \frac{\gamma_{Hg_2^{2+}}}{\gamma_{Hg^{2+}}} \qquad (3)$$

$$\text{Hence,} \quad \frac{x}{m-x} = p\left[K_1\left(\frac{\gamma_{Hg^{2+}}}{\gamma_{Hg_2^{2+}}}\right)\right] \frac{0.16}{T} \qquad (4)$$

where $\gamma_{Hg^{2+}}$ and $\gamma_{Hg_2^{2+}}$ are the activity coefficients of mercuric and mercurous ions respectively in the intracrystalline environment. For the first stage of the reduction m may be taken as 65% of the total mass of mercuric ions in the structure.

At a fixed temperature, equation (4) may be written

$$\frac{x}{(m-x)} = pK' \qquad (5)$$

which is Langmuir's isotherm. Diagram 3.3.5 shows a plot of $\left(\frac{x}{m-x}\right)$ against p for the data at 235.7°C. The graph is linear up to $\left(\frac{x}{m-x}\right) = 3$, having a slope of 5.77 cm^{-1}. In this region, therefore, the process may be regarded as a chemisorption, obeying Langmuir's isotherm. The data at 271.0°C give a plot similar to diagram 3.3.5, but with an initial slope of 2.70 cm^{-1}.

DIAGRAM 3.3.5

TEST OF LANGMUIR QUOTIENT HgX-Hg AT 235.7°C

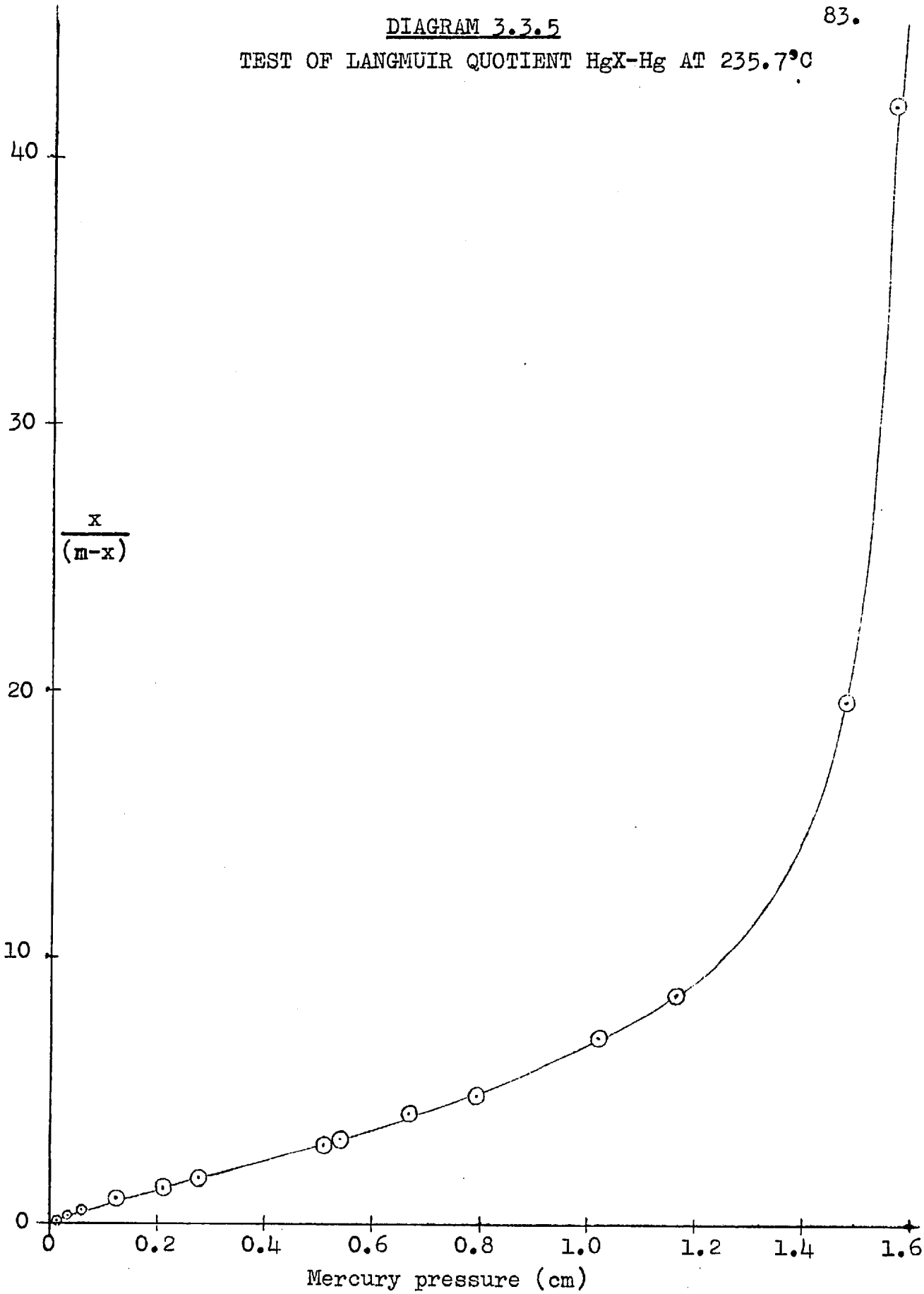

A standard energy change $(\Delta E^{\circ})'$ of reaction (1) may be calculated using the integrated form of the reaction isochore

$$\ell n\left(\frac{(K_1)_{T_1}}{(K_1)_{T_2}}\right) = \frac{(\Delta E^{\circ})'}{R}\left(\frac{1}{T_2} - \frac{1}{T_1}\right) \qquad (6)$$

if the assumption is made that ΔE° and the ratio of the activity coefficients $\gamma_{Hg^{2+}}$ and $\gamma_{Hg_2^{2+}}$ can be regarded as constant in the temperature range considered. Here $(K_1)_{T_1}$ and $(K_1)_{T_2}$ are the equilibrium constants at temperatures T_1 and T_2 defined in terms of concentrations.

If the approximation is made that in the intracrystalline environment of HgX, $\gamma_{Hg^{2+}} = \gamma_{Hg_2^{2+}}$, and hence $K_c = K_1$, a standard Helmholtz free energy change $(\Delta A^{\circ})'$ may also be calculated using

$$(\Delta A^{\circ})' = -RT\ell nK_c \quad . \qquad (7)$$

A standard entropy change $(\Delta S^{\circ})'$ can then be obtained using

$$(\Delta S^{\circ})' = \frac{(\Delta E^{\circ})' - (\Delta A^{\circ})'}{T} \quad . \qquad (8)$$

Values of $(\Delta E^{\circ})'$, $(\Delta A^{\circ})'$ and $(\Delta S^{\circ})'$ at the experimental temperatures are listed in table 3.3.4.

TABLE 3.3.4

Temperature °C	Temperature °A	$-(\Delta E^{\circ})'$ Kcal/g.atom	$-(\Delta A^{\circ})'$ Kcal/g.atom	$-(\Delta S^{\circ})'$ e.u.
235.7	508.9	10.6_8	9.9_1	1.5_1
271.0	544.2		9.8_4	1.5_4

These functions differ from the corresponding rigorous thermodynamic functions due to the approximations made in the ratios between activity coefficients. For example, the standard Helmholtz free energy change ΔA° is related to $(\Delta A^\circ)'$ through the relation

$$\Delta A^\circ = -RT\ell n\left(\frac{\gamma_{Hg_2^{2+}}}{\gamma_{Hg^{2+}}}\right) - RT\ell nK_c$$

$$= (\Delta A^\circ)' - RT\ell n\left(\frac{\gamma_{Hg_2^{2+}}}{\gamma_{Hg^{2+}}}\right) .$$

3.3.4 Silver Zeolite - Mercury Complexes

Silver ion-exchanged forms of zeolites also sorbed mercury rapidly and copiously at temperatures in the region of 250°C. The largest uptakes were recorded with AgX which can sorb nearly twice its own weight of mercury.

Diagram 3.3.6 shows the sorption branches of the isotherms recorded with AgX at 213.1°C and 282.6°C. The uptake rises rapidly as the pressure is increased, showing a strong interaction between mercury and the sorbent. The initial part of these isotherms is reversible, but when the uptake exceeds about 270 mg/g, the mercury sorption is no longer reversible. Diagram 3.3.7 shows the isotherm obtained at 235.2°C. A hysteresis loop open along the entire length of the isotherm was observed, and a residual uptake of 42 mg/g which could not be removed by further heating was recorded. The residual uptake increased progressively when isotherms were repeated. Diagram 3.3.8 shows successive isotherms with the same sample of AgX at 270.0°C. After the first

DIAGRAM 3.3.6

AgX-MERCURY ISOTHERMS

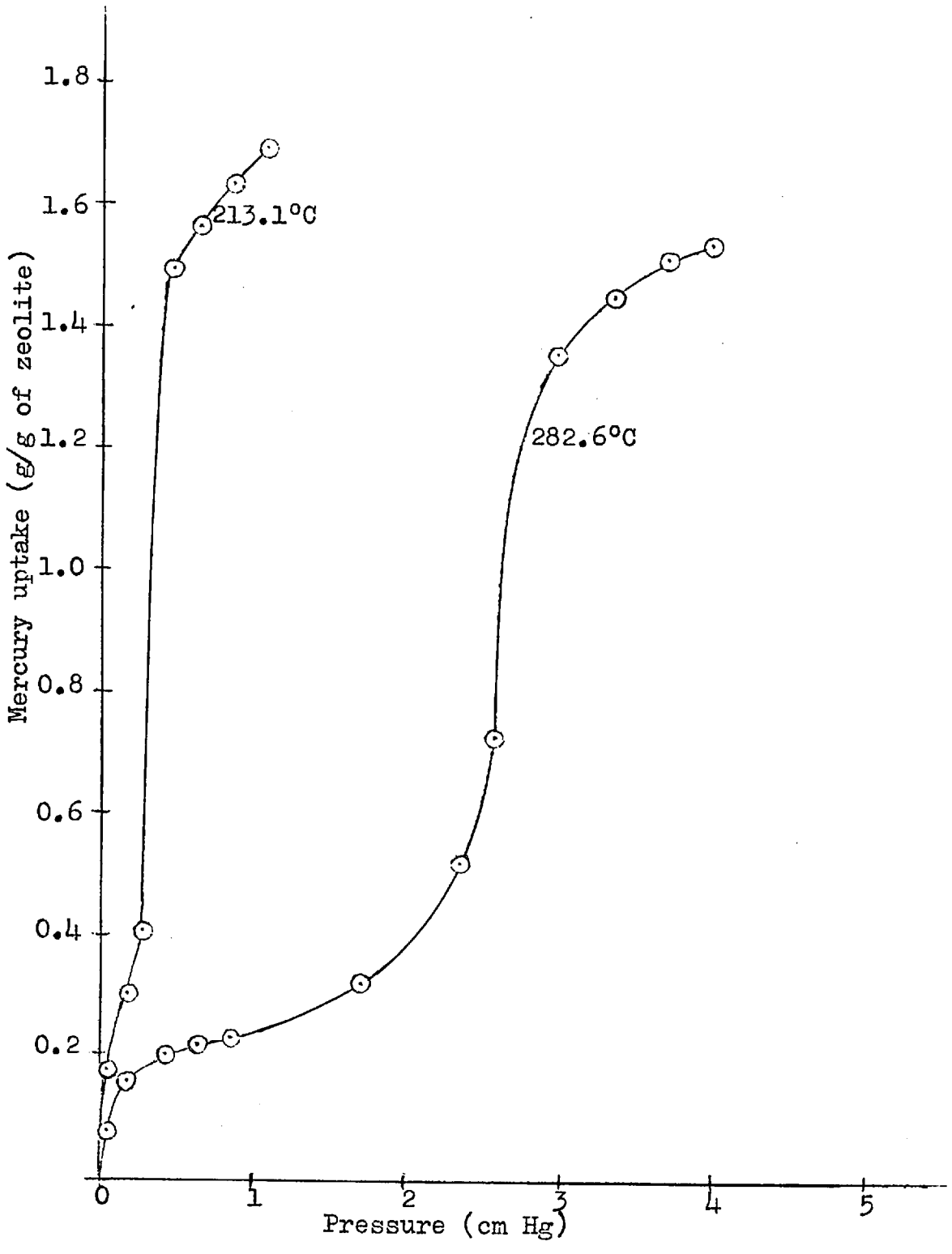

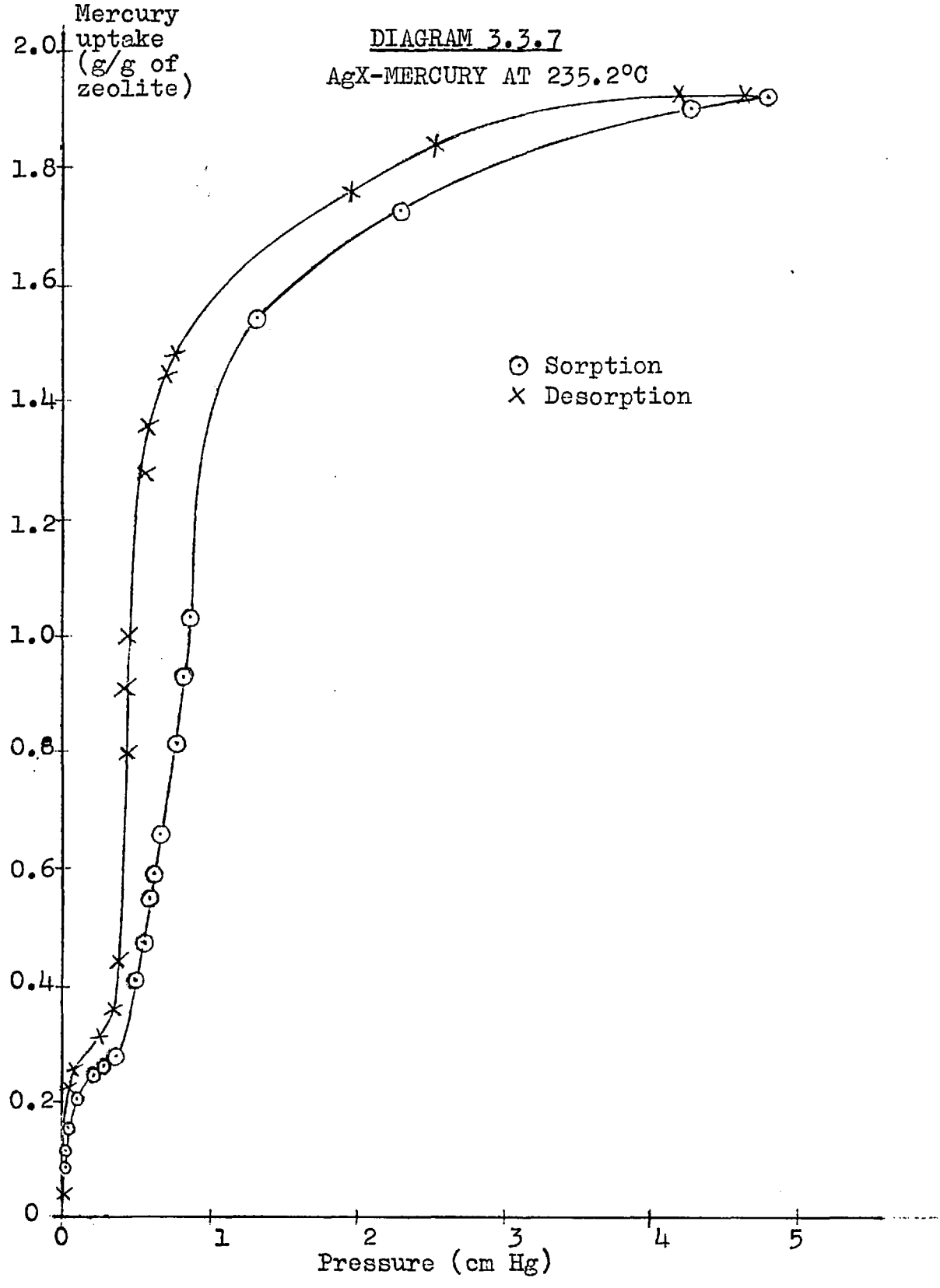

DIAGRAM 3.3.7

AgX-MERCURY AT 235.2°C

AgX – Mercury Isotherms at 270.0°C

DIAGRAM 3.3.8

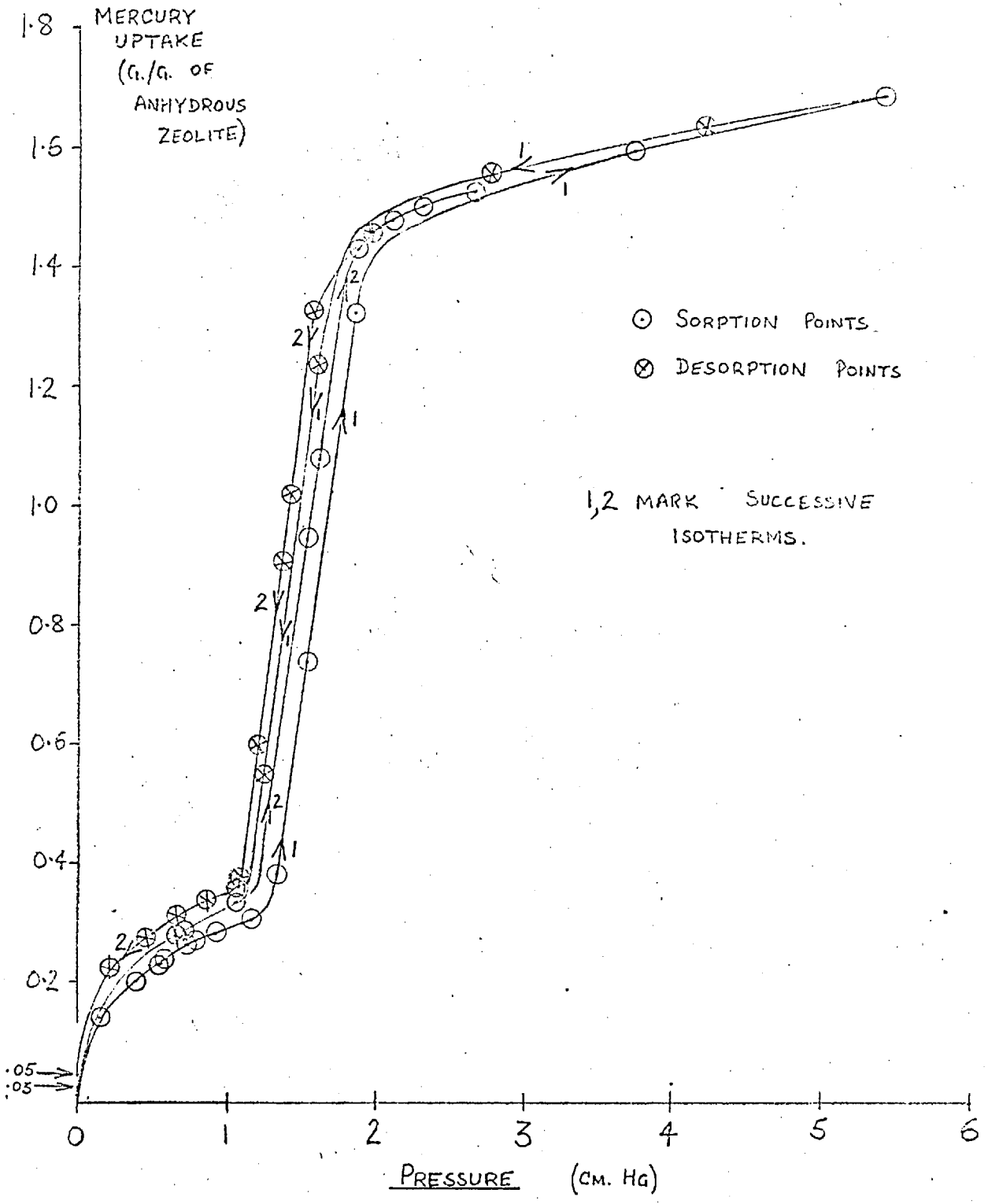

sorption cycle 30 mg of mercury per g of zeolite remained on the sorbent. The sorption branch of the second cycle followed the desorption branch of the first cycle until about 300 mg/g of mercury had been sorbed. The sorption then followed a course parallel to the first sorption. On lowering the pressure, the second desorption followed a course parallel to the first desorption, and a residual weight increase of 50 mg/g was recorded. In diagram 3.3.8 the successive cycles are numbered.

The copious uptake of mercury by AgX is in marked contrast to the very small mercury sorptions recorded with NaX and PbX. It is believed that the first process which takes place when a silver zeolite is exposed to mercury vapour is a reversible electron transfer between silver ions and mercury to give mercury ions and silver atoms. An electron transfer of this type would not be possible between sodium ions and mercury or between lead ions and mercury due to their relative positions in the electrochemical series.

The neutral silver atoms produced by the electron transfer mechanism may act as nucleation centres for the uptake of more mercury atoms. X-ray photographs of silver zeolites which have been round a cycle of mercury sorption and removal have additional lines which correspond with the structure of metallic silver. The sharpness of the lines indicates that the clusters of silver atoms are too large to be inside the structure of the zeolite. Some mercury cations must therefore remain inside the structure when the sorbed mercury is removed in order to maintain the electrical neutrality. The residual increase in weight of the zeolite, which remains after prolonged heating, is probably due to the presence of mercury cations.

The reactions which may occur include

(1) $2Ag^+ + Hg \rightleftarrows 2Ag + Hg^{2+}$ for which $K_1 = \dfrac{a_{Ag}^2 \; a_{Hg^{2+}}}{a_{Ag^+}^2 \; p}$

and

(2) $2Ag^+ + 2Hg \rightleftarrows 2Ag + Hg_2^{2+}$ for which $K_2 = \dfrac{a_{Ag}^2 \; a_{Hg_2^{2+}}}{a_{Ag^+}^2 \; p^2}$

where K_1 and K_2 are equilibrium constants, p is the vapour pressure of mercury, and a_{Ag}, a_{Ag^+}, $a_{Hg^{2+}}$ and $a_{Hg_2^{2+}}$ are the activities of silver atoms, silver ions, mercuric ions and mercurous ions respectively.

Subtracting (1) from (2) gives

$$Hg^{2+} + Hg \rightleftarrows Hg_2^{2+} \quad \text{for which } K_3 = \frac{a_{Hg_2^{2+}}}{a_{Hg^{2+}} \; p} \; . \qquad (3)$$

However

$$\frac{K_2}{K_1} = \frac{a_{Hg_2^{2+}}}{a_{Hg^{2+}} \; p} \quad \text{and therefore } K_3 = \frac{K_2}{K_1} \; .$$

Reactions (1) and (2) occurring in a volume V of sorbent in equilibrium with a pressure p of mercury vapour outside the crystal will produce x_1 g ions of mercuric ions, and x_2 g ions of mercurous ions. Hence from (3) we have

$$K_3 = \frac{x_2}{x_1 p} \frac{\gamma_{Hg_2^{2+}}}{\gamma_{Hg^{2+}}} \; .$$

If the assumption is made that the intracrystalline environment in the silver zeolite resembles that in HgX sufficiently for the ratios $(\gamma_{Hg^{2+}}/\gamma_{Hg_2^{2+}})$ in each case to be equated, then

$$\frac{x_2}{x_1 p_{Hg}} = \left[K_3\left(\frac{\gamma_{Hg^{2+}}}{\gamma_{Hg_2^{2+}}}\right)\right] = \left[K_c\left(\frac{\gamma_{Hg^{2+}}}{\gamma_{Hg_2^{2+}}}\right)\right] = 5.77 \text{ cm}^{-1} \text{ at } 235^\circ\text{C}.$$

It has been shown that zeolites containing a cation which is prohibited by its position in the electrochemical series from electron transfer with mercury occlude only very small amounts of mercury. For example, PbX occludes 1.8×10^{-6} moles per c.c. of sorbent volume for each cm of mercury vapour pressure. Therefore the assumption is made that the <u>initial</u> mercury uptake, q, of the zeolite is due to mercury ions produced by (1) and (2) and that mercury sorbed by the zeolite and by the silver atoms produced in the reactions can be neglected. We then have

$$q = x_1 + 2x_2 .$$

The volume V of silver zeolite initially contains m moles of Ag^+ ions. An uptake of q g.atoms of Hg corresponds to the production of 2q g.atoms of silver, leaving (m-2q) g.ions of silver ions. Then

$$K_1 = \frac{a_{Ag}^2 \, a_{Hg^{2+}}}{a_{Ag^+}^2 \, p} = \frac{(\frac{2q}{V})^2 \, \frac{x_1}{V}}{(\frac{m-2q}{V})^2 \, p} \, \frac{\gamma_{Ag}^2 \, \gamma_{Hg^{2+}}}{\gamma_{Ag^+}^2}$$

But at 235°C $\frac{x_2}{x_1} = 5.77 \, p$, $\therefore q = x_1(1+11.54 \, p)$

$$K_1' = K_1\left(\frac{\gamma_{Ag^+}^2}{\gamma_{Ag}^2 \gamma_{Hg^{2+}}}\right) = \frac{4q^2 x_1}{Vp(m-2q)^2} = \frac{4q^3}{V.p.(1+11.54p)(m-2q)^2}$$

Table 3.3.5 shows the experimental data at 235°C and the calculated values of K_1'.

As the pressure of mercury vapour is raised, K_1' rises at first, but then falls to a steady value of ca. 7.5×10^{-3}. When the mercury uptake exceeds 280 mg/g . K_1' rises rapidly as the pressure is increased. This

TABLE 3.3.5

Mercury Pressure p cm	Mercury Uptake mg/g of zeolite	K_1' $\left(= \frac{4q^3}{Vp(1+11.54p)(m-2q)^2}\right)$
.005	90	14.4×10^{-3}
.024	150	17.4×10^{-3}
.095	202	10.1×10^{-3}
.160	234	9.6×10^{-3}
.200	242	7.9×10^{-3}
.265	258	7.2×10^{-3}
.335	278	7.8×10^{-3}
.401	321	17.4×10^{-3}
.486	406	3.28

behaviour supports the proposed mechanism for the initial uptake of mercury.

Comparisons between the mercury uptakes of silver ion-exchanged forms of several zeolites reveal interesting differences between them. Isotherms at 235°C for AgA-Hg and Ag-chabazite-Hg are shown in diagram 3.3.9, while diagrams 3.3.7 and 3.3.10 show the isotherms recorded at this temperature for the systems AgX-Hg and Ag-gmelinite-Hg respectively. The initial part of each of these isotherms is similar in shape, suggesting that the electron transfer demonstrated in AgX is the first process to occur with each of the zeolites. Lowering the pressure during this part of the isotherm caused the sorption path to be retraced in each case. Raising the

DIAGRAM 3.3. 9

Ag-ZEOLITE-Hg ISOTHERMS AT 235.0°C

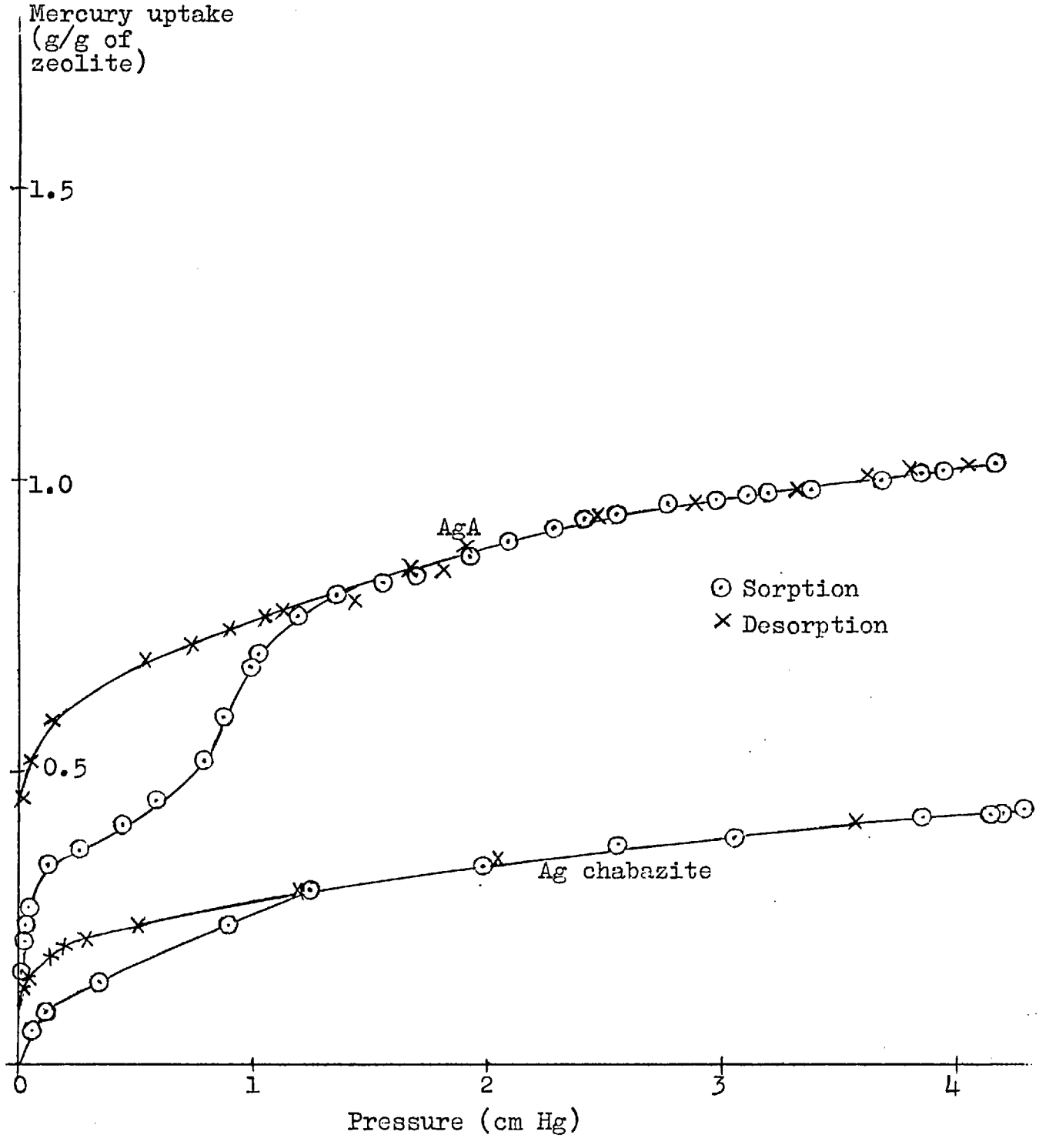

DIAGRAM 3.3.10

Ag GMELINITE-Hg AT 235.0°C

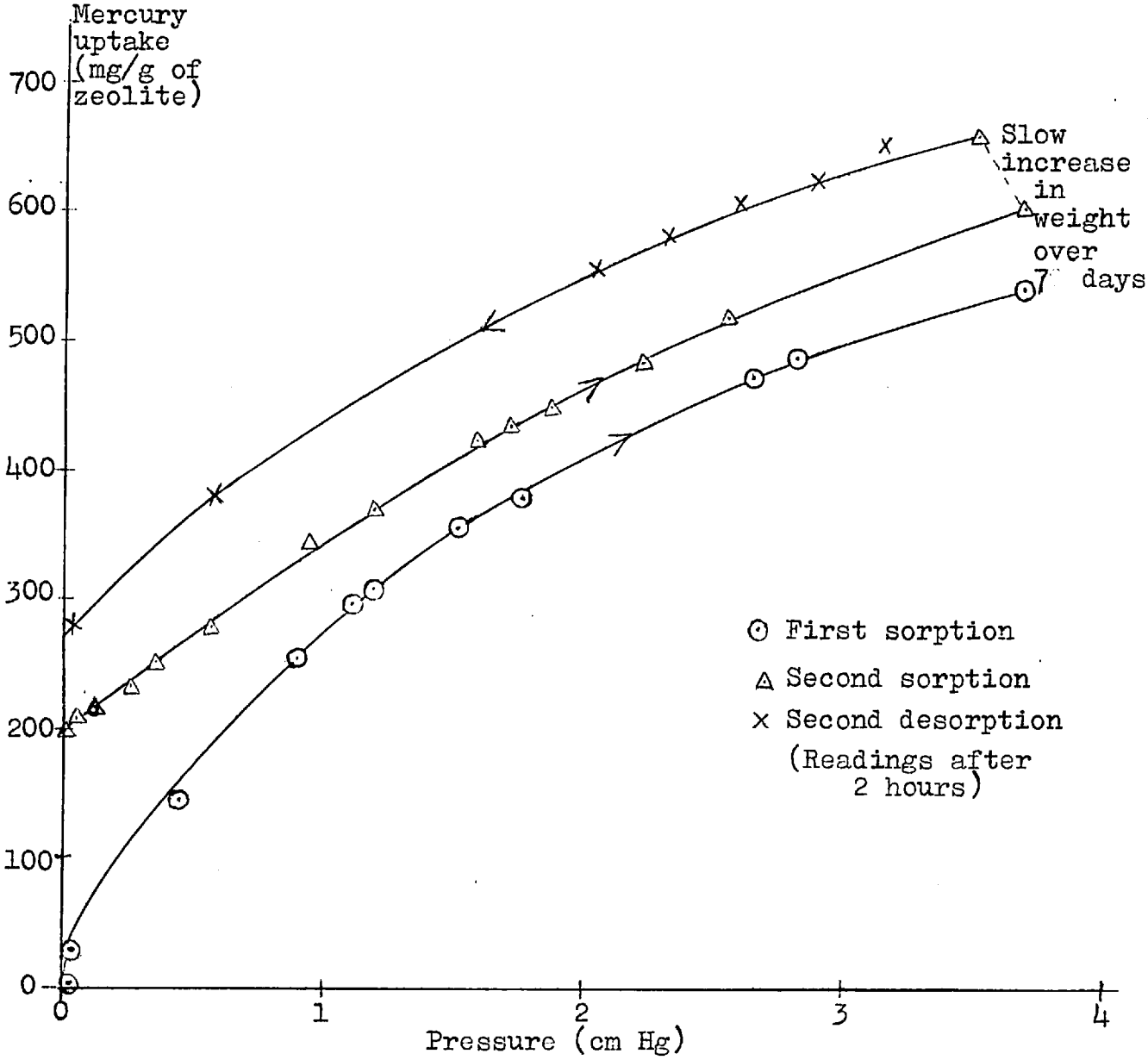

pressure took the isotherms out of this reversible section and here differences in behaviour between the sorbents were encountered. The isotherms for AgX-Hg and AgA-Hg rose steeply before a region of steadily increasing uptake was reached, while Ag chabazite and Ag gmelinite continued to take up mercury steadily, to relative pressures of unity. The maximum uptake recorded with each sorbent at 235°C is given in table 3.3.6. Also shown are the uptakes corresponding to complete filling of the free volume in each of the sorbents, and the ratio of the experimental uptake to the calculated saturation value, which represents the fractional filling if all the Hg uptake were intracrystalline.

TABLE 3.3.6

Sorbent	Maximum uptake at 235°C g/g	Calculated uptake corresponding to saturation g/g	Fractional filling
AgX	1.92	3.33	0.58
AgA	1.03	2.44	0.41
Ag gmelinite	0.67	3.12	0.22
Ag chabazite	0.44	3.44	0.13

The maximum uptakes recorded fall below the calculated saturation values to increasing extents as one goes down the table from the more open to the less open structures. Even with AgX the uptake corresponds to less than 60% filling. It is probable that some of the mercury clusters round silver atoms which have migrated outside the structure and the actual filling of the cages is even less than that shown in table 3.3.6.

This is supported by the observation with Ag gmelinite that while mercury was sorbed or desorbed rapidly when a change was made in the pressure, and an apparent steady value was reached within 2 hours, the uptake of mercury increased by 60 mg/g when the zeolite was exposed to nearly saturated vapour for 7 days. Silver atoms may not be able to act as nucleation centres while still inside the structure and the slow process may be the migration of silver atoms to the outside, where they may nucleate themselves to give metallic silver and also act as nucleation centres for further uptake of mercury. On desorption both AgA-Hg and Ag chabazite-Hg were reversible down to relative pressures of about 0.35 before hysteresis loops appeared. The hysteresis loop with AgX was open along the entire length of the isotherm.

Interesting differences arise between the residual uptakes of the zeolites. With AgX the residual uptake was only 2% of the maximum uptake, but in AgA, Ag gmelinite and Ag chabazite, the percentages of the maximum mercury uptakes which remained in the structure after prolonged evacuation at the isotherm temperature were 45%, 36% and 27% respectively.

4. SUMMARY AND CONCLUSIONS

A comparative study of the sorption of the elements sulphur, phosphorus and mercury, by a number of zeolites, has been made. The uptake of sulphur by the zeolites with more open structures is very rapid and gives type I isotherms which are remarkably rectangular in view of the high temperature of the sorbents. For uptakes near saturation of the crystals, a heat of inclusion for sulphur in NaX, $\Delta\bar{H}$ = -30.2 kcals/mole was calculated from the isotherms recorded at 320.2°C and 262.0°C. Isotherms for the 5A-sulphur system at 257.0°C and 323.7°C gave a corresponding heat of -24.5 kcal/mole. The saturation uptakes of sulphur in each sieve were compared with the theoretical maxima calculated by using the intracrystalline volume of the sieve and the density of liquid sulphur at the appropriate temperature. The comparison showed that the packing of sulphur molecules in the cages uses only 75-80% of the volumes available, suggesting that sulphur polymerises inside the structure. This view was supported by the study of the sorption of sulphur by chabazite. The occlusion of sulphur by this zeolite was very slow. Measurement of the rates of uptake at 320.2°C and 261.9°C showed the slow process to be an activated diffusion requiring an energy of 27.3 kcal/mole. These data are consistent with the diffusion of polymerised sulphur within the structure.

In contrast to the rapid occlusion of sulphur by sieves 5A and NaX the uptake of phosphorus by these sorbents is slow. In the case of NaX this is surprising since the cage windows are sufficiently large to admit P_4 molecules with ease. Another interesting feature

of the NaX-phosphorus system is that the isotherms obtained at 265.1°C and 323.8°C are of the rare type V. These are believed to be some of the first type V isotherms reported for sorption in a zeolite. Type V isotherms are found when the interaction between the sorbent and the molecules of the vapour is comparable with the interaction between the sorbed molecules themselves. Accordingly, it is found that the heat of inclusion, $-\Delta\overline{H}$, rises as the uptake proceeds and reaches a steady value of 27.5 kcal/mole when the sorption cavities are about 30% full and the isotherms are rising almost vertically.

The slow uptake of phosphorus by sieve 5A is to be expected since the concentration of P_2 molecules, which are the only species small enough to enter the cage windows, is very low at the temperature of the experiments. The form of the rate data and the variations of rate with sorbent temperature and sorbate pressure show that diffusion does not control the rate of uptake. The rate controlling factor may be the production of P_2 in an externally adsorbed layer of P_4 molecules. Measurements of the rate of desorption of phosphorus from sieve 5A at 323.2°C, 309.9°C and 295.0°C show desorption to be a first order process with an activation energy of 43.8 kcal/mole for the rate determining step.

Mercury is occluded by NaX to a much lesser extent than sulphur or phosphorus. At temperatures between 240°C and 320°C sorption isotherms are linear, yielding a heat of sorption of -8.2_8 kcal/g.atom of mercury. Since this heat is less negative than the heat of condensation of mercury, transfer of the element from liquid mercury to NaX is endothermal and hence is

favoured by high temperatures. The transfer of mercury to NaX will therefore be negligibly small at room temperature and below — an important conclusion in view of the use of mercury as the manometric fluid in sorption studies involving NaX.

The uptake of mercury by the lead form of sieve X at 200.9°C and 236.0°C was also small, the sorption heat being -9.1 kcal/g.atom of mercury. The uptakes of mercury by the sodium and lead forms of sieve X are unexpectedly modest in view of the strong interatomic forces in liquid mercury. Comparison of the experimental entropies of sorption with those calculated for various models of the sorbed state suggests that the mercury in these sorbents exists as isolated atoms and that it is the mercury-framework interactions which determine the extent of sorption. When electron interchange between mercury atoms and the cations in the zeolite is possible, much larger mercury uptakes are observed. In mercuric X the chemisorption of mercury by the mercuric ion leads to large uptakes of mercury. Reduction of mercuric ions to mercurous takes place in two stages, and at 235.7°C is complete by the time the partial pressure of mercury vapour has reached 0.79. The first stage appears to be the reversible reduction of the ions in certain positions within the structure and follows the Langmuir equation. The remainder of the mercuric ions are reduced in a second stage which is not thermodynamically reversible. On raising the partial pressure of mercury beyond 0.79 the uptake proceeds well beyond the point where every mercuric ion has been reduced. Desorption follows a different path, giving a hysteresis loop which closes

just above the reversible region. In the silver form of sieve X the transfer of electrons from mercury atoms to the silver ions allows still larger mercury uptakes to be achieved through the release of silver atoms which can act as sites for mercury uptake. This is also believed to be the mechanism of the large uptakes of mercury observed with the silver forms of chabazite, gmelinite and sieve A. Each of the silver forms takes up large amounts of mercury and the isotherms show hysteresis in every case. No correlation between the shapes of hysteresis loops and the size and accessibility of sorption cavities was detected, but the fractional filling of the sorption cages falls successively on going from the more open to the less open structures.

Direct comparison of the sorption of mercury, iodine, phosphorus and sulphur can be made from their behaviour in NaX. The interaction between sorbed molecules rises successively along the series of elements when they are arranged in the order of increasing molecular complexity, as above. The interaction between sorbed mercury atoms is negligibly small, and it is the mercury-framework interactions which determine the extent of sorption. In the iodine-NaX complex, sorbate-sorbate interactions contribute significantly to the heat of sorption only when the initial energetic heterogeneity of the sorption sites has died away (Barrer and Wasilewski, 1961). With phosphorus the intermolecular forces are strong and their interaction with the framework is less important. Sorbed sulphur molecules show the greatest interaction with each other and evidence suggests that polymerisation to form chain molecules of considerable length takes place.

REFERENCES

E. P. ADAMS and R. L. HIPPISLEY, 1922, Smithsonian Mathematical Formulae and Tables of Elliptic Functions, Smithsonian Institution, p. 129.

R. M. BARRER, 1956. Report to the 10th Solvay Council, "Physical Chemistry of some Non-Stoicheiometric Phases", Brussels.

R. M. BARRER, 1959. Brit.Chem.Eng., 4, 267.

R. M. BARRER and G. C. BRATT, 1960. J.Phys.Chem. Solids, 12, 130, 146 and 154.

R. M. BARRER and R. M. GIBBONS, 1963. Trans.Faraday Soc., 59, 2569 and 2875.

R. M. BARRER and R. M. GIBBONS, 1965. ibid., 61, 948.

R. M. BARRER and I. S. KERR, 1959. ibid., 55, 1915.

R. M. BARRER and W. M. MEIER, 1958. ibid., 54, 1074.

R. M. BARRER and L. V. C. REES, 1959. ibid., 55, 992.

R. M. BARRER and L. V. C. REES, 1961. ibid., 57, 999.

R. M. BARRER and P. J. REUCROFT, 1960. Proc.Roy.Soc., A.258, 431.

R. M. BARRER and M. SHAMSUZZOHA, 1964. Private communication.

R. M. BARRER and W. I. STUART, 1959. Proc.Roy.Soc., A.249, 464.

R. M. BARRER and J. W. SUTHERLAND, 1956. ibid., A.237, 439.

R. M. BARRER and A. J. WALKER, 1964. Trans.Faraday Soc., 60, 171.

R. M. BARRER and S. WASILEWSKI, 1960. J.Sci.Instruments, 37, 432.

R. M. BARRER and S. WASILEWSKI, 1961. Trans.Faraday Soc., 57, 1160.

R. M. BARRER and M. WOODHEAD, 1948. ibid., 44, 1001.

L. BROUSSARD and D. P. SHOEMAKER, 1960. J.Am.Chem.Soc., 82, 1041.

S. BRUNAUER, L. S. DEMING, W. E. DEMING and E. TELLER, 1940. ibid., 62, 1723.

S. BRUNAUER, P. H. EMMETT and E. TELLER, 1938. ibid., 60, 309.

J. CRANK, 1956. The Mathematics of Diffusion, O.U.P.

J. DONOHUE, A. CARON and E. GOLDISH, 1961. J.Am.Chem. Soc., 83, 3748.

D. H. EVERETT, 1955. Trans.Faraday Soc., 51, 1551.

D. H. EVERETT, 1957. Proc.Chem.Soc., 38.

D. H. EVERETT and W. I. WHITTON, 1952. Trans.Faraday Soc., 48, 749.

D. H. EVERETT and F. W. SMITH, 1954. ibid., 50, 187.

L. A. GARDEN and G. L. KINGTON, 1956. Trans. Faraday Soc., 52, 1397.

G. GEE, 1952. ibid., 48, 515.

F. GRANDJEAN, 1910. Bull.soc.franc.miner., 33, 5.

P. E. HALSTEAD and A. E. MOORE, 1962. J.Appl.Chem., 12, 413.

T. L. HILL, 1952. Advances in Catalysis (N.Y.Academic Press Inc.), 4, 211.

J. O. HIRSCHFELDER, R. J. BUEHLER, H. A. McGEE and J. R. SUTTON, 1958. Ind.Eng.Chem., 50, 375.

J. R. LACHER, 1937. Proc.Roy.Soc., A.161, 525.

I. LANGMUIR, 1918. J.Am Chem.Soc., 40, 1361.

C. S. LU and J. DONOHUE, 1944. ibid., 66, 818.

L. R. MAXWELL, V. M. MOSLEY and S. B. HENDRICKS, 1935. J.Chem.Phys., 3, 699.

K. H. MEYER and Y. GO, 1934. Helv.chim.Acta, 17, 1081.

W. J. C. ORR, 1939. Trans.Faraday Soc., 35, 1247.

L. PAULING, 1960. The Nature of the Chemical Bond, Cornell Univ. Press, Ithaca, N.Y., 189.

J. ROESER and P. WENSEL, 1941. Temperature, its measurement and control, Reinhold, 311.

B. E. WARREN and J. T. BURWELL, 1935. J.Chem.Phys., 3, 6.

A. F. WELLS, 1962. Structural Inorganic Chemistry, O.U.P.

J. R. WEST, 1950. Ind.Eng.Chem., 42, 713.

J. WYART, 1933. Bull.soc.franc.miner., 56, 81.